UNIVERSIDADE FEDERAL DO RIO GRANDE DO SUL
FACULDADE DE FARMÁCIA
PROGRAMA DE PÓS-GRADUAÇÃO EM CIÊNCIAS FARMACÊUTICAS

Desenvolvimento e avaliação in vivo de pós e grânulos contendo fenitoína nanoencapsulada

EDILENE GADELHA DE OLIVEIRA

Porto Alegre, 2018

UNIVERSIDADE FEDERAL DO RIO GRANDE DO SUL
FACULDADE DE FARMÁCIA
PROGRAMA DE PÓS-GRADUAÇÃO EM CIÊNCIAS FARMACÊUTICAS

Desenvolvimento e avaliação in vivo de pós e grânulos contendo fenitoína nanoencapsulada

Tese de Doutorado apresentada por **Edilene Gadelha de Oliveira** para obtenção do TÍTULO DE DOUTOR em Ciências Farmacêuticas

Orientador: Prof. Dr. Ruy Carlos Ruver Beck

Porto Alegre, 2018

Tese apresentada ao Programa de Pós-Graduação em Ciências Farmacêuticas, em nível de Doutorado Acadêmico, da Faculdade de Farmácia da Universidade Federal do Rio Grande do Sul e aprovada em 20 de março de 2018, pela Banca Examinadora constituída por:

Prof. Dra. Cristiane de Bona da Silva
Universidade Federal de Santa Maria

Prof. Dr. Diogo Losch de Oliveira
Universidade Federal do Rio Grande do Sul

Prof. Dr. Helder Ferreira Teixeira
Universidade Federal do Rio Grande do Sul

CIP - Catalogação na Publicação

de Oliveira, Edilene Gadelha
Desenvolvimento e avaliação in vivo de pós e grânulos contendo fenitoína nanoencapsulada / Edilene Gadelha de Oliveira. -- 2018.
194 f.
Orientador: Ruy Carlos Ruver Beck.

Tese (Doutorado) -- Universidade Federal do Rio Grande do Sul, , Porto Alegre, BR-RS, 2018.

1. Farmácia. 2. Nanotecnologia. 3. Nanocápsulas. 4. Fenitoína. I. Beck, Ruy Carlos Ruver, orient. II. Título.

Elaborada pelo Sistema de Geração Automática de Ficha Catalográfica da UFRGS com os dados fornecidos pelo(a) autor(a).

Este trabalho foi desenvolvido no Laboratório 405 da Faculdade de Farmácia da Universidade Federal do Rio Grande do Sul (UFRGS), com financiamento da CAPES, do CNPq e da FAPERGS. A autora recebeu bolsa de estudo da CAPES.

Aos meus pais Edson e Helena, a base de toda a minha educação, ao meu irmão Evérton por ser fonte de inspiração, e ao meu esposo Afonso pelo amor incondicional.

AGRADECIMENTOS

À Deus por ter me guiado durante toda a minha trajetória acadêmica.

Ao professor Ruy Beck, pela orientação deste trabalho, pelo acolhimento no grupo de pesquisa e pelos momentos de aprendizado nesses anos de estudo.

À professora Sílvia Guterres por ter sido minha tutora durante parte do meu doutorado, e pelos ensinamentos e à professora Adriana Pohlmann por ser fonte de conhecimento para todos.

Ao professor Mauro Schneider de Oliveira e aos seus alunos, pela parceria e ajuda na concretização deste trabalho.

Aos professores e funcionários desta Universidade pela colaboração direta e indireta.

À Universidade Federal do Rio Grande do Sul e ao Programa de Pós-Graduação em Ciências Farmacêuticas da UFRGS pela oportunidade.

À CAPES, órgão financiador da bolsa de pesquisa, e ao CNPq pelo apoio financeiro para realização deste trabalho.

Aos colegas e amigos do laboratório 405 na Faculdade de Farmácia e do K204 no Instituto de Química pelas contribuições de forma direta e indireta no desenvolvimento deste trabalho.

Ao laboratório Cristália Produtos Farmacêuticos Ltda, pela doação da fenitoína.

Aos amigos Clóvis e Cátia, pela amizade e pelo acolhimento em sua residência na cidade de Santa Maria/RS durante as atividades realizadas na UFSM.

Aos amigos do Rio Grande do Sul, pelos momentos de descontração, pelo apoio emocional e pela amizade imprescindível para a conclusão de mais uma etapa da minha vida.

Aos meus queridos professores do ensino fundamental e médio, pelo incentivo ao estudo e por me inspirarem na busca pelo conhecimento.

Aos meus pais Edson e Helena pelo amor incondicional, pelo apoio em todos momentos da minha vida e por me proporcionarem a melhor educação, ao meu irmão Evérton, por ser amigo e fonte de inspiração, e aos demais familiares pelo carinho que sempre me deram.

Ao meu esposo Afonso, pelo companheirismo, pela compreensão nos momentos de ausência e pelo amor, maior de todos os sentimentos.

Não siga onde o caminho pode levar. Vá onde não há caminho e deixe uma trilha.

Ralph Waldo Emerson

RESUMO

Este trabalho visou desenvolver pós e grânulos contendo nanocápsulas de fenitoína, avaliando suas propriedades físico-químicas e biológicas. Os pós foram obtidos por *spray-drying*, usando maltodextrina como adjuvante de secagem. Após a sua reconstituição em água, as características nanométricas da suspensão original foram recuperadas. As nanocápsulas revestidas com quitosana e carregadas com fenitoína, assim como seus pós redispersíveis, apresentaram boa estabilidade gastrointestinal e foram aptas a controlar a liberação do fármaco. Além disso, os pós redispersíveis melhoraram a atividade anticonvulsivante *in vivo*, em comparação com o fármaco não encapsulado. Em outra etapa do estudo, os grânulos foram produzidos em leito fluidizado, empregando nanocápsulas contendo fenitoína ou água, como aglutinantes, e uma mistura de maltodextrina e fenitoína, como substrato. O aumento no tamanho dos grânulos e as pontes sólidas foram responsáveis pelas melhores propriedades de fluxo dos grânulos contendo nanocápsulas. Suas características nanométricas foram recuperadas após reconstituição em água, apresentando boa redispersibilidade. A presença de nanocápsulas e o menor tamanho de partícula promoveram uma rápida liberação do fármaco a partir dos grânulos redispersos, os quais tiveram um efeito anticonvulsivante promissor, considerando que somente 10% do fármaco total está na forma nanoencapsulada. No intuito de explicar suas melhores propriedades tecnológicas e a performance superior *in vivo*, o efeito das nanocápsulas no crescimento do grânulo e em suas propriedades de mucoadesão foi avaliado. O crescimento do grânulo foi dependente do volume de aglutinante pulverizado. Um modelo esquemático da estrutura dos grânulos, proposto a partir das análises morfológicas, demonstrou que as nanocápsulas estão recobrindo a sua superfície e as pontes sólidas. Além disso, a principal barreira para controlar a liberação do fármaco foram as nanocápsulas, que circundam os aglomerados e são responsáveis por uma liberação lenta inicial, seguida por uma liberação rápida da fenitoína não encapsulada. Na última etapa, uma propriedade mucoadesiva superior foi encontrada para estes grânulos, sendo explicada pelo efeito combinado das nanocápsulas e da maltodextrina sobre a mucosa intestinal. Portanto, os pós e os grânulos contendo nanocápsulas de fenitoína melhoraram as propriedades tecnológicas e biológicas, apresentando-se como formas sólidas promissoras para reconstituição em água, na terapia anticonvulsivante para pacientes pediátricos e idosos.

Palavras-chave: pós; grânulos; nanocápsulas; fenitoína; atividade anticonvulsivante.

ABSTRACT

This study aimed to develop powders and granules containing phenytoin-loaded nanocapsules, evaluating their physicochemical and biological properties. The powders were obtained by spray-drying, using maltodextrin as drying adjuvant, and reconstituted in water, recovering the nanometric characteristics of the original suspension. The chitosan-coated phenytoin-loaded nanocapsules as well as their redispersible powders had good gastrointestinal stability and were able to control drug release. Moreover, the redispersible powders improved the *in vivo* anticonvulsant activity in mice in comparison with the non-encapsulated drug. In a next step, granules were produced using a fluid bed system, using phenytoin-loaded nanocapsules or water, as binders, and a mixture of maltodextrin and phenytoin, as substrate. The increase in the granule size and the solid bridges formed were responsible for the best flow properties of the granules containing nanocapsules. Their nanometric characteristics were recovered after reconstitution in water, showing good redispersibility. The presence of nanocapsules and the smallest particle size promoted a fast drug release from the redispersed granules, which had a promising *in vivo* anticonvulsant effect, considering that only 10% of the total drug is in the encapsulated form. In order to explain the better technological properties and the superior *in vivo* performance, the effect of the nanocapsules on the granule growth and their mucoadhesion properties was evaluated. The granule growth was dependent on the volume of the binder sprayed. A schematic model of its structure, built from the morphological analysis by SEM, demonstrated that the nanocapsules are covering the granule surface and the solid bridges. Furthermore, the main barrier for controlling the drug release were the nanocapsules surrounding the agglomerates and responsible for a slow initial drug release, followed by a fast non-encapsulated phenytoin release. In the last step, a promising mucoadhesive effect was found for the developed granules. The highest mucoadhesive property was explained by a combined effect on the intestinal mucosa of the nanocapsules and maltodextrin. Therefore, the powders and granules containing phenytoin-nanocapsules improved technological and biological properties, as promising solid dosage forms for reconstitution in the anticonvulsant treatment for paediatric and elderly patients.

Keywords: powders; granules; nanocapsules; phenytoin; anticonvulsant activity.

LISTA DE ILUSTRAÇÕES

CAPÍTULO 3

APÊNDICE A

LISTA DE TABELAS

LISTA DE ABREVIATURAS E SIGLAS

BHE	Barreira hematoencefálica
CI	Índice de Carr
CS-LNC	Nanocápsulas sem fenitoína revestidas com quitosana
D[3,2](v)	Diâmetro baseado na área superficial das partículas
D[4,3](v)	Diâmetro baseado no volume de partículas
D[4,3](n)	Diâmetro baseado no número de partículas
D0,1(v)	Diâmetro no percentil 10% da curva de distribuição cumulativa baseado no volume das partículas
D0,5(v)	Diâmetro no percentil 50% da curva de distribuição cumulativa baseado no volume das partículas
D0,9(v)	Diâmetro no percentil 90% da curva de distribuição cumulativa baseado no volume das partículas
D0,1(n)	Diâmetro no percentil 10% da curva de distribuição cumulativa baseado no número das partículas
D0,5(n)	Diâmetro no percentil 50% da curva de distribuição cumulativa baseado no número das partículas
D0,9(n)	Diâmetro no percentil 90% da curva de distribuição cumulativa baseado no número das partículas
EE	Eficiência de encapsulação
FB-LNC	Grânulos obtidos em leito fluidizado contendo nanocápsulas sem fenitoína
$FB\text{-}LNC_{PH}$	Grânulos obtidos em leito fluidizado contendo nanocápsulas carregadas com fenitoína
$FB\text{-}LNC_{PH1}$	Grânulos redispersos contendo nanocápsulas de fenitoína na concentração de 1 mg/mL
$FB\text{-}LNC_{PH3}$	Grânulos redispersos contendo nanocápsulas de fenitoína na concentração de 3 mg/mL
$FB\text{-}LNC_{PH5}$	Grânulos redispersos contendo nanocápsulas de fenitoína na concentração de 5 mg/mL
FB-PH	Grânulos obtidos em leito fluidizado contendo fenitoína
$FB\text{-}PH_3$	Grânulos redispersos contendo fenitoína na concentração de 3 mg/mL
GI	Índice de crescimento

HR	Razão de Hausner
LNC	Nanocápsulas de núcleo lipídico
LNC_{PH}	Nanocápsulas carregadas com fenitoína
MD	Maltodextrina
ρ_{bulk}	Densidade frouxa (*bulk*)
ρ_{tap}	Densidade de compactação
PDI	Índice de polidispersão
PCL	Poli(épsilon-caprolactona)
PCS	Espectroscopia de Correlação de Fótons
PH ou PHT	Fenitoína
PH-LNC	Nanocápsulas de núcleo lipídico carregadas com fenitoína
PHT-CS-LNC	Nanocápsulas de núcleo lipídico carregadas com fenitoína e revestidas com quitosana
PHT-LNC	Nanocápsulas de núcleo lipídico carregadas com fenitoína e não-revestidas
$PH\text{-}LNC_G$	Grânulos contendo nanocápsulas carregadas com fenitoína
$PH\text{-}LNC_{RG}$	Grânulos redispersos contendo nanocápsulas carregadas com fenitoína
PH_G	Grânulos contendo fenitoína
PH_{RG}	Grânulos redispersos contendo fenitoína
PH_S	Solução etanólica de fenitoína
%R	Porcentagem de redispersibilidade
RSD	Desvio padrão relativo
SD	Desvio padrão
SD-CS-LNC	Pós contendo nanocápsulas sem fenitoína e revestidas com quitosana
SD-PHT-CS-LNC	Pós contendo nanocápsulas carregadas com fenitoína e revestidas com quitosana
SD-PHT-LNC	Pós contendo nanocápsulas carregadas com fenitoína e não-revestidas
SEM	Microscopia Eletrônica de Varredura
SNC	Sistema Nervoso Central
SGF	Fluido Gástrico Simulado
SIF	Fluido Intestinal Simulado
SPAN	Polidispersão
$S\text{-}PH_3$	Solução etanólica de fenitoína na concentração de 3 mg/mL
TEM	Microscopia Eletrônica de Transmissão

SUMÁRIO

1 INTRODUÇÃO

1 INTRODUÇÃO

A epilepsia é um espectro de doenças que atinge mundialmente milhões de pessoas em todas as idades, sendo caracterizada pela recorrência de crises epilépticas, provocadas por eventos de atividade neuronal excessiva ou pela hipersincronia no momento da transmissão do impulso nervoso (BANERJEE; FILIPPI; HAUSER, 2009). O objetivo do tratamento da doença é reduzir o número de crises convulsivas, com um mínimo de efeitos adversos, melhorando a qualidade de vida do paciente (MINISTÉRIO DA SAÚDE, 2010).

A fenitoína é um fármaco utilizado no tratamento da epilepsia em adultos e crianças (BATCHELOR; APPLETON; HAWCUTT, 2015). Seu principal mecanismo de ação é o bloqueio de canais de sódio voltagem-dependentes. Devido à estreita janela terapêutica, este fármaco necessita de frequente monitoramento dos níveis séricos (MINISTÉRIO DA SAÚDE, 2010). Portanto, o controle da sua liberação a partir de nanopartículas pode diminuir as flutuações plasmáticas da fenitoína e, consequentemente, seus efeitos adversos tais como sonolência, hiperplasia gengival, deficiência de ácido fólico e vitamina K (SHORVON, 2010), arritmias cardíacas e hipotensão (BATCHELOR; APPLETON; HAWCUTT, 2015). Além disso, estes carreadores são promissores para o tratamento de doenças no Sistema Nervoso Central (SNC) devido à passagem pela barreira hematoencefálica (BHE) (PATEL et al., 2012; WONG; WU; BENDAYAN, 2012).

As nanocápsulas poliméricas são estruturas vesiculares compostas por um núcleo oleoso, envolvidas por uma parede polimérica e estabilizadas por um tensoativo (MORA-HUERTAS; FESSI; ELAISSARI, 2010; POHLMANN et al., 2013). Recentemente, nanocápsulas de núcleo lipídico (LNC) com propriedades mecânicas diferenciadas foram otimizadas. A sua principal diferença é a composição do núcleo oleoso, caracterizado como um organogel formado por monoestearato de sorbitano e óleo, sendo estabilizado por um tensoativo de alto EHL (polissorbato 80) (JÄGER et al., 2009; VENTURINI et al., 2011). Além disso, nanocápsulas de núcleo lipídico, estabilizadas com moléculas de polissorbato 80-lecitina e revestidas com quitosana na superfície também foram desenvolvidas (BENDER et al., 2012; CÉ et al., 2016). Os nanocarreadores têm sido propostos para aumentar o *delivery* cerebral de fármacos que atuam no SNC pelas vias oral e parenteral, melhorando sua eficácia

farmacológica e reduzindo os seus efeitos adversos (DIMER et al., 2014; RODRIGUES et al., 2016; ZANOTTO-FILHO et al., 2013).

A técnica de secagem por aspersão ou *spray-drying* tem sido empregada na produção de pós a partir de sistemas nanoestruturados, utilizando diferentes adjuvantes de secagem (MARCHIORI et al., 2012; TEWA-TAGNE; BRIANÇON; FESSI, 2007; ZUGLIANELLO et al., 2018). A produção destes pós permite melhorar a estabilidade físico-química das suspensões de nanocápsulas (GUTERRES; BECK; POHLMANN, 2009). O fundamento da técnica de *spray-drying* consiste na co-precipitação com evaporação do solvente, na qual o material a ser seco pode estar dissolvido, emulsionado ou disperso no meio líquido a ser atomizado (BECK et al., 2008; NANDIYANTO; OKUYAMA, 2011).

Por outro lado, a granulação por via úmida em leito fluidizado é uma das técnicas mais utilizadas na área industrial, estando bem estabelecida como etapa intermediária para a produção de comprimidos e cápsulas. Diante disso, esta técnica tem sido relatada na literatura para preparação de grânulos contendo nanopartículas (BASA et al., 2008; BOSE et al., 2012; HAKIM et al., 2005; YAMAMOTO et al., 2007). Friedrich et al. (2010) desenvolveram grânulos contendo nanocápsulas de dexametasona através de granulação por via úmida. Os autores demonstraram a boa estabilidade destes grânulos e a recuperação das características nanométricas da suspensão original. Recentemente, Andrade et al. (2018) desenvolveram grânulos obtidos por leito fluidizado contendo nanocápsulas de núcleo lipídico brancas como aglutinante, demonstrando o importante papel do revestimento catiônico na sua redispersão aquosa.

As limitações tecnológicas das formulações contendo fenitoína e a ausência de informações na literatura sobre o uso de nanocápsulas de núcleo lipídico com este fármaco na forma de pós e grânulos redispersíveis para uso oral motivou a escolha do tema de estudo. Diante disso, a hipótese do trabalho é que estes pós e grânulos, obtidos por secagem por aspersão e leito fluidizado, respectivamente, possam ser tecnologicamente viáveis como pós para reconstituição em água, recuperando as características das suspensões originais, com boa redispersibilidade, estabilidade físico-química e gastrointestinal, liberação controlada do fármaco e uma melhor ação anticonvulsivante. Portanto, o desenvolvimento e avaliação *in vivo* destes sistemas nanoestruturados visam à contribuição científica na produção de formulações seguras e eficazes como alternativa ao tratamento anticonvulsivante convencional.

2 OBJETIVOS

2 OBJETIVOS

2.1 Objetivo geral

- Desenvolver pós e grânulos redispersíveis contendo nanocápsulas de núcleo lipídico carregadas com fenitoína para administração oral, empregando as técnicas de secagem por aspersão e granulação em leito fluidizado, e avaliando a estabilidade em fluido gastrointestinal e as propriedades de mucoadesão, respectivamente, bem como seus efeitos *in vivo* sobre a atividade anticonvulsivante, em um modelo de crises convulsivas induzidas por pilocarpina em camundongos.

2.2 Objetivos específicos

- Desenvolver nanocápsulas de núcleo lipídico carregadas com fenitoína e revestidas ou não com quitosana;
- Desenvolver pós contendo nanocápsulas de núcleo lipídico carregadas com fenitoína, empregando a técnica de secagem por aspersão (*spray-drying*), avaliando as suas características físico-químicas, incluindo a reconstituição em água;
- Avaliar a estabilidade das suspensões e respectivos pós secos por aspersão nos fluidos gástrico e intestinal simulados, considerando a distribuição de tamanho de partícula das nanocápsulas, assim como dos pós redispersíveis;
- Desenvolver grânulos contendo nanocápsulas de núcleo lipídico carregadas com fenitoína, utilizando a granulação em leito fluidizado, avaliando suas características físico-químicas, assim como a formação dos grânulos e seu comportamento mucoadesivo após redispersão aquosa.
- Avaliar os perfis de liberação *in vitro* da fenitoína a partir de nanocápsulas e dos respectivos pós e grânulos redispersíveis.
- Estudar o efeito anticonvulsivante *in vivo* da nanoencapsulação da fenitoína, a partir da administração dos pós e grânulos redispersíveis, em modelo de crises induzidas por pilocarpina em camundongos.

3 REVISÃO DA LITERATURA

3 REVISÃO DA LITERATURA

3.1 Epilepsia

A epilepsia é considerada um problema de saúde pública, pois acomete aproximadamente 50 milhões de pessoas em todo o mundo, atingindo todas as idades, sendo uma das principais enfermidades que atinge o SNC (WHO, 2016). A epilepsia compreende um grupo de distúrbios neurológicos, caracterizados pela recorrência de crises epilépticas (GOLDENBERG, 2010; WHO, 2016). As crises parciais se originam em áreas isoladas, enquanto que as crises generalizadas atingem ambos os hemisférios do cérebro (BENNEWITZ; SALTZMAN, 2009).

As crises epilépticas podem ser controladas por meio de farmacoterapia em 70% dos casos. Diante disso, a sua alta incidência pode estar relacionada a fatores socioeconômicos como o acesso limitado à assistência médica, ou mesmo, de causa idiopática (BANERJEE; FILIPPI; HAUSER, 2009). A discriminação social em torno da doença perdura até os dias atuais, impactando na qualidade de vida dos pacientes e de suas famílias (WHO, 2016).

Os fármacos anticonvulsivantes são utilizados principalmente para evitar crises epilépticas, mas podem ser usados na clínica em casos específicos de enxaqueca, transtorno afetivo bipolar e dor neuropática. Eles agem através de diferentes mecanismos: bloqueio dos canais de sódio e cálcio, inibição de receptores $GABA_A$ ou ligação à proteína SV2A da vesícula sináptica (ROGAWSKI; LÖSCHER, 2004). Como exemplos de fármacos anticonvulsivantes, têm-se a carbamazepina, clobazam, etossuximida, fenitoína, fenobarbital, gabapentina, primidona, topiramato, lamotrigina, vigabatrina e ácido valproico (MINISTÉRIO DA SAÚDE, 2010).

A fenitoína tem sido bastante efetiva em controlar crises parciais (focais) e tônico-clônicas (MEGIDDO et al., 2016) e está disponível em diferentes formas farmacêuticas como comprimidos (100 mg), cápsulas (100 mg), suspensões orais (20 mg/mL) e solução injetável (50 mg/mL).

3.2 Fenitoína

3.2.1 Características físico-químicas

A fenitoína (5,5-difenilhidantoína) é um fármaco anticonvulsivante convencional utilizado em crises epilépticas parciais e generalizadas, mas não em crises de ausência (MEGIDDO et al., 2016). Possui natureza fracamente ácida (pKa = 8,31) e baixa solubilidade em água, o que pode ocasionar problemas durante a absorção no trato gastrointestinal (BURSTEIN et al., 1999). No Sistema de Classificação Biofarmacêutico, é classificado como classe II, sendo portanto considerado um fármaco de baixa solubilidade e alta permeabilidade (SOUZA; FREITAS; STORPIRTIS, 2007).

A fenitoína possui um anel hidantoína e dois grupos substituintes fenila, como demonstrado na Figura 1. Tem sido proposto pela literatura que o anel aromático ligado ao grupo amida da hidantoína possui afinidade pelos canais de sódio voltagem-dependentes, sendo responsável por sua atividade anticonvulsivante (LIPKIND; FOZZARD, 2010; UNVERFERTH et al., 1998; ZHA; BROWN; BROUILLETTE, 2004).

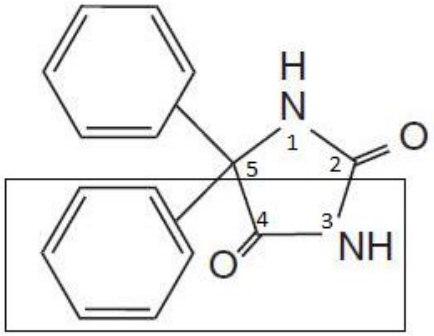

Figura 1 – Estrutura química da fenitoína e seu núcleo farmacofórico.

3.2.2 Mecanismo de ação

As crises epilépticas são resultado de descargas elétricas excessivas nos neurônios do cérebro, as quais podem ser graves e prolongadas. A fenitoína possui uma ação inibitória nos canais de sódio voltagem-dependentes, levando à uma diminuição da atividade elétrica neuronal (DAVIES, 1995). Esse processo envolve uma inativação lenta dos canais de sódio, sendo que o início e a recuperação tardia

destes contribui para retardar a alta frequência dos potenciais de ação que ocorrem como resultado da despolarização prolongada ou repetitiva (ROGAWSKI; LÖSCHER, 2004).

3.2.3 Farmacocinética

A biodisponibilidade oral da fenitoína é de 95%, seu pico máximo é variável com um $T_{máx}$ de 4 a 12 horas, possui um volume de biodistribuição de 0,5 a 0,8 L/kg, liga-se à 70-95% das proteínas plasmáticas e apresenta amplo tempo de meia-vida (7-42 horas). Quando é administrada na forma de sal sódico, a preparação é absorvida lentamente pelo trato gastrointestinal. O fator limitante para a sua absorção é a dissolução no meio, pois a fenitoína é praticamente insolúvel no pH ácido do estômago, enquanto que há um aumento da sua solubilidade em pH mais alto. Além disso, este fármaco é predominantemente absorvido pelo intestino, sendo que a presença de alimentos pode alterar a sua absorção (SHORVON, 2010).

A fenitoína tem um índice terapêutico estreito, o que requer monitoramento plasmático. Em pessoas idosas, isso se torna ainda mais importante, pois há alterações relacionadas à idade na distribuição, no metabolismo e na eliminação de fármacos. Além disso, a polimedicação pode contribuir para a interação da fenitoína com outros agentes terapêuticos (BATTINO et al., 2004). A maioria dos fármacos possui cinética de 1ª ordem, na qual existe uma relação linear entre a dose e os níveis séricos. No entanto, a fenitoína apresenta um tipo de cinética conhecida como Michaelis-Menten, em que a sua eliminação é não linear devido à saturação do metabolismo. Em altas concentrações plasmáticas, há um aumento da meia-vida e diminuição do clearence. Portanto, um pequeno acréscimo na dose pode elevar desproporcionalmente os níveis séricos e, consequentemente, atingir concentrações tóxicas (DELEU; AARONS; AHMED, 2005). Os efeitos adversos da fenitoína incluem: sonolência, tonturas, sedação, dor de cabeça, perda da libido, hiperplasia gengival, deficiência de ácido fólico e vitamina K, hepatite, disfunção hormonal, alterações de humor, defeitos na coagulação (SHORVON, 2010) e outros mais graves como arritmias cardíacas, hipotensão e efeitos colaterais neurológicos em concentrações séricas mais altas (BATCHELOR; APPLETON; HAWCUTT, 2015).

3.3 Nanopartículas poliméricas

Nanopartículas são carreadores de fármacos, na escala nanométrica (1 a 1000 nm), que podem ser biodegradáveis ou não, utilizados em sistemas de liberação de fármacos. As nanopartículas poliméricas podem ser classificadas em nanocápsulas e nanoesferas, as quais diferem quanto à organização estrutural (Figura 2). As nanoesferas são sistemas matriciais, constituídas por uma rede polimérica, na qual o fármaco pode estar dissolvido ou disperso, enquanto que as nanocápsulas são sistemas vesiculares formados por um núcleo oleoso envolvido por um invólucro polimérico, onde o fármaco pode estar dissolvido no núcleo ou adsorvido à parede polimérica (REIS et al., 2006; SCHAFFAZICK et al., 2003).

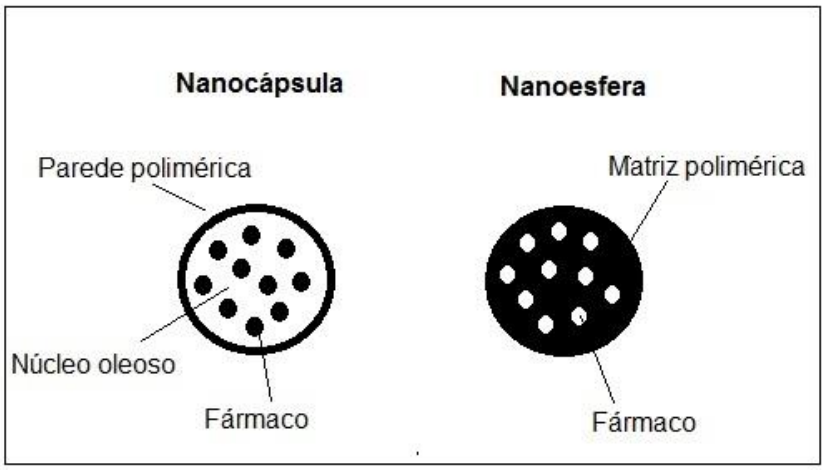

Figura 2 – Esquema representativo da estrutura de nanocápsulas e nanoesferas.
Fonte: adaptado de Schaffazick et al. (2003).

Vários métodos de preparação de nanopartículas têm sido relatados na literatura, pelos quais se obtêm partículas, geralmente de tamanho entre 100 e 500 nm. Estes podem ser classificados em duas principais categorias: por reação de polimerização (*in situ*) e deposição interfacial do polímero pré-formado (QUINTANAR-GUERRERO et al., 1998; REIS et al., 2006). A polimerização interfacial é baseada no uso de uma fase contínua aquosa e outra orgânica. Na fase aquosa contínua, o monômero é dissolvido em água, sem necessidade de adição de tensoativos. O processo se inicia quando a molécula do monômero colide com um iniciador (íon ou radical livre) e o crescimento da cadeia ocorre quando os íons formados colidem com outras moléculas de monômero. Na fase orgânica contínua, há uma dispersão do

monômero em um meio não-solvente ou em uma emulsão. A vantagem deste método é a obtenção de nanocápsulas a partir da formação do polímero *in situ* ao redor da fase interna óleo/água ou água/óleo (REIS et al., 2006). Apesar de ser o método mais rápido e de fácil escalonamento, resíduos de monômeros e oligômeros do processo de polimerização poderiam limitar o uso destas nanopartículas (FESSI et al., 1989).

A técnica de deposição interfacial do polímero pré-formado foi descrita por Fessi et al. (1989) e envolve a emulsificação espontânea de uma fase interna, na qual o polímero está dissolvido em um solvente orgânico miscível em água (acetona ou etanol), em uma fase aquosa externa, com presença ou não de um tensoativo. O processo envolve a rápida difusão do solvente, o qual pode ser eliminado sob pressão reduzida, favorecendo a deposição do polímero na interface água-solvente orgânico, formando instantaneamente nanocápsulas ou nanoesferas.

No caso da produção de nanocápsulas, o óleo utilizado na fase orgânica favorece a alta eficiência de encapsulação de fármacos lipofílicos (QUINTANAR-GUERRERO et al., 1998; REIS et al., 2006), juntamente com outros fatores como características físico-químicas do fármaco, o tipo de tensoativo utilizado, a natureza do polímero e o pH do meio (SCHAFFAZICK et al., 2003). As principais desvantagens da técnica de deposição interfacial do polímero pré-formado é a limitada disponibilidade de solventes orgânicos miscíveis em água, resquícios de solventes que podem ser tóxicos à saúde e baixa eficiência em encapsular fármacos hidrofílicos (REIS et al., 2006).

As nanopartículas poliméricas têm sido bastante estudadas na área farmacêutica (FANG et al., 2016; FONSECA et al., 2014; RODRIGUES et al., 2016; VENTURINI et al., 2011). Os sistemas nanoestruturados são promissores carreadores de fármacos devido às inúmeras vantagens tais como proteção do fármaco contra fotodegradação (FRIEDRICH et al., 2015; OURIQUE et al., 2014; PAESE et al., 2009) e melhora das respostas biológicas como o efeito neuroprotetor da indometacina na doença de Alzheimer e o efeito antioxidante do resveratrol e da curcumina (BERNARDI et al., 2012; CORADINI et al., 2014).

Niwa et al. (2011) desenvolveram uma nanosuspensão contendo fenitoína na forma de *beads* a partir da combinação de duas técnicas: nano-moagem (*nano-milling*) e secagem por aspersão (*spray-drying)*. O pó seco obtido a partir desta nanosuspensão apresentou uma alta dispersibilidade e recuperação do tamanho nanométrico original e imediata liberação do fármaco no meio gastrointestinal. Fang

et al. (2016) produziram nanopartículas de poli(butilcianoacrilato) revestidas com Pluronic P85 contendo fenitoína e demonstraram que estas nanoestruturas atravessam a barreira hematoencefálica, liberando o fármaco no interior do cérebro em ratos resistentes (superexpressão de glicoproteína-P) ao tratamento com este anticonvulsivante. Wang et al. (2016) desenvolveram hidrogéis de nanopartículas eletroresponsivas, que possibilitaram um aumento do efeito anticonvulsivante da fenitoína sódica em um modelo de crises tônico-clônicas induzidas em ratos, comparado ao das não-eletroresponsivas e ao da solução do fármaco.

3.3.1 Nanocápsulas de núcleo lipídico

Recentemente, nanocápsulas de núcleo lipídico, envolvidas por uma membrana polimérica de poli(ε-caprolactona) (PCL), estabilizadas com polissorbato 80, foram desenvolvidas, utilizando o método de deposição interfacial do polímero pré-formado. A proporção entre os componentes da formulação foi otimizada no intuito de obter exclusivamente nanocápsulas, evitando a contaminação por nanoesferas e/ou nanoemulsões (JÄGER et al., 2009; VENTURINI et al., 2011).

O núcleo lipídico é formado por um lipídeo sólido (monoestearato de sorbitano) e um lipídeo líquido (óleo). A composição deste núcleo está relacionada à solubilidade do fármaco no óleo. Além disso, a viscosidade do núcleo lipídico influencia diretamente a permeabilidade do fármaco e, consequentemente, a sua liberação (JÄGER et al., 2009). Zanotto-Filho e colaboradores (2013) utilizaram o óleo de semente de uva para nanoencapsulação da curcumina e avaliaram a sua atividade no tratamento de gliomas. Os autores observaram uma diminuição do tumor e aumento da sobrevida dos animais, sugerindo que as nanocápsulas aumentaram a eficácia farmacológica do fármaco.

As características de biocompatibilidade e biodegradabilidade de polímeros como a poli(ε-caprolactona) são requisitos importantes para o uso biológico de nanocarreadores (SINHA et al., 2004). A PCL é um poliéster alifático semicristalino, cuja temperatura de transição vítrea e de fusão são, aproximadamente, -60 °C e 59-64 °C, respectivamente. É obtida através de polimerização por abertura de anel de um monômero (ε-caprolactona). É solúvel em solventes como diclorometano e clorofórmio, parcialmente solúvel em acetonitrila e acetona e insolúvel em água (LABET; THIELEMANS, 2009).

A degradação da PCL é dependente do peso molecular, do grau de cristalinidade e das condições de degradação. Inicialmente, a fase amorfa degrada, resultando em um aumento da cristalinidade. A reação de degradação é catalisada por ácidos carboxílicos liberados a partir da hidrólise do grupo éster, o que ocasiona perda de massa. Na natureza, os microorganismos podem degradá-la completamente e as enzimas aceleram este processo. Por outro lado, a fagocitose tem um papel importante no estágio final de degradação *in vivo* deste polímero (LABET; THIELEMANS, 2009; SINHA et al., 2004). Além disso, outras vantagens do uso da PCL em nanoestruturas é o controle da liberação do fármaco, da penetração/permeação na pele, melhora da estabilidade química e aumento da resposta biológica (POHLMANN et al., 2013).

3.3.2 Nanocápsulas para delivery cerebral

O Sistema Nervoso Central (SNC) é constituído por duas grandes barreiras, a barreira hematoencefálica (BHE) e a barreira sangue-líquido cefalorraquidiano (BSLCR). A BHE é composta de células endoteliais, caracterizadas pela presença de *tight junctions* que formam uma barreira celular, limitando a entrada de células (macrófagos), compostos endógenos e xenobióticos. No entanto, moléculas de baixo peso molecular podem atravessá-la facilmente (<1000 Da). A regulação do fluxo de substâncias do sangue para o fluido intersticial é modulada por transportadores de membrana como a glicoproteína-P (P-gp), a qual é uma bomba de efluxo que utiliza energia celular para bombear fármacos de volta para o lúmen do vaso, diminuindo o acúmulo destes no cérebro (BENNEWITZ; SALTZMAN, 2009; WONG; WU; BENDAYAN, 2012).

A limitada passagem de moléculas pela BHE é um desafio para o *delivery* cerebral de fármacos (PATEL et al., 2012). Algumas estratégias para aumentar a sua penetração e a permanência no cérebro é o uso de nanopartículas poliméricas, lipossomas, dendrímeros e carreadores lipídicos nanoestruturados (BENNEWITZ; SALTZMAN, 2009; YANG, 2010). Vários mecanismos têm sido propostos para explicar o transporte de nanopartículas através da BHE. As duas principais rotas são a transcitose adsortiva e a transcitose mediada por receptor através da interação de um ligante com porções expressas nas células endoteliais no cérebro (HERVÉ; GHINEA; SCHERRMANN, 2008; YANG, 2010). Proteínas catiônicas (por exemplo, a

albumina) e a quitosana têm sido investigadas como nanocarreadores, pois podem aumentar o *delivery* cerebral via transcitose adsortiva (YANG, 2010).

Em algumas infecções bacterianas e virais, Doença de Alzheimer, epilepsia e tumores cerebrais pode haver um comprometimento da integridade desta barreira, alterando a sua permeabilidade (WONG; WU; BENDAYAN, 2012). Em distúrbios cerebrais, como as crises epilépticas, há uma abertura transitória da BHE devido à regulação positiva do receptor de toxina diftérica (RTD), o qual é responsável pelo transporte de internalização de fármacos no cérebro (GAILLARD; BRINK; DE BOER, 2005). Diante disso, o *targeting* de moléculas poderia ser favorecido. No entanto, esse processo torna o entendimento do transporte via paracelular ainda mais complexo, considerando a limitação de resultados *in vivo* sob condições patológicas (CHEN et al., 2013).

De acordo com estudos prévios, nanocápsulas de núcleo lipídico são aptas para aumentar a biodisponibilidade de fármacos no cérebro pelas vias oral (RODRIGUES et al., 2016) e parenteral (DIMER et al., 2015; FIGUEIRÓ et al., 2013; FROZZA et al., 2010; ZANOTTO-FILHO et al., 2013), reduzindo seus efeitos colaterais (DIMER et al., 2014). Rodrigues e colaboradores (2016) demonstraram que as nanocápsulas de núcleo lipídico atravessam a barreira hematoencefálica, liberando o fármaco no cérebro após administração intravenosa e oral.

Outra estratégia interessante em *delivery* de fármacos no SNC é o revestimento de nanocápsulas com quitosana, a qual tem sido bastante utilizada como revestimento catiônico para a modificação de superfície de nanopartículas (BENDER et al., 2012; NAFEE et al., 2009; OYARZUN-AMPUERO et al., 2010; PREGO et al., 2005). Isso ocorre devido à interação entre a carga negativa de fosfolipídeos e a carga positiva de moléculas de quitosana (PREGO et al., 2005). Este revestimento é adsorvido na superfície da nanocápsula, através da adição de uma solução de quitosana, sob agitação moderada e tempo pré-determinados, em uma etapa posterior ao método de nanoprecipitação (MORA-HUERTAS; FESSI; ELAISSARI, 2010).

A quitosana é um polissacarídeo linear obtido a partir da N-desacetilação da quitina, a qual é um biopolímero comumente encontrado no exoesqueleto de invertebrados e parede celular de fungos. Este polímero possui unidades de β-(1,4)-2-amino-2-D-glucosamina (desacetilada) e β-(1,4)-2-acetamido-2-D-glucosamina (acetilada), cujo grau de desacetilação é dado pelo número de unidades desacetiladas (KHOR; LIM, 2003; PRASHANTH; KITTUR; THARANATHAN, 2002). Ela possui

propriedades de biocompatibilidade, biodegradabilidade e mucoadesão (KHOR; LIM, 2003; OYARZUN-AMPUERO et al., 2010) bem como a habilidade em alterar as *tight junctions* pela via paracelular, facilitando a passagem desses sistemas nanoestruturados através da barreira intestinal (PREGO et al., 2005).

Considerando que a maior parte das células do trato gastrointestinal são produtoras de muco, então o uso de polímeros bioadesivos, como a quitosana, é desejável para administração oral de fármacos no intuito de prolongar o contato entre as nanopartículas e a mucosa (bioadesão), sendo absorvidas em uma etapa posterior (JUNG et al., 2000; PREGO et al., 2006). Além disso, outros fatores devem ser levados em consideração para aumentar sua absorção, como o tamanho, a carga de superfície e a hidrofobicidade (JUNG et al., 2000). Nanocarreadores de fármacos com revestimento positivo têm se mostrado promissores devido à melhora da sua estabilidade na presença de íons Ca^{2+} e maior interação com membranas biológicas carregadas negativamente (CALVO; REMUNAN-LOPEZ, 1997). Bender et al. (2012) avaliaram a hemocompatibilidade *in vitro* de nanocápsulas de núcleo lipídico estabilizadas com polissorbato 80 e lecitina (carga negativa), e revestidas com quitosana (carga positiva). Os resultados demonstraram que as nanocápsulas foram hemocompatíveis, não sendo observada hemólise e agregação plaquetária significativa.

3.4 Secagem por aspersão

A técnica de secagem por aspersão (*spray-drying*) é bastante utilizada na área industrial química, farmacêutica e alimentícia devido à sua versatilidade e fácil escalonamento. Esse método foi descrito pela primeira vez por Percy (1872) como um processo simultâneo de atomização e secagem de substâncias. O processo de secagem por aspersão envolve três etapas principais: (1) atomização do precursor em forma de gotículas; (2) conversão das gotículas em partículas através da evaporação do solvente e (3) coleta de partículas, como demonstrado na Figura 3 (SINGH; VAN DEN MOOTER, 2016). Na 1ª fase, um precursor (solução, suspensão ou emulsão) é atomizado em forma de gotículas, cujo tamanho é dependente do tipo de atomizador utilizado, no qual atuam forças como a centrífuga, eletrostática e ultrasônica (ISKANDAR, 2009; NANDIYANTO; OKUYAMA, 2011). Estas gotículas entram em contato com um fluxo de ar aquecido ou atmosfera inerte (nitrogênio). Em seguida, há

a conversão destas gotículas em partículas através da remoção do solvente (ISKANDAR, 2009; RHODES, 2008). Na última etapa, as partículas são separadas e coletadas no ciclone e/ou coletor eletrostático, em função da massa de pó e/ou do tamanho da partícula (RHODES, 2008).

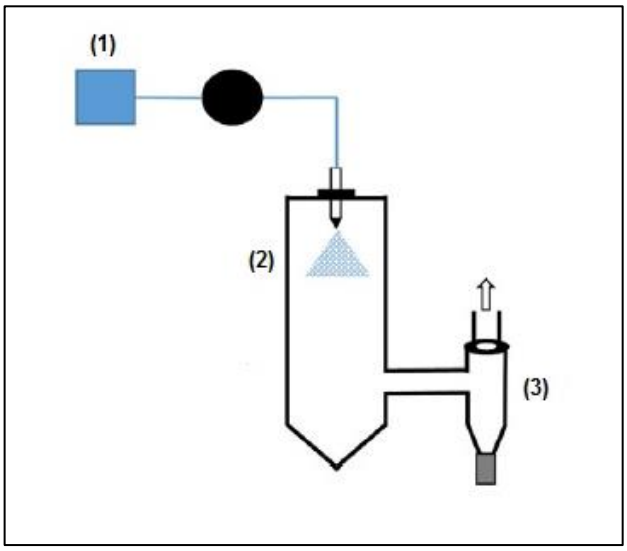

Figura 3 – Etapas do processo de secagem por aspersão (*spray-drying*).
Fonte: adaptado de Singh e Mooter (2016).

As variáveis inerentes ao processo incluem temperatura de entrada e saída, taxa de alimentação, fluxo de gás de secagem e parâmetros da atomização (tipo de atomizador). Além disso, há outros parâmetros que determinam as propriedades do produto final, tais como pressão de vapor e taxa de evaporação do solvente, concentração do precursor e razão fármaco/polímero (SINGH; VAN DEN MOOTER, 2016). Esta técnica de secagem é útil para o controle do tamanho e morfologia das partículas, as quais podem ser esféricas, uniformes e de escala nano a micrométrica. Através desse método, é possível a obtenção de pós nanoestruturados, compostos por nanopartículas coloidais (partículas primárias) e/ou pós submicrométricos que possuem propriedades na escala nanométrica (NANDIYANTO; OKUYAMA, 2011).

Müller e colaboradores (2000) aplicaram a técnica *spray-drying* pela primeira vez para a secagem de suspensões de nanocápsulas poliméricas. O dióxido de silício foi utilizado como adjuvante de secagem devido à forte adesão dos nanocarreadores às paredes do equipamento. Além disso, os autores confirmaram a presença de nanopartículas na superfície de micropartículas esféricas. Portanto, este método poderia ser utilizado para a obtenção de pós secos contendo nanoestruturas. A forma

sólida permite a eliminação da água destas suspensões coloidais, ocasionando uma melhora da estabilidade físico-química e microbiológica das formulações durante seu armazenamento (GUTERRES; BECK; POHLMANN, 2009).

Tewa-Tagne e colaboradores (2007) avaliaram diferentes adjuvantes de secagem solúveis em água para a secagem por aspersão de nanocápsulas, ressaltando a potencialidade desta técnica para esta aplicação. Além disso, pós com melhores características de morfologia e redispersão foram obtidos, utilizando a concentração de 10% (m/v) de lactose. Marchiori et al. (2012) avaliaram a influência do processo de *spray-drying* nas características físico-químicas de nanocápsulas de núcleo lipídico de tretinoína. Os autores concluíram que a técnica de secagem não alterou a estrutura supramolecular das nanocápsulas, preservando a propriedade de proteção da tretinoína contra a degradação ultravioleta.

A maltodextrina é constituída por uma mistura de sacarídeos (polissacarídeo) de diferentes massas molares, sendo produto da degradação enzimática do amido e caracterizada pela dextrose equivalente (DE < 20), principal parâmetro responsável por suas propriedades reológicas e funcionais (YUSRAINI; HARIYADI; KUSNANDAR, 2013). Este excipiente exibe propriedades tensoativas (PYCIA et al., 2016) e, após passar por um processo de secagem por aspersão, apresenta-se como um pó amorfo que pode reduzir o *caking*, o *stickness* e melhorar o fluxo, aumentando a estabilidade de processamento e armazenamento de sólidos (DESCAMPS et al., 2013).

A maltodextrina é um excipiente solúvel em água, o que poderia facilitar a redispersão do pó (HOFFMEISTER et al., 2012; TEWA-TAGNE; BRIANÇON; FESSI, 2007). Além disso, ela possui aprovação pelo FDA (BOUREZG et al., 2012), compatibilidade com nanocápsulas para posterior secagem por aspersão (TEWA-TAGNE; BRIANÇON; FESSI, 2007) e boa segurança quando usada em formulações pediátricas (EMA, 2013). Além disso, excipientes como a lactose, apesar de ser bastante utilizado em pós para redispersão aquosa (OURIQUE et al., 2014; RIBEIRO et al., 2016), não seria adequado para uso pediátrico devido à intolerância de crianças à lactose, relacionada à sintomas tais como desidratação, diarreia e acidose metabólica (EMA, 2006; ROWE; SHESKEY; OWEN, 2012), limitando, assim, a sua aplicação.

Tewa-Tagne e colaboradores (2007) desenvolveram pós contendo nanocápsulas poliméricas através da técnica de *spray-drying*, avaliando diferentes adjuvantes de secagem em relação às propriedades físico-químicas tais como a

morfologia das partículas e a recuperação do tamanho original das nanocápsulas. Os pós contendo 10% de maltodextrina (m/v) apresentaram partículas grandes com ampla distribuição de tamanho. Além disso, a presença de aglomerados influenciou o aumento do tamanho inicial da suspensão de nanocápsulas, após o processo de secagem por aspersão. Por outro lado, Hoffmeister et al. (2012) também avaliaram a maltodextrina (10% m/v) como adjuvante de secagem para a obtenção de pós secos contendo nanocápsulas de núcleo lipídico de melatonina. Os autores observaram que os pós foram redispersíveis em água e adequados para a incorporação em hidrogéis.

Bourezg et al. (2012) avaliaram três métodos de secagem (liofilização, secagem por aspersão e granulação em leito fluidizado) para obtenção de nanopartículas lipídicas redispersíveis. Dentre os adjuvantes de secagem utilizados (polióis, maltodextrina e celulose microcristalina), a combinação de maltodextrina e polióis (manitol ou sorbitol) foi a mais adequada para obter pós redispersíveis para uso pediátrico. No entanto, houve um aumento do tamanho de partícula em relação ao tamanho da suspensão primária após redispersão dos pós obtidos pelos diferentes métodos de secagem.

3.5 Granulação empregando leito fluidizado

A granulação úmida tem sido bastante empregada nos processos industriais, principalmente na produção de comprimidos e cápsulas. No entanto, pode ser utilizada para produzir grânulos esféricos de liberação modificada e/ou uso pediátrico. Uma de suas vantagens é o aumento da uniformidade de conteúdo em produtos que requerem baixa dose do fármaco e melhorar as propriedades de fluxo (FAURE; YORK; ROWE, 2001; PARIKH, 2005).

A granulação pode ser definida como um processo em que partículas pequenas se aglomeram em outras maiores, nas quais as partículas primárias ainda podem ser identificadas (IVESON et al., 2001; PARIKH, 2005). No método por via seca, no qual não se usa líquido, os grânulos podem ser formados por pontes sólidas (*solid bridges*) através de forças de adesão entre as partículas promovidas pelo aglutinante. No método por via úmida, no qual utiliza algum líquido para unir as partículas, os aglomerados são ligados através de forças de coesão entre as partículas por meio de pontes líquidas (*liquid bridges*) (PARIKH, 2005).

A granulação em leito fluidizado (Figura 4) utiliza a técnica de via úmida no processo de obtenção dos grânulos. A aspersão de um líquido aglutinante é realizada no interior de um leito de pó fluidizado e, subsequentemente, ocorre a secagem dos aglomerados em um mesmo equipamento (JOSHI et al., 2017). A mistura do pó é mantida fluidizando através de um fluxo de ar injetado para cima a partir do fundo do granulador e a solução do aglutinante é pulverizada sobre o leito do pó em uma direção oposta ao fluxo de ar (FAURE; YORK; ROWE, 2001). Os parâmetros que devem ser controlados durante a granulação são aqueles inerentes ao processo (pressão de atomização, tamanho da gota e razão de adição do aglutinante, velocidade do ar de secagem e umidade), às propriedades do aglutinante, como viscosidade e tensão superficial, e do substrato de granulação (IVESON et al., 2001).

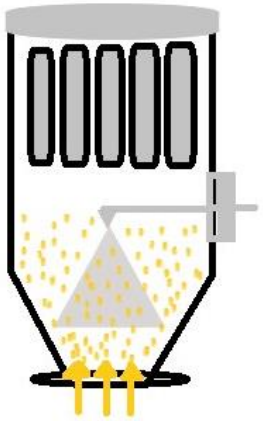

Figura 4 – Desenho esquemático da granulação em leito fluidizado.
Fonte: adaptado do manual do fabricante (Glatt Air Techniques Inc.).

Friedrich e colaboradores (2010) utilizaram a granulação por via úmida para a produção de grânulos contendo nanocápsulas de núcleo lipídico para aumentar a estabilidade físico-química das suspensões originais. No intuito de otimizar o processo de obtenção destes grânulos, a granulação em leito fluidizado é uma abordagem promissora. Diante disso, grânulos a partir de nanosuspensões de fármacos ou moléculas ativas foram obtidos por esta técnica de secagem. Basa e colaboradores (2008) desenvolveram grânulos para produção de comprimidos a partir de uma nanosuspensão de cetoconazol e lactose como substrato para granulação, no intuito de aumentar a velocidade de dissolução do fármaco, melhorando sua biodisponibilidade. Os autores demonstraram que a incorporação de grânulos

contendo a nanosuspensão aos comprimidos aumentou a taxa de dissolução do cetoconazol quando comparado à formulação comercial.

Além disso, Bose et al. (2012) avaliaram a viabilidade de uma nanosuspensão de vitamina E TPGS em uma forma sólida através do processo de granulação em leito fluidizado, utilizando manitol e lactose monohidratada *spray-dried* como substrato. Os autores observaram que os grânulos contendo manitol apresentaram uma melhor dissolução do fármaco e, consequentemente, nos parâmetros farmacocinéticos da nanosuspensão primária e na forma de grânulos em relação à suspensão grosseira. Recentemente, Andrade e colaboradores (2018) desenvolveram grânulos contendo nanocápsulas de núcleo lipídico brancas através da técnica de leito fluidizado. O revestimento catiônico melhorou a redispersão aquosa dos grânulos, facilitando a recuperação das propriedades nanométricas da suspensão original.

3.5.1 Mecanismos envolvidos em um processo de granulação úmida

Há diferentes mecanismos de formação do grânulo durante o processo de granulação úmida, sendo que os principais incluem (IVESON et al., 2001): molhagem e nucleação das partículas (1); consolidação e crescimento por colisões do material no granulador (2); atrito e ruptura (3). Estes mecanismos ocorrem simultaneamente em um processo de granulação em leito fluidizado (BURGGRAEVE et al., 2013). Na primeira etapa, o aglutinante entra em contato com o pó, sendo distribuído pelo leito para formar os núcleos dos grânulos. A zona de nucleação (*wetting zone*) é definida como a área na qual o líquido entra em contato com a superfície do pó, formando o núcleo inicial. Os fatores que influenciam esta fase são o ângulo de contato entre o líquido e o pó, a espalhabilidade do aglutinante e o tamanho das partículas primárias.

Na etapa de consolidação e crescimento, ocorrem colisões entre dois grânulos, entre grânulos e partículas primárias, levando à compactação ou coalescência e ao crescimento dos mesmos. Este crescimento pode iniciar logo que o líquido é adicionado ao leito do pó, bem como simultaneamente com o estágio de nucleação, e pode continuar após o término da adição do aglutinante. O tamanho do grânulo é determinado pelas condições de nucleação. Durante esta fase, os grânulos gradativamente se consolidam, aumentando a saturação de seus poros e alterando suas propriedades mecânicas.

Em seguida, os grânulos úmidos ou secos quebram devido ao impacto no granulador, ou durante o posterior manuseio do produto. Essa quebra dos grânulos pode influenciar na distribuição do tamanho de partícula final. Contudo, o atrito dos grânulos secos pode levar à geração de finos, o que pode ser inconveniente do ponto de vista tecnológico, considerando que o processo de granulação geralmente visa à remoção dos mesmos.

APRESENTAÇÃO

O primeiro capítulo da tese abordou o desenvolvimento de pós obtidos a partir de secagem por aspersão (*spray-drying*), contendo nanocápsulas de núcleo lipídico carregadas com fenitoína, revestidas ou não com quitosana. Posteriormente, estes pós foram reconstituídos em água no intuito de se avaliar a sua redispersibilidade, recuperação das propriedades nanométricas, estabilidade físico-química e gastrointestinal, liberação do fármaco *in vitro* e avaliação do efeito anticonvulsivante em modelo de crises induzidas por pilocarpina em camundongos. O fármaco de escolha foi a fenitoína devido à sua farmacocinética não-linear, a qual depende da saturação do metabolismo, e ao índice terapêutico estreito, o que requer frequente monitoramento plasmático. A fenitoína é um agente anticonvulsivante utilizado no tratamento da epilepsia. A proposta do estudo foi desenvolver um pó para reconstituição em água que recupere as características nanométricas da suspensão original, possua estabilidade em fluido gastrointestinal e efeito anticonvulsivante superior em relação ao fármaco não encapsulado. Este artigo será submetido em fase de redação para posterior submissão a periódico científico de circulação internacional.

Redispersible spray-dried phenytoin-loaded nanocapsules improve the *in vivo* phenytoin anticonvulsant effect and the survival time in mice

Edilene Gadelha de Oliveira[a], Aline Marquez Cardoso[a], Karina Paese[b], Karine Coradini[a], Clarissa Vasconcelos de Oliveira[d], Mauro Schneider Oliveira[d] Adriana Raffin Pohlmann[c], Sílvia Stanisçuaski Guterres[a], Ruy Carlos Ruver Beck[a*]

[a]Programa de Pós-Graduação em Ciências Farmacêuticas, Universidade Federal do Rio Grande do Sul, Porto Alegre, RS, Brazil

[b]Departamento de Produção e Controle de Medicamentos, Universidade Federal do Rio Grande do Sul, Porto Alegre, RS, Brazil

[c]Departamento de Química Orgânica, Instituto de Química, Universidade Federal do Rio Grande do Sul, Porto Alegre, RS, Brazil

[d]Programa de Pós-Graduação em Farmacologia, Universidade Federal de Santa Maria, Santa Maria, RS, Brazil

*Author to whom correspondence should be addressed: Prof R.C.R. Beck; Departamento de Produção e Controle de Medicamentos, Universidade Federal do Rio Grande do Sul, Avenida Ipiranga, 2952, 90610-000, Porto Alegre, RS, Brazil; Phone +55 51 33085215; E-mail: ruy.beck@ufrgs.br

ABSTRACT

This study evaluated the *in vivo* anticonvulsant effect of a spray-dried powder for reconstitution containing phenytoin-loaded lipid-core nanocapsules. The effect of chitosan coating on redispersibility, gastrointestinal stability, and drug release from nanoparticles was evaluated during the development of the powders. Maltodextrin was used as adjuvant in the spray-drying process. Chitosan coating played an important role in redispersibility. Moreover, the highest concentration of solids in the feed increased particle size (> 100 µm). However, after aqueous redispersion, volume-based particle size was reduced to about 1 µm. The release of nanoparticles from the surface of the spherical microagglomerates (roundness index = 0.75) was confirmed by SEM analysis. Powders reconstituted in water partially recovered the nanometric properties of the original suspensions and were stable for 24 h. Phenytoin-loaded chitosan-coated nanocapsules and their redispersible powders have good gastrointestinal stability, and are able to control drug release in simulated gastric and intestinal fluids. Besides that, the reconstitution powder containing chitosan-coated nanocapsules exhibited improved anticonvulsant activity against seizures induced by pilocarpine in mice, compared to the non-encapsulated drug, representing an important approach in anticonvulsant treatments of children and adults.

Keywords: anticonvulsant, chitosan, nanocapsules, phenytoin, powder, spray-drying.

1. Introduction

Polymeric nanoparticles have been studied as an alternative to conventional antiepileptic treatment (Fang et al., 2016; Leyva-Gómez et al., 2014). Antiepileptic drugs often fail to completely control seizures and, therefore, to prevent undesired side effects. Phenytoin (PHT) is a blockade of voltage-dependent sodium channels used in the treatment of epilepsy. Besides severe adverse effects that include cardiac arrhythmias, hypotension and neurological side effects (Batchelor et al., 2015), the narrow therapeutic index of PHT demands plasma monitoring in treatments based on this drug (Deleu et al., 2005), making it an interesting candidate for nanoencapsulation. Despite that, no effective and safe therapy that (i) controls PHT release, (ii) crosses the blood brain barrier (BBB) (Wang et al., 2016) and (iii) mitigates *in vivo* effects of the drug has been developed.

Lipid-core nanocapsules (LNC) are core-shell nanocarriers comprising a lipid core composed of sorbitan monostearate and medium chain triglycerides (MCT). This lipid core is coated with a poly(ε-caprolactone) polymeric membrane, whose particles are stabilized by polysorbate 80 micelles on their surface (Venturini et al., 2011). Lipid-core nanocapsules stabilized with polysorbate 80-lecithin and coated with chitosan on the surface of LNC have been also proposed, showing good *in vitro* hemocompatibility (Bender et al., 2012), and improved antimicrobial activity of drugs (Cé et al., 2016). Moreover, different administration routes have been proposed to improve brain delivery of drugs by nanocarriers in the treatment or prevention of central nervous system (CNS) diseases (Rodrigues et al., 2016; Zanotto-Filho et al., 2013).

However, LNC are produced as aqueous dispersions and may have limited physicochemical stability during storage, leading to polymer hydrolysis, particle aggregation, and microbiological growth in some cases (Guterres et al., 2009). Spray-drying has been reported to increase the stability of those polymeric nanocarriers, converting them in powders (Beck et al., 2008; Hoffmeister et al., 2012; Ribeiro et al., 2016). On the other hand, due to difficulty to swallow tablets or capsules, oral liquid formulations are usually considered more acceptable by elderly patients and pediatric patients alike, compared with solid dosage forms. As an alternative, liquid preparations are prepared by reconstitution from stable solid oral dosage forms (powders and granules), with improved dose flexibility and homogeneity, easy administration, and better palatability (EMA, 2013).

Although spray-drying has been reported as an alternative to produce dried nanocapsules, the efficiency of process depends on a suitable amount of a drying adjuvant added to the original formulation (Müller et al., 2000; Tewa-Tagne et al., 2006). The choice of the drying adjuvant is crucial to ensure redispersibility of dried products, to prevent phase separation (Tewa-Tagne et al., 2007), and to reach the suitable level of safety needed for adult and pediatric formulations (EMA, 2013). As a product of enzymatic degradation of starch, maltodextrin is a polysaccharide characterized by dextrose equivalent (DE) lower than 20, which defines its rheological and functional properties (Pycia et al., 2016). It is a water soluble excipient approved by the FDA for oral formulations, and has surfactant properties (Hoffmeister et al., 2012; Ourique et al., 2014; Paese et al., 2017; Pycia et al., 2016; Tewa-Tagne et al., 2007), making it suitable for the preparation of spray-dried nanocapsules to facilitate aqueous redispersion (Hoffmeister et al., 2012; Tewa-Tagne et al., 2007).

Nanoparticles have been studied concerning different administration routes, like parenteral (Leyva-Gómez et al., 2014; Paese et al., 2017), oral (Beck et al., 2008; Rodrigues et al., 2016), pulmonary (Ourique et al., 2014), and topical (Hoffmeister et al., 2012; Marchiori et al., 2012). In the oral route, the gastrointestinal tract is an important barrier to drug loaded-polymeric nanoparticles, which may influence the pharmacological effect of drugs due to degradation induced by pH variation and agglomeration resulting from the presence of enzymes or bile salts (Tobío et al., 2000). In addition, the lipase activity of pancreatin in the intestinal fluid could facilitate the digestion of lipid formulations. The shell structure of nanocarriers has an important role in lipid degradation. For instance, an added coating could protect the lipid substrate from the action of lipase (Klinkesorn and McClements, 2009; Roger et al., 2009). Therefore, the gastrointestinal stability of lipid nanocarriers like polymeric nanoparticles (Tobío et al., 2000), emulsions (Mun et al., 2006), lipid nanocapsules (Roger et al., 2009), nanoemulsions (Li et al., 2016), and polymeric nanocapsules (Niu et al., 2017) has been investigated. However, there is a lack of information about the gastrointestinal stability of LNC and the behavior of their respective redispersible powders in biological fluids.

In this scenario, this study described the development and production of spray-dried LNC as a powder for reconstitution and oral administration, assessing their *in vivo* anticonvulsant activity in mice. The analyses were designed to understand the role of chitosan coating in the aqueous redispersion behavior of the spray-dried powders as

well as the effect of the spray-drying process on their gastrointestinal stability and drug release profile. To the best of our knowledge, no previous report has been published on the evaluation of *in vivo* efficacy of drug-loaded nanocapsules after their aqueous reconstitution from spray-dried powders.

2. Materials and methods

2.1 Materials

Poly(ε-caprolactone) (PCL) (molecular weight, MW = 80,000 g mol^{-1}), low MW chitosan (MW = 50,000-190,000 g mol^{-1}; 75-85% deacetylation), sorbitan monostearate, maltodextrin (dextrose equivalent 16.5 – 19.5), pepsin from porcine stomach mucosa, pancreatin from porcine pancreas, and pilocarpine were supplied by Sigma Aldrich (São Paulo, Brazil). Grape seed oil was obtained from Delaware (Porto Alegre, Brazil) and polysorbate 80 was acquired from Vetec (Rio de Janeiro, Brazil). Soybean lecithin (Lipoid® S75) was obtained from Lipoid (Ludwigshafen, Germany). Phenytoin was kindly donated by Cristália (São Paulo, Brazil). All other reagents and solvents were analytical or pharmaceutical grade.

2.2 Preparation and characterization of the lipid-core nanocapsules

Lipid-core nanocapsules (LNC) were prepared by interfacial deposition of preformed polymer as previously described (Jäger et al., 2009; Venturini et al., 2011). Two different formulations were prepared: uncoated and chitosan-coated LNC. To obtain the uncoated LNC, poly(ε-caprolactone) (0.25 g), grape seed oil (412.5 µL), sorbitan monostearate (0.0962 g) and phenytoin (0.00625 g) were dissolved in acetone (60 mL) at 40°C. Concomitantly, soybean lecithin (0.15 g) was solubilized in ethanol (7.5 mL) and added to the organic phase. This mixture was injected into an aqueous solution (135 mL) containing polysorbate 80 (0.1925 g) under moderate stirring at 40°C for 10 min. After, acetone was eliminated, and the suspension was concentrated under reduced pressure. The final volume was adjusted to 25 mL (0.25 mg.mL^{-1} of phenytoin) in a volumetric flask. This formulation was named phenytoin-loaded LNC (PHT-LNC). The cationic coating of the nanocapsules was prepared using a chitosan solution (0.6% w/v) in 1% acetic acid, adapted from Bender et al. (2012). This coating was optimized based on the narrower particle size distribution when different concentrations of chitosan (0.3, 0.6, and 0.9% w/v) were tested. Then, the chitosan solution was slowly

poured into these nanocapsules at the concentration of 0.225 mg.mL^{-1}, and the mixture was kept under magnetic stirring overnight at room temperature (25°C). This formulation was named as phenytoin-loaded chitosan-coated LNC (PHT-CS-LNC).

Particle size distribution was determined by laser diffraction (Mastersizer 2000, Malvern Instruments, UK). Samples were directly placed in the wet sample dispersion unit. Particle size (mean diameter) and zeta potential were evaluated using a Zetasizer Nano ZS (Malvern Instruments, UK) diluting the samples in ultrapure water (1:500) and in 10 mM NaCl aqueous solution, respectively. The dilution media was filtered (0.45 µm) before analyses. pH values were measured using a calibrated potentiometer (Digimed, DM-22, Campo Grande, Brazil). Each analysis was performed in triplicate batches.

Morphological analyses were evaluated by transmission electron microscopy (MET JEM 1200 Exll, *Centro de Microscopia Eletrônica*, UFRGS, Brazil) operating at 80 kV. Suspensions were diluted in ultrapure water (1:10) and deposited on specimen grid (Formvar-carbon support film) using uranyl acetate solution (2% w/v) as negatively stained standard.

Phenytoin was assayed by high-performance liquid chromatography (HPLC). The apparatus consisted of a Shimadzu LC-20A system (LC-20AT pump), a CBM-20A system controller, a SPD-M20A photodiode-array detector, a SIL-20A auto-sampler (Tokyo, Japan), and a Phenomenex C18 column (150 mm x 4.6 mm, 5 µm, Gemini). The mobile phase was composed of acetonitrile:water (50:50 v/v). The injected volume was 20 µL at an isocratic flow rate of 1.0 mL.min^{-1} and the detection wavelength was 210 nm. The retention time of phenytoin was 5.6 min. The HPLC method afforded good linearity in the range of 1.00 to 20.00 µg.mL^{-1} ($r = 0.9999$), suitable inter and intra-day variability (< 2.0%), good accuracy between 96.10% and 98.16%, and a limit of quantification of 0.80 µg.mL^{-1}. Total drug was determined after dissolving nanocapsules in acetonitrile (1:25 v/v) followed by ultrasonic homogenization for 30 min, centrifugation at 1597 x g for 20 min, and filtration (0.45 µm) before HPLC analysis.

The encapsulation efficiency assay (EE%) was performed according to an ultrafiltration-centrifugation technique (Ultrafree-MC 10,000 MW, Millipore, Billerica, USA) at 1820 x g for 10 min. The difference between total concentration of drug in the formulation and its concentration in the aqueous phase of the suspension was calculated. To determine the presence of drug nanocrystals, the suspensions were

separated in two flasks, stocked at room temperature, and protected from light according to a protocol previously proposed (Pohlmann et al., 2008). The first flask was kept immobilized throughout the experiment (21 days), while the second flask was shaken before HPLC analysis. Each analysis was performed in triplicate.

2.3 Preparation and characterization of spray-dried lipid-core nanocapsules

Spray-dried phenytoin-loaded LNC as well as spray-dried unloaded nanocapsules were prepared (Spray Dryer B-290, Büchi, Switzerland) using maltodextrin as drying adjuvant at different concentrations (5% and 1.75%). The effect of cationic coating was evaluated comparing the behavior of the powders containing uncoated LNC (SD-PHT-LNC) and chitosan-coated LNC (SD-PHT-CS-LNC). Maltodextrin was added to the nanocapsules suspension 20 min before the spray-drying process and kept under magnetic stirring. The drying process was carried out according to the following parameters (Marchiori et al., 2012): inlet temperature (120 ± 1°C); outlet temperature (68 ± 5°C); sample feed rate (4.5 $mL.min^{-1}$); drying gas flow (approx. 35 $m^3.h^{-1}$); spray gas flow of 600 $NL.h^{-1}$. The equipment has two-fluid nozzle (cap diameter: 0.7 mm), operating at a co-current flow. All formulations were prepared in triplicate, kept in desiccator, and protected from light at room temperature (25°C) before analyses.

Process yield (%) was calculated by the ratio between the weight of the produced powder and all solid components of the formulation. Loss on drying was assessed by heating an amount of sample until 105°C for 1 min by means of an infrared moisture analyzer (Ohaus MB45, Parsippany, USA). The particle size distribution and geometric mean diameter were measured by laser diffraction (Mastersizer 2000, Malvern, UK) using the dry powder dispersion unit (Scirocco 2000, Malvern, UK). The redispersion profile of the spray-dried powders was evaluated in water (Hydro 2000 sample dispersion unit, Malvern, UK) as a function of time. Aliquots were analyzed every 1 min for 5 min.

Morphological analyses of powders before and after aqueous redispersion were carried out by scanning electron microscopy (SEM; JEOL, JSM 6060, Tokyo, Japan) at the *Centro de Microscopia Eletrônica*-UFRGS (Porto Alegre, Brazil) at 10 kV. The powders were deposited on silicon wafer and covered with water for 5 min, which was removed using absorbent paper. The samples were also spread on a double-adhesive tape adhered to aluminum stubs and sputter-coated with gold. Roundness index or circularity of particles before and after aqueous redispersion were obtained from SEM

images using the software ImageJ (version 1.50i, National Institutes of Health, USA). The parameters were calculated using the formula: circularity = 4π (area/perimeter^2). In accordance with the roundness scale (Powers, 1953), the index ranges from 0 to 1, with 1 indicating a perfect circle.

2.3.1 Reconstitution of spray-dried powders and redispersibility analysis

The spray-dried powders were reconstituted in ultrapure water and vortexed for 2 min to a final concentration of 0.25 mg.mL^{-1} of phenytoin. The pH values of the redispersion were determined using a potentiometer (Digimed, DM-22, Campo Grande, Brazil). In order to assay the drug content of spray-dried powders before and after reconstitution, these samples were dispersed in the mobile phase, sonicated for 60 min, centrifuged at 1597 x g for 20 min, and filtered (0.45 µm) before HPLC analysis. Particle size was measured by laser diffraction (Mastersizer 2000, Malvern, UK). The aqueous redispersibility of the spray-dried powders was evaluated by gravimetry and laser diffraction analyses were performed to obtain the particle size distribution of the reconstituted powders. This procedure was adapted from Kho et al. (2010). In the first step of the experiment, the reconstituted powder was gently shaken for 30 min. Then, it was centrifuged at 7,280 *x* g for 10 min after which the supernatant containing nanocapsules and excipient was withdrawn, and replaced with same volume of ultrapure water, and centrifuged again. These steps were repeated five times to ensure that all the redispersed nanocapsules and dissolved excipient were removed. In each step, an aliquot of the supernatant was withdrawn for laser diffraction analysis. After the last centrifugation, the supernatant was discarded, and the sediment was dried at 40°C until constant weight for 72 h. The percentage of redispersibility of the spray-dried powders was calculated from the initial mass of powder and the mass of the final sediment of the non-redispersed aggregates. Furthermore, aliquots of reconstituted powder were filtered (0.45 µm) and analyzed by photon correlation spectroscopy (Zetasizer Nano ZS, Malvern, UK) for obtaining the mean particle size and zeta potential (electrophoretic mobility). The measurements were conducted in triplicate.

2.4 Stability study in simulated gastrointestinal fluids

Gastrointestinal stability of phenytoin-loaded LNC and the redispersible powders were evaluated in simulated gastric fluid (SGF) containing 0.32% (w/v) pepsin (pH 1.2) and simulated intestinal fluid (SIF) composed of 1% (w/v) pancreatin (pH 7.5) according to

Roger et al. (2009). Samples were diluted in different media (1:9), kept on magnetic stirring, and incubated at 37°C. Freshly prepared formulations and samples collected 0, 1, 2, and 3 h after were analyzed by laser diffraction (Mastersizer 2000, Malvern, UK). SIF was centrifuged at 1597 x g for 20 min to eliminate aggregates of pancreatin that could interfere in the laser diffraction analysis.

2.5 In vitro drug release

In vitro drug release studies of phenytoin-loaded LNC and the redispersible powders were carried out using a dialysis membrane method at 37°C. Four milliliters of each sample were placed in a dialysis bag (10 kDa molecular weight cutoff, Sigma Aldrich, Brazil), which was put in a beaker containing 80 mL of release medium (SGF and SIF) under moderate stirring, ensuring sink conditions. At predetermined time intervals, aliquots (2 mL) were collected and replaced with fresh medium. The samples were filtered (0.45 µm) and analyzed by HPLC according to the method previously described. SIF samples were centrifuged at 7280 x g for 10 min before filtering due to the risk of membrane saturation by aggregates of pancreatin. A solution of phenytoin (0.25 $mg.mL^{-1}$) was prepared in ethanol: water (60:40 v/v) to evaluate the diffusion profile of the non-encapsulated drug in both media. Mathematical modeling (MicroMath Scientist® 2.0) was performed to evaluate the profiles of the drug release. The data were fitted to model-dependent biexponential (Eq. 1).

$$C = Ae^{-k1t} + Be^{-k2t} \quad (1)$$

Where C is the amount of drug released at time *t* (h), *A* (burst phase) and *B* (sustained phase) are the initial drug concentrations, and k_1 and k_2 (h^{-1}) are the kinetics constants.

2.6 In vivo experiments

2.6.1 Animals

In vivo studies were approved by the Ethics Committee for Animal Research of the Federal University of Santa Maria (protocol # 3273040416). They were carried out in accordance with National guidelines of the Council for Control of Animal Experiments (CONCEA) and U.S. Public Health Service's Policy on Humane Care and Use of Laboratory Animals (PHS Policy). Adult C57BL/6 mice (25-35 g, 30 – 90 days old) of

both genders were used in the experiments. Animals were kept at constant room temperature (24 ± 1°C), relative humidity (55%), under a 12:12 h light-dark cycle with free access to water and food until 4 h before the experiments because of the interaction of phenytoin with food, which could decrease its oral bioavailability.

2.6.2 Drug administration and behavioral evaluation of pilocarpine-induced seizures model

Mice were treated daily with water (control), non-encapsulated PHT suspension in water, redispersible powders containing phenytoin-loaded cationic nanocapsules (SD-PHT-CS-LNC), and powder containing unloaded cationic nanocapsules (SD-CS-LNC). The dose of all compounds used was 10 $mg.kg^{-1}.day^{-1}$ (n = 5) for 7 days. Powders were reconstituted in water at a concentration of 1 $mg.mL^{-1}$ and administered by gavage (p.o.). The weight of the animals was monitored daily. On the 7^{th} day of treatment, 60 min after the last oral administration, pilocarpine dissolved in 0.9% NaCl was injected (300 $mg.kg^{-1}$, i.p.) to induce seizures following standard procedures (Borges et al., 2003; Funck et al., 2014; Velíšek, 2005). The animals were observed for 60 min. Latency to limbic seizures, latency to generalized seizures, seizure severity, and survival were observed and recorded. Seizure severity was scored according to the modified Racine Scale (Racine, 1972): 0 = normal behavior; 1 = Facial movement, hyperactivity; 2 = head nodding, tremor; 3 = unilateral forelimb clonus; 4 = bilateral forelimb clonus and rearing; 5 = bilateral forelimb clonus with loss of posture; 6 = generalized tonic-clonic seizures, status epilepticus, or death. Stages 1-3 were recognized as limbic seizures and stages 4–6 as generalized seizures.

2.7 Statistical Analysis

Data were expressed as mean ± standard deviation (SD). Statistical analysis was carried out using a one-way analysis of variance (ANOVA), the Student's t test, and the Kruskal-Wallis test in GraphPad Prism 5 (GraphPad Software, San Diego, USA). Differences were considered significant when $p < 0.05$.

3. Results and Discussion

3.1 Lipid-core nanocapsules

Uncoated and chitosan-coated LNC were prepared as aqueous dispersions as previously described. Our goal was to evaluate the role and influence of the chitosan-coating layer of the nanocapsules on the properties of spray-dried powders and their redispersion behavior. Both formulations (coated and uncoated) were homogeneous, white-bluish, and opalescent in aspect, regardless of whether they were coated with chitosan. Formulations analyzed by TEM showed spherical shaped and nanometric particles for phenytoin-loaded LNC (PHT-LNC) (Fig. 1A) and phenytoin-loaded chitosan-coated LNC (PHT-CS-LNC) (Fig. 1B). Besides that, radar charts were built from their particle size distribution data by laser diffraction analysis [Fig.1 (A1) and (B1)]. Radar charts have been used to assess a variety of healthcare or pharmaceutical data (Perez-Vega et al., 2014). Consequently, specific fingerprints of the LNC [Fig.1 (A1) and (B1)] were similar as a consequence of their monomodal particle size distribution with low polydispersity, as previously established for LNC (Bianchin et al., 2015). Also, d0.9(v) was smaller than 350 nm and d0.5(n) was smaller than 70 nm for both formulations, confirming their nanometric properties. D[4,3] values were 177 ± 13 nm and 193 ± 16 nm for uncoated- and chitosan-coated nanocapsules, respectively. These results indicated that chitosan coating did not cause any agglomeration or precipitation of particles.

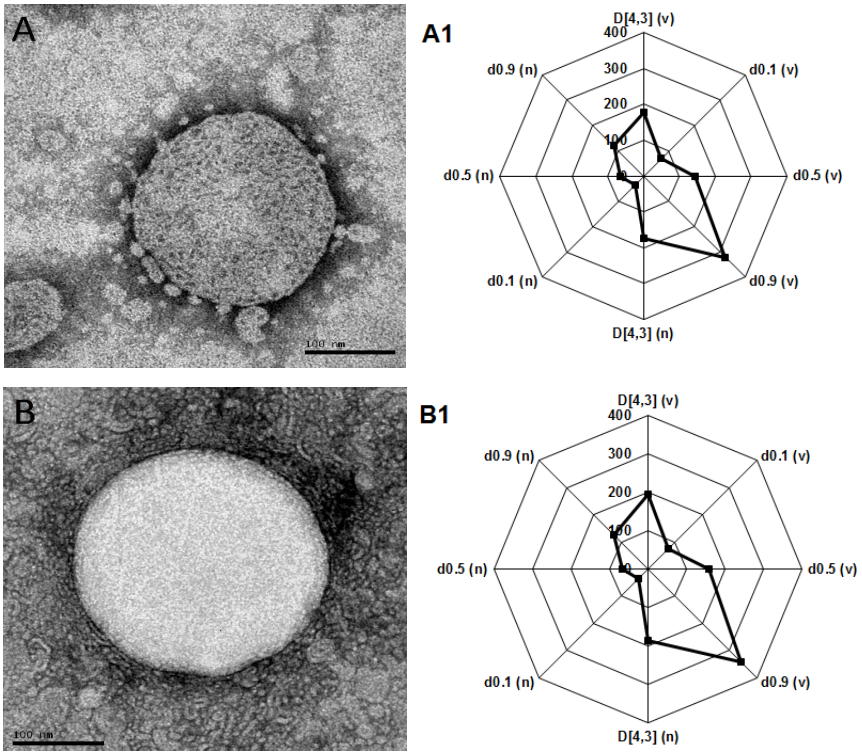

Fig. 1. Photomicrographs obtained by TEM (bar = 100 nm). **A, B**: phenytoin-loaded uncoated nanocapsules (PHT-LNC), phenytoin-loaded chitosan-coated nanocapsules (PHT-CS-LNC and their fingerprints obtained by laser diffraction (**A1, B1**), respectively. D[4,3] (v): mean diameter based on volume-weighted; d0.1 (v): diameter based on volume at percentile 10 of the cumulative size distribution; d0.5 (v): diameter based on volume at percentile 50 of the cumulative size distribution; d0.9 (v): diameter based on volume at percentile 90 of the cumulative size distribution; D[4,3] (n): mean diameter based on number-weighted; d0.1 (n): diameter based on number at percentile 10 of the cumulative size distribution; d0.5 (n): diameter based on number at percentile 50 of the cumulative size distribution; d0.9 (n): diameter based on number at percentile 90 of the cumulative size distribution.

Table 1 shows the detailed physicochemical characteristics of unloaded (LNC and CS-LNC) and phenytoin-loaded LNC (PHT-LNC and PHT-CS-LNC). They presented hydrodynamic mean diameter between 158 and 168 nm and narrow particle size distribution (PDI < 0.2). No change was observed in particle size after cationic coating ($p > 0.05$), in agreement with the laser diffraction analysis.

Table 1. Physicochemical characteristics of unloaded and PHT-loaded lipid-core nanocapsules (n = 3, mean ± SD).

Formulation	Mean diameter (nm)	PDI[a]	ZP[b] (mV)	Drug content ($mg.mL^{-1}$)	EE[c] (%)
LNC	165 ± 4	0.14 ± 0.02	-19.1 ± 0.6	-	-
CS-LNC	167 ± 4	0.16 ± 0.02	+17.0 ± 0.6	-	-
PHT-LNC	158 ± 8	0.17 ± 0.03	-10.4 ± 0.8	0.25 ± 0.01	94 ± 1.34
PHT-CS-LNC	168 ± 4	0.15 ± 0.01	+16.2 ± 1.5	0.23 ± 0.01	93 ± 1.02

[a] Polydispersity index; [b] Zeta potential; [c] Encapsulation Efficiency

Unloaded and PHT-loaded uncoated lipid-core nanocapsules (LNC and PHT-LNC) had negative zeta potential due to the presence of polysorbate 80 molecules on the surface of lecithin phospholipids and its free fatty acids, which act as stabilizers at the particle/water interface (Bender et al., 2012). On the other hand, unloaded and PHT-loaded chitosan-coated LNC (CS-LNC and PHT-CS-LNC) had a positive zeta potential, which confirm the chitosan coating on the particle surface due to the interaction of its ionized amino groups with the negative phosphate group of lecithin (Bender et al., 2012; Cé et al., 2016).

The drug contents of 0.25 $mg.mL^{-1}$ (PHT-LNC) and 0.23 $mg.mL^{-1}$ (PHT-CS-LNC) were close to the concentration established, showing that the preparation technique did not interfere in drug stability. Furthermore, both nanocapsule suspensions presented encapsulation efficiency of about 95%, demonstrating that chitosan coating had no influence on this parameter. Besides that, there was a 12-fold increase in the aqueous solubility of drug (0.02 $mg.mL^{-1}$) (Alvarez-Núñez and Yalkowsky, 1999) after its nanoencapsulation, confirming this strategy as a tool for improving the aqueous solubility of poorly soluble drugs (Coradini et al., 2014).

LNC and PHT-LNC showed pH values of 6.41 ± 0.12 and 6.57 ± 0.36, respectively. A decrease of pH values to 4.00 ± 0.08 for both chitosan-coated LNC was observed, compared to the uncoated formulations due to 1% acetic acid aqueous solution used to dissolve chitosan. In addition, the presence of drug nanocrystals in the formulations as a function of time was assessed to prevent precipitation as nanocrystals during the preparation due to its low water solubility. The initial concentration of phenytoin in nanocapsules (PHT-LNC and PHT-CS-LNC) remained constant for 21 days in both

shaken and immobilized samples ($p > 0.05$), regardless of the presence of chitosan coating (**Supplementary material Fig.S1 and Fig. S2**).

3.2 Spray-dried nanocapsules: redispersion studies and physicochemical characteristics

LNC were spray-dried using maltodextrin as a drying adjuvant to increase physicochemical stability and to develop a powder for reconstitution and oral administration. Although lactose has been widely used in the production of spray-dried powders (Lebhardt et al., 2011; Ourique et al., 2014; Ribeiro et al., 2016), maltodextrin was chosen due to its water solubility, which facilitates powder redispersion in water (Bourezg et al., 2012; Rowe et al., 2012). Moreover, lactose is not suitable for pediatric use due to lactose intolerance, which has been associated with symptoms such as diarrhea, dehydration, and metabolic acidosis in infants (EMA, 2006; Rowe et al., 2012). Therefore, replacing it with other adjuvants is highly desirable.

On the other hand, one of the main problems in the preparation of spray-dried powders is the non-homogeneous character of the mixture of the two or more components in the sample to be fed during the spray-drying process. If the sample is homogeneous, weak or moderate interactions are expected, favoring stable dispersions without sedimentation or flocculation in the feeding sample during the drying process, leading to the production of well-separated particles that should have a good redispersion in water (Tewa-Tagne et al., 2006). Consequently, homogeneous spray-dried powders would be produced if spontaneous phase separation of dispersion is avoided during sample feeding. In this regard, the good compatibility of maltodextrin and polymeric nanocapsules, with no visible phase separation, was previously reported (Tewa-Tagne et al., 2007), supporting our choice in selecting this adjuvant.

Figure 2 shows the redispersion behavior of the spray-dried powders containing uncoated LNC (SD-PHT-LNC) and chitosan-coated LNC (SD-PHT-CS-LNC) using maltodextrin at 5% (w/v), demonstrating the effect of chitosan coating on redispersion behavior of spray-dried powders. A better redispersion behavior was clearly observed for the spray-dried powders containing chitosan-coated LNC (D[4,3]: 690 nm; SPAN: 2.921) compared with those prepared from the uncoated nanocapsules (D[4,3]: 25 µm; SPAN: 3.369). This result suggests that the surface charge and/or coating layer of LNC has an important role on redispersion behavior. To maintain the stability of colloidal systems after the drying process, steric and electrostatic repulsions need to overcome

the van der Waals attractive forces between particles close to each other (Hong et al., 2014). In this study, chitosan-coated nanocapsules were stabilized by electrostatic forces due to positive charge between particles as well as by steric hindrance (Bender et al., 2012), while uncoated nanocapsules were stabilized by the predominance of steric repulsions generated by the polysorbate 80-lecithin layer on the particle/water interface (Ezhilarasi et al., 2016). Observing the behavior of the reconstituted powders in water allowed suggesting that saccharide-saccharide interactions (maltodextrin-chitosan) are stronger than saccharide-lipid ones (maltodextrin-lecithin), probably due to the hydrogen bonds formed by the saccharide-saccharide interaction, since these are more stable than the dipole-dipole interactions in the saccharide-lipid interaction. However, hydrogen bonds are quickly undone in water as they reach the water-particle interface, establishing hydrogen bonds between the water and the saccharide molecules, undoing saccharide-saccharide interactions, promoting the redispersibility of powders. This mechanism does not occur when there are dipole-dipole interactions, leading to non-redispersible powders. Moreover, coating with surfactant of low glass transition temperature (e.g. lecithin) may induce high cohesive forces between the particles (Vehring, 2008).

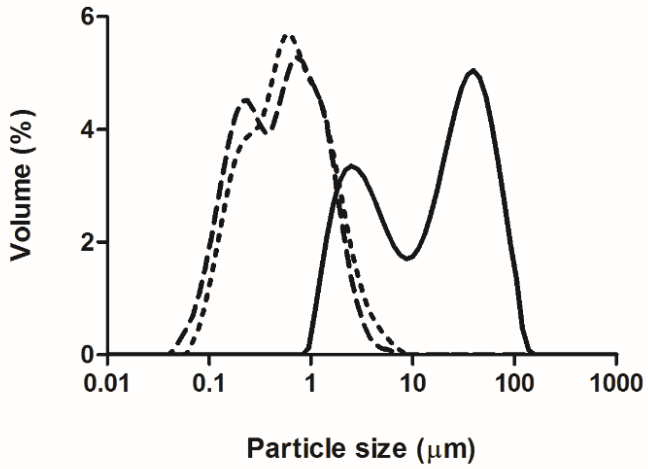

Fig.2. Particle size distribution of powders containing phenytoin-loaded uncoated nanocapsules using 5% maltodextrin (solid line) and phenytoin-loaded chitosan-coated nanocapsules with 5% (dashed line) and 1.75% (w/v) maltodextrin (dotted line).

However, in order to improve drug content (mg of phenytoin/g of powder) in the final spray-dried powder, a minimal amount of adjuvant would be desirable. Therefore, a

lower concentration of maltodextrin (1.75% w/v) was tested. At this concentration, the yield of the process to dry the uncoated nanocapsules was 0% due to the high powder adherence to the equipment walls. In this case, the nanocarriers can affect the stickiness of the powder, enhancing it adhesive and plastic features during the drying process (Drapala et al., 2017). When the concentration of the adjuvant is not high enough to protect nanocapsules from the thermal stress, high adherence on the cyclone wall is expected (Müller et al., 2000; Tewa-Tagne et al., 2006). Moreover, high MW molecules (e.g. chitosan) usually are more stable to stress, compared to those of low MW such as lecithin (Drapala et al., 2017). Consequently, the powders prepared from chitosan-coated nanocapsules using maltodextrin at 1.75 % (w/v) had a yield of 65% and a good redispersion profile, as observed in Fig. 2, with a D[4,3] value of 951 nm and SPAN of 3.008. The redispersibility behavior of the spray-dried powders were highly dependent on the surface composition of the LNC.

Based on the data discussed above, the powder containing chitosan-coated nanocapsules was selected for further studies. Firstly, their detailed physicochemical characteristics (SD-CS-LNC and SD-PHT-CS-LNC) were evaluated, as shown in Table 2. The process of spray-drying had high yields (70-74%), with low residual water content in powders (< 2%), confirming the suitability of the operational conditions. Phenytoin content (3.97 ± 0.18 $mg.g^{-1}$) was similar to the expected drug loading (3.96 $mg.g^{-1}$). The powder containing phenytoin presented larger geometric mean diameter (114 ± 6 µm) than that without it (69 ± 9 µm) due to the higher particle density, which increases agglomeration under the action of the air flow used in the laser diffraction technique.

Table 2. Physicochemical characteristics of spray-dried powders containing chitosan-coated nanocapsules with and without drug (n = 3; mean ± SD).

Formulation	Yield (%)	Residual water (%)	Drug content ($mg.g^{-1}$)	Particle size distribution*	
				D[4,3] µm	SPAN
SD-CS-LNC	74 ± 2	1.63 ± 1.55	-	69 ± 9	3.03 ± 0.59
SD-PHT-CS-LNC	70 ± 1	1.79 ± 0.29	3.97 ± 0.18	114 ± 6	3.38 ± 0.13

*dry dispersion in the laser diffraction analysis.

In order to further evaluate their water redispersion behavior, these powders were dispersed directly into the wet sample dispersion unit and characterized by laser

diffraction. Data were obtained as volume (Fig. 3A) and number-weighted particle size distribution (Fig. 3B). Initially, particle size distribution of the dried particles was evaluated for 5 min, every 1 min. However, practically no change in the volume-based redispersion profile was observed after 2 min, and all subsequent analyses were stopped after this time had elapsed. The volume-based redispersion profiles indicated that both formulations had large particle size distribution (Fig. 3A). The values of D[4,3] were 1038 ± 166 nm and 1041 ± 79 nm for powders prepared with unloaded and phenytoin-loaded chitosan-coated LNC, respectively, demonstrating that the particle size of the original dry powders decreased (Table 2).

In order to evaluate the influence of the micrometric population in the particle size distribution, both profiles were analyzed as number-weighted particle size distribution (Fig. 3B). The mean surface area moment values (D[3,2]) were 425 nm ± 160 nm (SD-CS-LNC) and 436 nm ± 19 nm (SD-PHT-CS-LNC), revealing the existence of a negligible micrometric population. Furthermore, the particle size distribution obtained by laser diffraction as well as the drug content of powders were assessed for 90 days. These values remained similar to their initial ones (data not shown), which indicates a good physicochemical physical stability of the spray-dried powders during storage at room temperature (25°C) and protected from light.

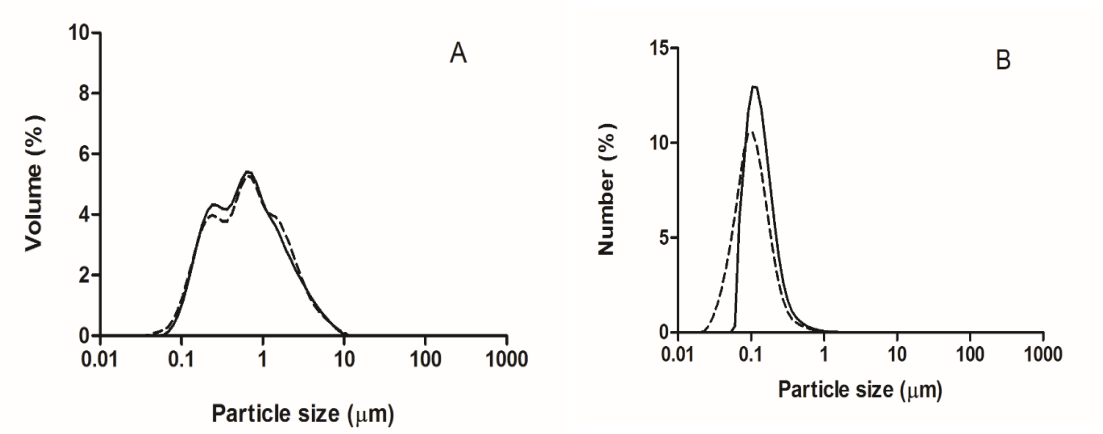

Fig.3. Volume (A) and number-weighted (B) particle size distribution of powder containing unloaded chitosan-coated lipid-core nanocapsules (dashed line) and phenytoin-loaded chitosan-coated lipid-core nanocapsules (solid line) 2 min into analysis.

Morphology of the spray-dried powders as well as the recovery of nanocapsules after their redispersion in water were analyzed by SEM (Fig. 4). Dried particles of different

sizes arranged as large ‘bunch of grape’-type microagglomerates (Drapala et al., 2017) (Fig. 4A), corroborating the broad particle size distribution of the powders as measured by laser diffraction. However, after redispersion in water (Fig. 4B), these microagglomerates disintegrated and the nanocapsules adsorbed on their surface were released into the aqueous medium. This structure, composed of a coating layer of the nanocapsules, can be explained considering the droplet-to-particle conversion during the drying process. When two components of different sizes are mixed (maltodextrin and nanocapsules, in the present study), single particles are formed. In the beginning of the drying process, these components are distributed homogeneously in the droplet. But during solvent evaporation, the meniscus region induces capillary flow, causing the self-assembly of the nanoparticles into the close-packed structure. Due to the buoyancy force, small particles can move easier and faster to the meniscus region than large particles. For this reason, this process is responsible for the coating of larger components by the smaller particles (Nandiyanto and Okuyama, 2011). Moreover, to confirm that the nanostructures observed by SEM after powder redispersion were due to the presence of nanocapsules, an additional powder was prepared from a dispersion of phenytoin, polysorbate 80, sorbitan monostearate, and lecithin without any polymer and oil. Larger microagglomerates were obtained (Fig. 4C). After contact with water, these particles were solubilized, and all components were leached on absorbent paper (Fig. 4D), demonstrating the absence of hydrophobic nanostructures. As the last step in this morphological evaluation, the sphericity of the microagglomerates calculated from the SEM images showed roundness indices of about 0.75 before and after redispersion. According to the Powers’ Scale of Roundness (Powers, 1953), indices between 0.70 and 1.00 indicate almost spherical particles. This index represents the spherical shape of the dried microagglomerates, the nanocapsules released after redispersion in water, as well as the remaining nanocapsules/maltodextrin agglomerates.

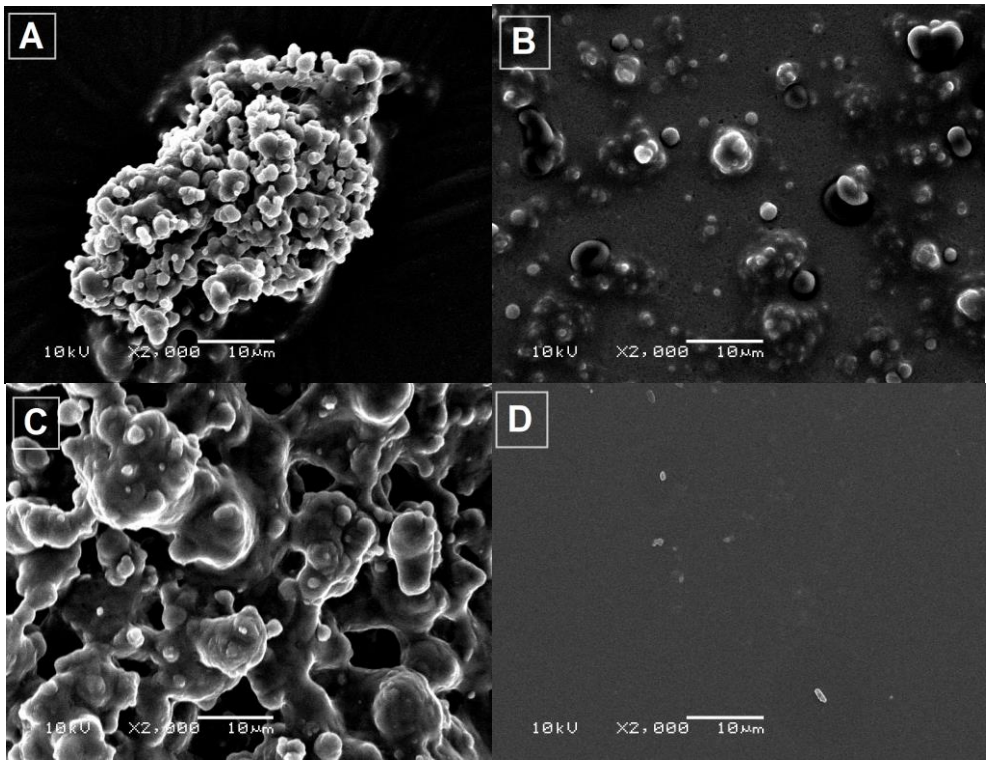

Fig.4. SEM images of (A) spray-dried phenytoin-loaded chitosan-coated LNC, (B) nanocapsules in the aqueous redispersion of the spray-dried powder, (C) spray-dried dispersion of phenytoin (without polymer or oil) and (D) aqueous redispersion of the spray-dried dispersion of phenytoin (2,000x).

3.2.1 Reconstitution of spray-dried powders in water: physicochemical properties

For better understanding of the results this issue, reconstitution was defined as the returning to the liquid state by adding water while redispersion or redispersibility is the capacity of recovering the nanometric profile of the original suspension. In extemporaneous preparations, like powders for reconstitution, it is necessary to ensure good redispersibility and stability. Therefore, particle size, zeta potential, pH, and drug content were evaluated after reconstitution of the spray-dried powders containing phenytoin-loaded chitosan-coated nanocapsules. Nanoparticles have a natural tendency to aggregate due to attractive interaction of their surfaces when they are close to each other, reducing the number of primary nanoparticles in dry systems. During a reconstitution procedure, sometimes it is necessary to use external energy such as ultrasound, stirring, and mechanical vibration to overcome attractive forces between nanoparticles (Hakim et al., 2005). In this study, only the mechanical agitation was evaluated to reconstitute the powders, since it is an easy, fast, and viable method for further *in vivo* experiments and therapeutic applications. Hence, the powders were

reconstituted in ultrapure water to recover drug content of the original nanocapsules (0.25 $mg.mL^{-1}$) in a vortex-shaker for 2 min. The reconstituted powder had a redispersibility index of 72 ± 4%, compared to the original nanocapsules suspension, and their profiles of particle size distribution do not alter during the redispersibility analyses (Fig. 5) and they were similar to the redispersion profile of the spray-dried powder previously discussed in Fig. 3. These results confirm that the powders are redispersible, partly recovering their original nanometric population. Spray-dried powders that have redispersibility > 90% are considered fully redispersible, while powders with < 50% is considered non-redispersible (Hong et al., 2014).

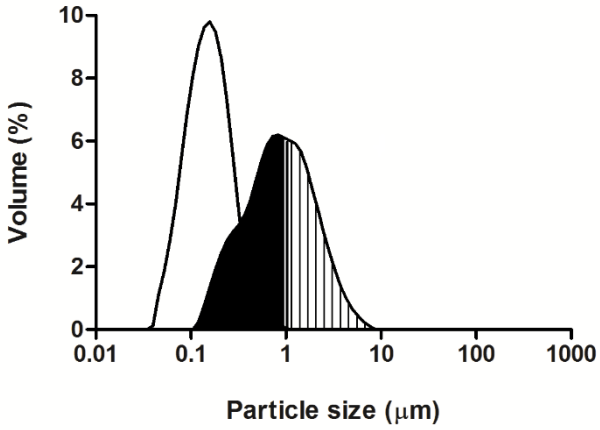

Fig.5. Particle size distribution of chitosan-coated lipid-core nanocapsules (white area) and their reconstituted powder (black/hatched area). The black area represents the percent volume of particles with exclusively nanometric profile in the redispersion.

Furthermore, Table 3 shows the detailed physicochemical properties of the reconstituted powder just after the reconstitution and after 24 h of storage at room temperature (25°C) and protected from light. They had a mean diameter of 345 ± 1 nm and polydispersity index of 0.36 ± 0.04, confirming the nanometric population. These results were in the range between the mean diameter of the original nanocapsules and the dry powder, indicating the presence of released LNC and LNC/maltodextrin agglomerates, as demonstrated by SEM analyses. The agglomeration of the particles may have been caused by the high initial feed concentration (Nandiyanto and Okuyama, 2011; Tewa-Tagne et al., 2006; Vehring, 2008), as previously discussed.
The positive surface charge of chitosan-coated nanocapsules (+20 ± 4 mV) remained unchanged, showing that no destabilization of the chitosan coating on nanocapsules

occurred during the spray-drying process and after the powder reconstitution in water, as redispersed particles. The drug content was similar to the expected concentration (0.25 mg.mL^{-1}), suggesting no precipitation of phenytoin in the reconstitution medium. Also, the pH value was higher compared to the original suspension, which can be explained by the presence of hydroxyl moieties of the maltodextrin in the aqueous medium. As phenytoin is a weakly acidic drug and has a low water solubility, higher pH values could be considered even more adequate to avoid its precipitation in an acidic environment (Alvarez-Núñez and Yalkowsky, 1999).

In addition, it is important to ensure the minimum physical stability of the reconstituted powder. Consequently, it was kept immobilized after reconstitution in water for 24 h, when it was mildly stirred before analysis. No significant difference was found in the mean particle diameter (359 ± 64 nm), polydispersity index (0.42 ± 0.15), drug content (0.257 ± 0.01 mg.mL^{-1}), and zeta potential (+18 ± 2 mV) in comparison to initial parameters (p > 0.05). A slight increase in pH (6.00 ± 0.04) was observed. These results showed that the reconstituted powder was stable for 24 h, considering that the chemical nature of the powder's surface after reconstitution in water is a critical factor for its physicochemical characteristics.

Table 3. Physicochemical characterization of reconstituted powder containing phenytoin-loaded chitosan-coated nanocapsules just after reconstitution (0 h) and after 24 h of storage (n = 3, mean ± SD).

Physicochemical parameters	0 h	24 h
Mean diameter (nm)	345 ± 1	359 ± 64
Polydispersity index	0.36 ± 0.04	0.42 ± 0.10
Zeta potential (mV)	+20 ± 4	+18 ± 2
pH	5.86 ± 0.03[a]	6.00 ± 0.04[a]
Drug content (mg.mL^{-1})	0.255 ± 0.01	0.257 ± 0.01

[a] statistical difference between 0 and 24 h (p < 0.05; test t-Student).

3.3 Stability study in simulated gastrointestinal fluid

Besides the good physicochemical stability, nanotechnological formulations for oral administration should have appropriate gastrointestinal stability. In the literature, simulated gastrointestinal media have been used to evaluate the stability of nanocarriers (Li et al., 2016; Roger et al., 2009) due to the variation in pH and the presence of enzymes that could trigger the aggregation of nanoparticles in these fluids (Roger et al., 2009). In addition, the lipolysis (digestion) of oral lipid-based formulations in the gastrointestinal tract can affect the solubility, dissolution, and bioavailability of poorly water-soluble drugs. Many of the compounds present in the lipid nanocarriers, such as phospholipids and polysorbates, have ester groups that may be hydrolyzed by lipases, like the pancreatic lipase, the main enzyme involved in this process and present in the intestinal medium (Carrière, 2016). Therefore, particle size should be monitored in these fluids, evaluating the degradation of lipid nanosystems (Carrière, 2016; Klinkesorn and McClements, 2009).

The stability of phenytoin-loaded chitosan-coated LNC suspension and its respective reconstituted powder in SGF and SIF were evaluated. In order to rule out the interference of SGF and SIF in the laser diffraction analyses, these media were also analyzed without any formulation. No influence of SGF was observed due to the complete solubilization of all components of this medium, which did not reach the obscuration index (2%) during the laser diffraction analysis. However, the particles dispersed in SIF were 567 nm in mean size. Table 4 shows particle size distribution data of chitosan-coated nanocapsules and their redispersible powders in simulated fluids at times 0, 1, 2, and 3 h, which corresponds to gastric emptying time. The nanocapsules had D[4,3] (v) values ranging from 195 to 231 nm, which were close to their original size (193 ± 16 nm). No agglomeration of particles was observed after precipitation in SIF and SGF. Although no changes were observed in particle size distribution of chitosan-coated nanocapsules in both media, a shift was observed in d0.9(v) values in SIF compared to SGF, corresponding to an increase from 354 ± 3 nm to 405 ± 10 nm ($p < 0.05$). This may be explained based on the influence of the nanometric size of the particles of the intestinal medium (around 500 nm), as discussed above, in particle size distribution profile of chitosan-coated nanocapsules. This hypothesis can be supported also by increase in size observed in the d0.9(v) values for uncoated nanocapsules, from 333 ± 04 nm (SGF) to 347 ± 10 nm (SIF) ($p < 0.05$) (**Supplementary Material Fig.S3)**.

Regarding the reconstituted powders, no statistical difference was found in the particle size distribution over time in SGF and SIF ($p > 0.05$). The D[4,3] (v) of redispersible powders containing chitosan-coated nanocapsules varied from 1082 to 1112 nm, which are similar to their initial mean particle size (1109 ± 7 nm). The d0.9(v) values of 2232 ± 16 nm in SGF were also similar to those observed in SIF (2210 ± 36 nm) ($p > 0.05$). The constituent particles of SIF influenced redispersed powder data less intensely, compared with those nanocapsules data, probably due to its higher mean particle size. Despite this, chitosan-coated nanocapsules as well as their redispersible powders showed good gastrointestinal stability.

Table 4. Particle size distribution data for phenytoin-loaded chitosan-coated lipid-core nanocapsules and their redispersible powder in simulated gastric fluid (SGF) and simulated intestinal fluid (SIF) at 0, 1, 2, and 3 h.

Diameter	Nanocapsule suspension (mean, µm ± SD)		Redispersible powder (mean, µm ± SD)	
	SGF*	SIF*	SGF*	SIF*
D[4,3] (v)	196 ± 1	225 ± 6	1104 ± 6	1097 ± 15
d0.1 (v)	76 ± 0	81 ± 2	290 ± 3	288 ± 9
d0.5 (v)	162 ± 1	177 ± 4	842 ± 6	837 ± 9
d0.9 (v)	354 ± 3	405 ± 10	2232 ± 16	2210 ± 36

* time interval of 0 – 3 h in each fluid.

3.4 In vitro drug release

Although the spray-dried powder containing chitosan-coated LNC showed suitable physicochemical and aqueous redispersion properties as a powder for reconstitution, it is important to evaluate the impact of the spray-drying process on their drug release profiles in the gastrointestinal environment. Therefore, *in vitro* drug release profiles of phenytoin-loaded chitosan-coated LNC (PHT-CS-LNC) and their redispersible powder (SD-PHT-CS-LNC) in SGF and SIF were studied.

Figure 6 shows the drug diffusion profile from a phenytoin solution (Fig. 6A), and the release profiles from chitosan-coated LNC and their redispersible powder (Fig. 6B). Non-encapsulated phenytoin reached 85% and 100% of diffusion across the dialysis bag after 8 h in SGF and SIF, respectively. The lower non-encapsulated drug diffusion in the gastric fluid may be explained by its lower solubility in this fluid (acidic pH).

Chitosan-coated LNC controlled drug release in both media in comparison with non-encapsulated phenytoin, releasing 74% and 72% of drug in SGF and SIF, respectively, after 48 h. These data showed that the influence of pH-dependent solubility on the drug release profiles could be overcome by drug nanoencapsulation. Similar data were observed for the reconstituted powder, which released 69% and 64% of the drug in SGF and SIF, respectively, at the same time interval. Besides that, no significant difference was observed between the drug release profiles from nanocapsules and redispersible powder through analysis of their kinetic constants in gastric (K_2= 0.014 h^{-1} ± 0.001 and K_2 = 0.013 h^{-1} ± 0.001) and intestinal medium (K_2= 0.013 h^{-1} ± 0.003 and K_2 = 0.011 h^{-1} ± 0.000), respectively (p> 0.05), showing that the spray-dried process controlled phenytoin release by the LNC.

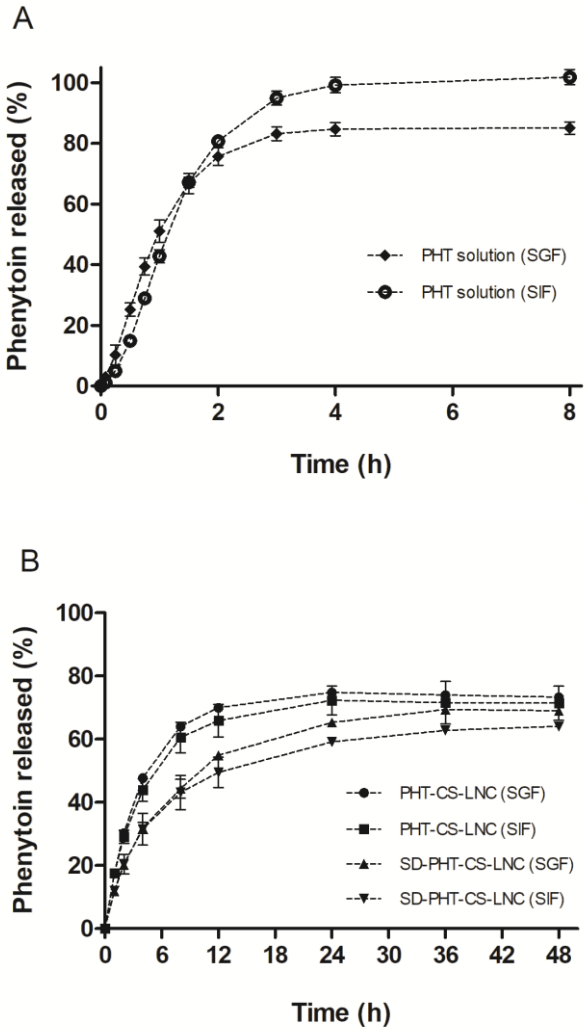

Fig.6. Drug released (%) from phenytoin solution (A), phenytoin-loaded chitosan-coated lipid-core nanocapsules, and their redispersible powder (B) in simulated gastrointestinal fluids.

3.5 In vivo experiments

A pilocarpine-induced seizures model, which was first described by Turski et al. (1983), was used to evaluate the *in vivo* anticonvulsant efficacy of the reconstituted spray-dried powder containing nanoencapsulated phenytoin. This model was chosen due to similarity to human temporal lobe epilepsy (TLE) (Borges et al., 2003). In the present study, an acute model was used to chemically induce seizures by pilocarpine, which are characterized by a typical pattern of action in mice, such as salivation, for example, which is caused by activation of muscarinic receptors. Moreover, pilocarpine activates phospholipase C, producing diacylglycerol and inositol triphosphate, and promoting alterations in calcium and potassium gradients, hence promoting excitability (Tawfik, 2011).

Animals were divided in four different groups, which were given (1) water (control), (2) non-encapsulated phenytoin (PHT) suspension in water, (3) powder containing unloaded cationic nanocapsules (placebo powder, SD-CS-LNC), and (4) redispersible powders containing phenytoin-loaded cationic nanocapsules (SD-PHT-CS-LNC). Phenytoin 10 $mg.kg^{-1}day^{-1}$ was administrated by gavage to groups 2 and 3, whereas a similar volume of water or resuspended placebo powder were administered for groups 1 and 4. The treatment lasted 7 days in order to reach steady-state plasma concentration due to nonlinear pharmacokinetic of phenytoin. Body weight of all animals in all groups was essentially constant throughout the treatment time ($p > 0.05$) (**Supplementary material Fig.S4**).

In pilot experiments, the dose of 2.5 $mg.kg^{-1}day^{-1}$ in the group treated with phenytoin-loaded nanocapsules did not show significant anticonvulsant effect in mice. Before that, the powder containing phenytoin-loaded nanocapsules was resuspended in water (1 $mg.mL^{-1}$), according to the procedure described in section *2.3.1* in order to reach the maximum drug concentration to keep suitable physicochemical characteristics, such as nanometric particle size (840 ± 36 nm), pH (5.86 ± 0.09), and drug content (1.04 ± 0.03 $mg.mL^{-1}$), and to ensure appropriate oral gavage in mice. The powder containing unloaded nanocapsules also presented similar properties (819 ± 65 nm; pH 5.97 ± 0.03) with the dilution with the same volume of water.

Figure 7 shows the effect of all groups on pilocarpine-induced seizures. No differences were observed between treatments in the latency to myoclonic seizures ($p > 0.05$; Fig. 7A). On the other hand, an increase in latency to generalized seizures in the group treated with redispersible powder containing phenytoin-loaded cationic LNC was observed (Fig. 7B), showing a superior anticonvulsant effect compared with non-encapsulated phenytoin suspension ($p < 0.05$) and the placebo powder ($p < 0.05$). Besides that, this redispersible powder reduced the severity of seizures (Fig. 7C) and significantly increased the survival time of animals ($p < 0.05$; Fig. 7D). These data confirm the results published by Wang et al. (2016) using the pilocarpine model, who developed phenytoin-loaded non-electroresponsive and electroresponsive nanoparticles. The authors observed that the group treated with the phenytoin solution did not show significant increase in latency to generalized seizures, compared to a control, while mice treated with electroresponsive nanoparticles showed higher latency to generalized seizures as opposed to rats treated with non-electroresponsive nanoparticles.

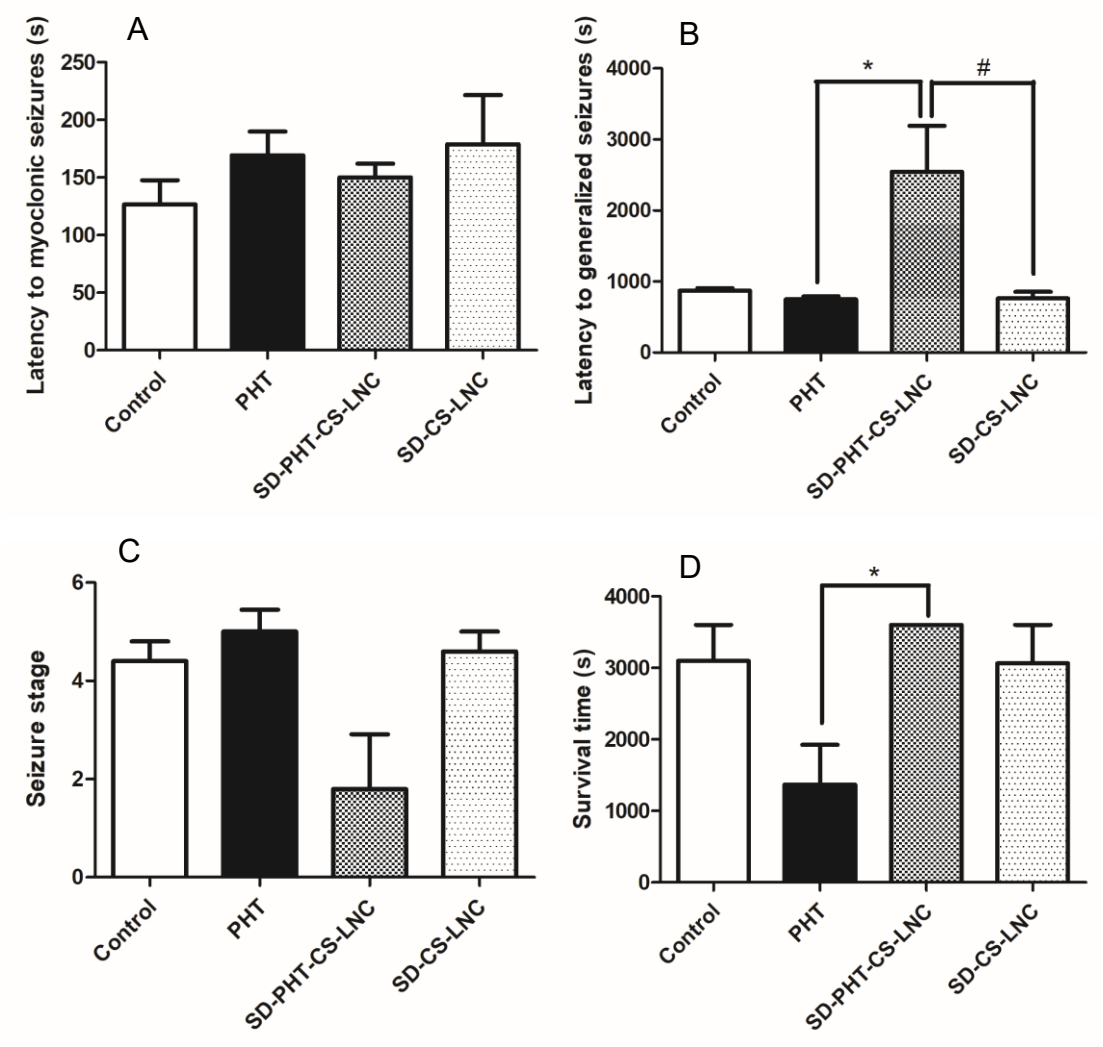

Fig.7. The *in vivo* anticonvulsant effect of the powder containing nanocapsules in the pilocarpine-induced seizures model. The effect of non-encapsulated phenytoin (PHT), redispersible powder containing phenytoin-loaded cationic nanocapsules (SD-PHT-CS-LNC) and redispersible powder containing unloaded cationic nanocapsules (SD-CS-LNC) on the latency to myoclonic seizures (A), on the latency to generalized seizures (B), seizure stage (C), and survival time of the animals (D). * $p < 0.05$, compared to non-encapsulated phenytoin; $^{\#}p < 0.05$, compared to SD-CS-LNC.

The group of mice treated with redispersible powder containing phenytoin-loaded nanocapsules showed better response to generalized seizures compared to those treated with the non-encapsulated drug, which exhibited no effect after treatment with this dose. In addition, the placebo redispersible powder did not have significant

anticonvulsant effect. This finding suggests that the nanoencapsulated drug is responsible for its activity. Ying et al. (2014) demonstrated that unloaded electroresponsive hydrogel nanoparticles modified with angiopep-2 did not present antiepileptic effect on amygdala-kindled seizures, compared to saline. However, they were able to transport phenytoin into the brain, improving its anticonvulsant effect. Based on the results described above, chitosan-coated LNC could be used as drug shuttles through the blood brain barrier (BBB), as proposed by Rodrigues et al. (2016) for polysorbate-80-coated LNC. However, the mechanism underlying drug targeting from cationic nanocapsules into the brain after oral administration has not been clarified, requiring further research based on the novel *in vivo* data obtained in this study.

4. Conclusion

Spray-dried powders containing chitosan-coated lipid-core nanocapsules were formulated using maltodextrin (1.75% w/v) as a powder for reconstitution. Chitosan coating was fundamental to improve the aqueous redispersibility of powders. Moreover, the spray-dried powders had good physicochemical and gastrointestinal stability after reconstitution in water, partially recovering the nanometric properties of the original suspensions. The spray-drying process did not alter the drug release behavior in gastric and intestinal fluids. Moreover, redispersible powders containing phenytoin-loaded nanocapsules improved pilocarpine-induced seizures, being a promising approach for adult and pediatric anticonvulsant treatment.

Declaration of interest

The authors report no conflicts of interest.

Acknowledgements

E.G.O. thanks CAPES for the PhD fellowship. The authors thank the financial support of CNPq/Brazil, CAPES/Brazil and FAPERGS. We also would like to thank Cristália Produtos Químicos e Farmacêuticos Ltda for gently providing the phenytoin raw material.

References

ALVAREZ-NÚÑEZ, F. A.; YALKOWSKY, S. H. Buffer capacity and precipitation control of pH solubilized phenytoin formulations. **International Journal of Pharmaceutics**, v. 185, n. 1, p. 45–49, 1999.

BATCHELOR, H.; APPLETON, R.; HAWCUTT, D. B. Comparing paediatric intravenous phenytoin doses using physiologically based pharmacokinetic (PBPK) modelling software. **Seizure**, v. 33, p. 8–12, 2015.

BECK, R. C. R. et al. Surface morphology of spray-dried nanoparticle-coated microparticles designed as an oral drug delivery system. **Brazilian Journal of Chemical Engineering**, v. 25, n. 2, p. 389–398, 2008.

BENDER, E. A. et al. Hemocompatibility of poly(ε-caprolactone) lipid-core nanocapsules stabilized with polysorbate 80-lecithin and uncoated or coated with chitosan. **International Journal of Pharmaceutics**, v. 426, n. 1–2, p. 271–279, 2012.

BIANCHIN, M. D. et al. Radar charts based on particle sizing as an approach to establish the fingerprints of polymeric nanoparticles in aqueous formulations. **Journal of Drug Delivery Science and Technology**, v. 30, p. 180–189, 2015.

BORGES, K. et al. Neuronal and glial pathological changes during epileptogenesis in the mouse pilocarpine model. **Experimental Neurology**, v. 182, p. 21–34, 2003.

BOUREZG, Z. et al. Colloids and Surfaces A: Physicochemical and Engineering Aspects Redispersible lipid nanoparticles of Spironolactone obtained by three drying methods. **Colloids and Surfaces A: Physicochemical and Engineering Aspects**, v. 413, p. 191–199, 2012.

CARRIÈRE, F. Impact of gastrointestinal lipolysis on oral lipid-based formulations and bioavailability of lipophilic drugs. **Biochimie**, v. 125, p. 297–305, 2016.

CÉ, R. et al. Colloids and Surfaces A: Physicochemical and Engineering Aspects Chitosan-coated dapsone-loaded lipid-core nanocapsules: Growth inhibition of clinical isolates, multidrug-resistant Staphylococcus aureus and Aspergillus ssp. **Colloids and Surfaces A: Physicochemical and Engineering Aspects**, v. 511, p. 153–161, 2016.

CORADINI, K. et al. Co-encapsulation of resveratrol and curcumin in lipid-core nanocapsules improves their in vitro antioxidant effects. **European Journal of Pharmaceutics and Biopharmaceutics**, v. 88, p. 178–185, 2014.

DELEU, D.; AARONS, L.; AHMED, I. A. Estimation of population pharmacokinetic parameters of free-phenytoin in adult epileptic patients. **Archives of Medical Research**, v. 36, n. 1, p. 49–53, 2005.

DRAPALA, K. P. et al. Influence of emulsifier type on the spray-drying properties of model infant formula emulsions. **Food Hydrocolloids**, v. 69, p. 56–66, 2017.

EMA. **Committee for Medicinal Products for Human Use (CHMP) Reflection Paper: Formulations of Choice for the Paediatric Population**. Disponível em: <http://www.ema.europa.eu/docs/en_GB/document_library/Scientific_guideline/2009/09/WC500003782.pdf>. Acesso em: 3 fev. 2017.

EMA. **Committee for Medicinal Products for Human Use (CHMP) Guideline on pharmaceutical development of medicines for paediatric use**. Disponível em: <http://www.ema.europa.eu/docs/en_GB/document_library/Scientific_guideline/2013/07/WC500147002.pdf>. Acesso em: 3 fev. 2017.

EZHILARASI, P. N.; MUTHUKUMAR, S. P.; ANANDHARAMAKRISHNAN, C. Solid lipid nanoparticle enhances bioavailability of hydroxycitric acid compared to a microparticle delivery system. **RSC Advances**, v. 6, n. 59, p. 53784–53793, 2016.

FANG, Z. et al. Pluronic P85-coated poly(butylcyanoacrylate) nanoparticles overcome phenytoin resistance in P-glycoprotein overexpressing rats with lithium-pilocarpine-induced chronic temporal lobe epilepsy. **Biomaterials**, v. 97, p. 110–121, 2016.

FUNCK, V. R. et al. Long-term decrease in Na+,K+-ATPase activity after pilocarpine-induced status epilepticus is associated with nitration of its alpha subunit. **Epilepsy Research**, v. 108, n. 10, p. 1705–1710, 2014.

GUTERRES, S. S.; BECK, R. C. R.; POHLMANN, A R. Spray-drying technique to prepare innovative nanoparticulated formulations for drug administration: a brief overview. **Brazilian Journal of Physics**, v. 39, n. 1A, p. 205–209, 2009.

HAKIM, L. F. et al. Aggregation behavior of nanoparticles in fluidized beds. **Powder Technology**, v. 160, n. 3, p. 149–160, 2005.

HOFFMEISTER, C. R. et al. Hydrogels containing redispersible spray-dried melatonin-loaded nanocapsules: a formulation for transdermal-controlled delivery. **Nanoscale Research Letters**, v. 7, n. 1, p. 251, 2012.

HONG, L. et al. Colloids and Surfaces A: Physicochemical and Engineering Aspects Impact of particle size and surface charge density on redispersibility of spray-dried powders. **Colloids and Surfaces A: Physicochemical and Engineering Aspects**, v. 459, p. 274–281, 2014.

JÄGER, E. et al. Sustained release from lipid-core nanocapsules by varying the core viscosity and the particle surface area. **Journal of Biomedical Nanotechnology**, v. 5, n. 1, p. 130–140, 2009.

KLINKESORN, U.; MCCLEMENTS, D. J. Influence of chitosan on stability and lipase digestibility of lecithin-stabilized tuna oil-in-water emulsions. **Food Chemistry**, v. 114, n. 4, p. 1308–1315, 2009.

LEBHARDT, T. et al. European Journal of Pharmaceutics and Biopharmaceutics Surfactant-free redispersible nanoparticles in fast-dissolving composite microcarriers for dry-powder inhalation. **European Journal of Pharmaceutics and Biopharmaceutics**, v. 78, n. 1, p. 90–96, 2011.

LEYVA-GÓMEZ, G. et al. Nanoparticle formulation improves the anticonvulsant effect of clonazepam on the pentylenetetrazole-induced seizures: Behavior and electroencephalogram. **Journal of Pharmaceutical Sciences**, v. 103, n. 8, p. 2509–2519, 2014.

LI, J. et al. Effects of chitosan coating on curcumin loaded nano-emulsion: Study on stability and in vitro digestibility. **Food Hydrocolloids**, v. 60, p. 138–147, 2016.

MARCHIORI, M. C. L. et al. Spray-dried powders containing tretinoin-loaded engineered lipid-core nanocapsules: development and photostability study. **Journal of Nanoscience and Nanotechnology**, v. 12, n. 3, p. 2059–2067, 2012.

MÜLLER, C. R. et al. Preparation and Characterization of Spray-Dried Polymeric Nanocapsules. **Drug Development and Industrial Pharmacy**, v. 26, n. 3, p. 343–347, 2000.

MUN, S. et al. Influence of interfacial composition on in vitro digestibility of emulsified lipids: Potential mechanism for chitosan's ability to inhibit fat digestion. **Food Biophysics**, v. 1, n. 1, p. 21–29, 2006.

NANDIYANTO, A. B. D.; OKUYAMA, K. Progress in developing spray-drying methods for the production of controlled morphology particles: From the nanometer to submicrometer size ranges. **Advanced Powder Technology**, v. 22, n. 1, p. 1–19, 2011.

NIU, Z. et al. Rational design of polyarginine nanocapsules intended to help peptides overcoming intestinal barriers. **Journal of Controlled Release**, v. 263, p. 4–17, 2017.

OURIQUE, A. F. et al. Redispersible liposomal-N-acetylcysteine powder for pulmonary administration: Development, in vitro characterization and antioxidant activity. **European Journal of Pharmaceutical Sciences**, v. 65, p. 174–182, 2014.

PAESE, K. et al. Production of Isotonic, Sterile, and Kinetically Stable Lipid-Core Nanocapsules for Injectable Administration. **AAPS PharmSciTech**, v. 18, n. 1, p. 212–223, 2017.

PEREZ-VEGA, S.; HIDALGA, A. N.; SHARRATT, P. N. Journal of Loss Prevention in the Process Industries Tools for an enhanced solvent properties screening in the early stages of pharmaceutical process development. **Journal of Loss Prevention in the Process Industries**, v. 29, p. 300–312, 2014.

POHLMANN, A. R. et al. Determining the simultaneous presence of drug nanocrystals in drug-loaded polymeric nanocapsule aqueous suspensions: A relation between light scattering and drug content. **International Journal of Pharmaceutics**, v. 359, n. 1–2, p. 288–293, 2008.

POWERS, M. C. A new roundness scale for sedimentary particles. **Journal of Sedimentary Petrology**, v. 23, n. 2, p. 117–119, 1953.

PYCIA, K. et al. Maltodextrins from chemically modified starches. Selected physicochemical properties. **Carbohydrate Polymers**, v. 146, p. 301–309, 2016.

RACINE, R. J. Modification of seizure activity by electrical stimulation: II. Motor seizure. **Electroencephalography and Clinical Neurophysiology**, v. 32, p. 281–294, 1972.

RIBEIRO, R. F. et al. Spray-dried powders improve the controlled release of antifungal tioconazole-loaded polymeric nanocapsules compared to with lyophilized products. **Materials Science and Engineering C**, v. 59, p. 875–884, 2016.

RODRIGUES, S. F. et al. Lipid-core nanocapsules act as a drug shuttle through the blood brain barrier and reduce glioblastoma after intravenous or oral administration. **Journal of Biomedical Nanotechnology**, v. 12, n. 5, p. 986–1000, 2016.

ROGER, E.; LAGARCE, F.; BENOIT, J. P. The gastrointestinal stability of lipid nanocapsules. **International Journal of Pharmaceutics**, v. 379, n. 2, p. 260–265, 2009.

ROWE, R. C.; SHESKEY, P. J.; OWEN, S. C. **Handbook of Pharmaceutical Excipients**. 5. ed. London: Pharmaceutical Press, 2012.

TAWFIK, M. K. Coenzyme Q10 enhances the anticonvulsant effect of phenytoin in pilocarpine-induced seizures in rats and ameliorates phenytoin-induced cognitive impairment and oxidative stress. **Epilepsy and Behavior**, v. 22, n. 4, p. 671–677, 2011.

TEWA-TAGNE, P.; BRIANÇON, S.; FESSI, H. Spray-dried microparticles containing polymeric nanocapsules: Formulation aspects, liquid phase interactions and particles characteristics. **International Journal of Pharmaceutics**, v. 325, n. 1–2, p. 63–74, 2006.

TEWA-TAGNE, P.; BRIANÇON, S.; FESSI, H. Preparation of redispersible dry nanocapsules by means of spray-drying: Development and characterisation. **European Journal of Pharmaceutical Sciences**, v. 30, n. 2, p. 124–135, 2007.

TOBÍO, M. et al. The role of PEG on the stability in digestive fluids and in vivo fate of PEG-PLA nanoparticles following oral administration. **Colloids and Surfaces B: Biointerfaces**, v. 18, p. 315–323, 2000.

TURSKI, W. A. et al. Limbic seizures produced by pilocarpine in rats: behavioural, electroencephalographic and neuropathological study. **Behavioural Brain Research**, v. 9, p. 315–335, 1983.

VEHRING, R. Pharmaceutical particle engineering via spray drying. **Pharmaceutical Research**, v. 25, n. 5, p. 999–1022, 2008.

VELÍŠEK, L. Models of Chemically-Induced Acute Seizures. In: PITKÄNEN, A., SCHWARTZKROIN, P., MOSHÉ, S. (Ed.). . **Models of Seizures and Epilepsy**. New York: Elsevier Academic Press, 2005. p. 127–151.

VENTURINI, C. G. et al. Formulation of lipid core nanocapsules. **Colloids and Surfaces A: Physicochemical and Engineering Aspects**, v. 375, n. 1–3, p. 200–208, 2011.

WANG, Y. et al. Electroresponsive Nanoparticles Improve Antiseizure Effect of Phenytoin in Generalized Tonic-Clonic Seizures. **Neurotherapeutics**, v. 13, n. 3, p. 603–613, 2016.

YING, X. et al. Angiopep-conjugated electro-responsive hydrogel nanoparticles: Therapeutic potential for epilepsy. **Angewandte Chemie - International Edition**, v. 53, n. 46, p. 12436–12440, 2014.

ZANOTTO-FILHO, A. et al. Curcumin-loaded lipid-core nanocapsules as a strategy to improve pharmacological efficacy of curcumin in glioma treatment. **European Journal of Pharmaceutics and Biopharmaceutics**, v. 83, n. 2, p. 156–167, 2013.

Supplementary material

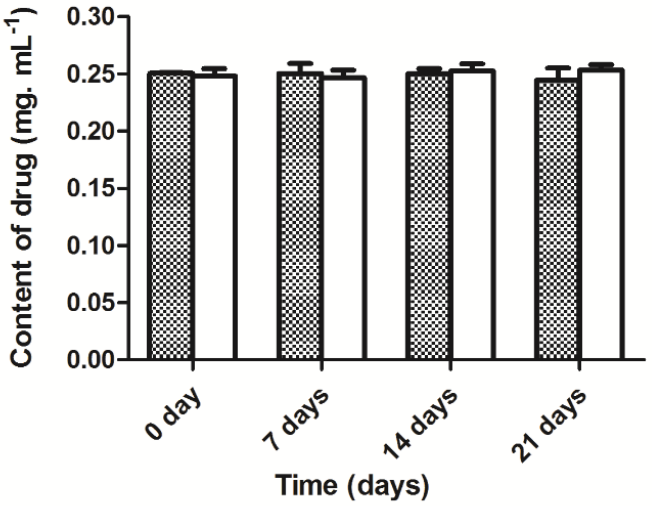

Fig. S1. Drug content (mg.mL^{-1}) as a function of the storage time (days) for shaken (shaded bars) and immobilized (hollow bars) of a suspension of phenytoin-loaded uncoated lipid-core nanocapsules (PHT-LNC).

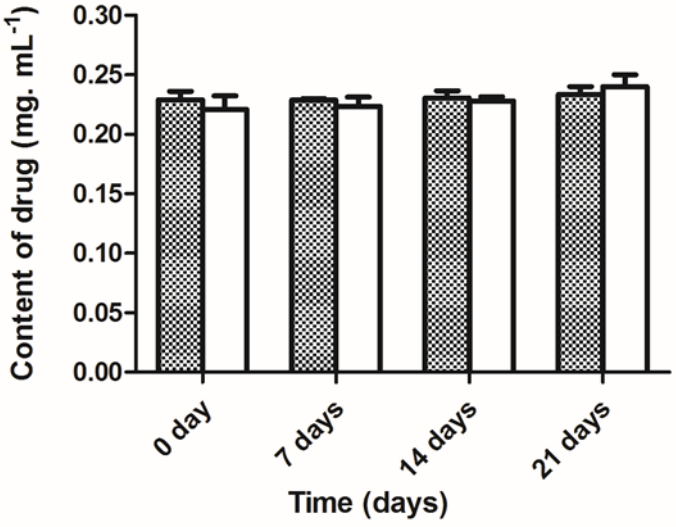

Fig. S2. Drug content (mg.mL^{-1}) as a function of the storage time (days) for shaken (shaded bars) and immobilized (hollow bars) of suspension of phenytoin-loaded chitosan-coated lipid-core nanocapsules (PHT-CS-LNC).

5 CAPÍTULO 2

APRESENTAÇÃO

O segundo capítulo da tese avaliou o uso de nanocápsulas de núcleo lipídico carregadas com fenitoína como uma abordagem inovadora para melhorar as características tecnológicas e a performance *in vivo* de grânulos obtidos por leito fluidizado. Essa técnica consiste de uma etapa única de granulação e secagem, em um mesmo equipamento, a qual tem sido empregada para a produção de grânulos com boas propriedades de fluxo, estabilidade e aumento da velocidade de dissolução do fármaco. Os grânulos foram produzidos a partir de um substrato, composto por maltodextrina e fenitoína, e uma suspensão de nanocápsulas de fenitoína e/ou água como aglutinante, obtendo-se grânulos contendo uma combinação de fenitoína encapsulada (10%) e não encapsulada (90%) ou somente o fármaco não encapsulado, respectivamente. Em seguida, os grânulos foram avaliados em relação às propriedades físico-químicas e de fluxo, à recuperação das características nanométricas após redispersão aquosa, à liberação do fármaco *in vitro* em fluido intestinal e ao efeito anticonvulsivante dos grânulos redispersos. Este artigo está em fase de redação para posterior submissão a periódico científico de circulação internacional.

Polymeric nanocapsules as an approach to improve the technological properties and *in vivo* performance of fluid bed granules containing phenytoin

Edilene Gadelha de Oliveira[a], Mauro Schneider Oliveira[c] Adriana Raffin Pohlmann[b], Sílvia Stanisçuaski Guterres[a], Ruy Carlos Ruver Beck[a*]

[a] Programa de Pós-Graduação em Ciências Farmacêuticas, Universidade Federal do Rio Grande do Sul, Porto Alegre, RS, Brazil

[b] Departamento de Química Orgânica, Instituto de Química, Universidade Federal do Rio Grande do Sul, Porto Alegre, RS, Brazil

[c] Programa de Pós-Graduação em Farmacologia, Universidade Federal de Santa Maria, Santa Maria, RS, Brazil

*Author to whom correspondence should be addressed: Prof R.C.R. Beck; Departamento de Produção e Controle de Medicamentos, Universidade Federal do Rio Grande do Sul, Avenida Ipiranga, 2952, 90610-000, Porto Alegre, RS, Brazil; Phone +55 51 33085215; E-mail: ruy.beck@ufrgs.br

ABSTRACT

Fluid bed is a drying technique used to produce pharmaceutical granules with good flowability properties, stability and enhanced drug dissolution. In this study, the use of phenytoin-loaded nanocapsules suspension as binder in the production of fluidized bed granules of phenytoin (PH) was evaluated on their flow, granulometric properties, *in vitro* drug release and anticonvulsant effect. Granules showed good yields (73-82%) and low moisture content (< 5%). An increase in the granule mean size (122 µm) was observed compared with maltodextrin primary particles (50 µm) due to the formation of solid bridges in the granules containing nanocapsules (FB-LNC_{PH}), whose increase was not observed for granules prepared with the non-encapsulated drug (FB-PH). Moreover, FB-LNC_{PH} granules presented a good flow, moderate cohesion and no caking. Their nanometric properties were recovered after reconstitution in water (3 $mg.mL^{-1}$ of phenytoin), releasing the nanocapsules from the granule surface, showing redispersibility around 90%. The drug release from redispersed granules was slower than from ethanolic solution in the intestinal fluid. The presence of nanocapsules and the particle size influenced on this process. The granules containing phenytoin-nanocapsules increased the latency to myoclonic and generalized seizures. Taking into account that 10% of the total drug is in the encapsulated form, redispersed granules had a promising anticonvulsant effect. Hence, the use of nanocapsules as binder was an innovative approach to produce fluidized bed granules of phenytoin with improved technological and biological properties.

Keywords: fluidized bed granules, nanocapsules, phenytoin, flowability, redispersibility, anticonvulsant effect.

1. Introduction

Lipid-core nanocapsules (LNC) are nanocarriers that have an organogel structure (core) composed of a liquid and a solid lipid surrounded by a polymeric wall and stabilized by polysorbate 80 micelles (CÉ et al., 2016; VENTURINI et al., 2011). In order to improve the biological effects, their surface may be chemically modified by electrostatic interactions between lecithin and chitosan molecules in a coating layer (BENDER et al., 2012). Besides that, the improvement of the pharmacological effects of encapsulated drugs that act in the Central Nervous System has been demonstrated (CARREÑO et al., 2016; DIMER et al., 2015; RODRIGUES et al., 2016). According to these studies, LNC cross the blood-brain barrier (BBB) delivering the drug into brain by oral and intravenous route. In this scenario, the nanoencapsulation of an anticonvulsant drug as phenytoin (PH), which is used in the treatment of the epilepsy and requires plasma monitoring due to its narrow therapeutic index and its adverse effects such as hypotension, arrhythmia and gingival hyperplasia (BATCHELOR; APPLETON; HAWCUTT, 2015; DELEU; AARONS; AHMED, 2005; MEGIDDO et al., 2016) is a subject to be investigated.

Moreover, LNC suspensions can be converted into dried powders through different drying process in order to increase their physicochemical and microbiological stability. Freeze-drying has been described as a good technological strategy to dry nanocapsules, depending on the choice of the cryoprotect or drying excipient. However, the great disadvantage is the poor flow properties of the freeze-dried powders (SCHAFFAZICK et al., 2003). On the other hand, spray-drying has been widely applied to dry polymeric nanocapsules (HOFFMEISTER et al., 2012; RIBEIRO et al., 2016; TEWA-TAGNE; BRIANÇON; FESSI, 2006). This method is known to produce size-controlled and specific morphology particles by handling the process parameters (NANDIYANTO; OKUYAMA, 2011). Moreover, it is necessary to select an adequate drying adjuvant to avoid or reduce stickiness, and consequently the wall deposition, with impact on the cohesion and flowability properties of the final product (KESHANI et al., 2015; TEWA-TAGNE; BRIANÇON; FESSI, 2006).

Regarding the production of solid dosage forms containing nanocapsules, Friedrich et al. (2010) produced granules containing dexamethasone-loaded nanocapsules using a wet granulation process, which consisted of multi-steps: wet mixture, sieving and drying. The granules had good physicochemical stability (until 6 months), recovering

the nanocapsules after redispersion in water. However, these granules showed poor flow properties. More recently, fluidized bed granules containing blank nanocapsules were developed by our research group, evaluating the role of the cationic coating in the production of redispersible granules and on their physicochemical properties (ANDRADE et al., 2018). Fluidized bed granulation has been widely used in the pharmaceutical industry to produce granules because it can be easily scalable, has large capacity and low capital cost (BRIENS; BOJARRA, 2010). It comprises a single-step granulation process, reducing the production time. Besides that, in general, it provides granules with good flowability and drug content uniformity (BRIENS; BOJARRA, 2010; BURGGRAEVE et al., 2013). Taking these comments altogether, fluid bed granulation represents an interesting tool to produce solid dosage forms from liquid nanocapsule suspensions, as an approach to turn them in a commercial product. However, there is still a lack of knowledge about the effects of using drug-loaded nanocapsules as a liquid binder in the production of fluid bed granules. Therefore, the aim of this study was to evaluate the use of phenytoin-loaded nanocapsules suspension as binder on the technological properties and *in vivo* performance of fluidized bed granules containing phenytoin. These granules were produced using water or phenytoin-loaded nanocapsules as the binder system and a mixture of maltodextrin and non-encapsulated phenytoin as the substrate. Consequently, they were produced with the non-encapsulated drug or the combination of non-encapsulated and encapsulated phenytoin. The effects of the presence of nanocapsules in the binder system were evaluated on the technological properties of granules, recovery of the original nanometric characteristics, *in vitro* drug release and *in vivo* performance using an anticonvulsant model in mice.

2. Materials and methods

2.1 Materials

Maltodextrin (dextrose equivalent 9 – 15%) was supplied by Fagron (São Paulo, Brazil). Low molar weight chitosan (MW = 50,000-190,000 $g.mol^{-1}$; 75-85% deacetylation), Poly(ε-caprolactone) (PCL) (MW = 80,000 $g.mol^{-1}$), sorbitan monostearate, pancreatin from porcine pancreas, and pilocarpine were obtained from Sigma Aldrich (São Paulo, Brazil). Soybean lecithin (Lipoid® S75) was obtained from Lipoid (Ludwigshafen, Germany). Polysorbate 80 was acquired from Vetec (Rio de

Janeiro, Brazil) and grape seed oil was obtained from Delaware (Porto Alegre, Brazil). Phenytoin was kindly donated by Cristália (São Paulo, Brazil). All other reagents and solvents were analytical or pharmaceutical grade.

2.2 Preparation of the lipid-core nanocapsule suspension

Unloaded and phenytoin-loaded nanocapsules (0.225 $mg.mL^{-1}$) were obtained by interfacial deposition of preformed polymer as previously described (VENTURINI et al., 2011). Phenytoin (0.025 g), poly(ε-caprolactone) (1.00 g), sorbitan monostearate (0.385 g), and grape seed oil (1.65 mL) were dissolved in acetone (240 mL) at 40°C. In parallel, soybean lecithin (0.60 g) was solubilized in ethanol (30 mL) and added to the organic phase. This mixture was injected into an aqueous solution (540 mL) containing polysorbate 80 (0.77 g). After, acetone was eliminated, and the suspension was concentrated under reduced pressure. The final volume was adjusted in a volumetric flask to 100 mL (LNC_{PH}). The cationic coating of the nanocapsules was prepared using a chitosan solution (0.6% w/v) in 1% acetic acid, kept under magnetic stirring overnight at room temperature (25°C), as previously standardized.

2.3 Preparation of granules by fluid bed granulation

Fluid bed granulation was performed using a MiniGlatt (Glatt Air Techniques Inc., Ransey, NJ, USA). A mixture (100 g) of maltodextrin and phenytoin (1:0.004 w/w) was used as the substrate and the binder system (nanocapsule suspension or water) was sprayed from the top down onto the fluidized bed. Granulation process was carried out in the top spray mode, using the following parameters: inlet air temperature (80ºC), air flow (10 - 13 $m^3.h^{-1}$), and atomizing air pressure (0.7 bar). The batch size varied 100 to 110 g, depending on the solid mass of the nanocapsules. A volume of 200 mL of suspension or 25 mL of water was pumped through a peristaltic pump at a constant rate of 0.1 $g.min^{-1}$ and sprayed onto the granulation substrate, reaching a final drug concentration around 4.00 $mg.g^{-1}$. Granules containing unloaded nanocapsules (FB-LNC) were also produced as described above for comparison. Three batches of each formulation were produced. At the end of the spraying process, the powder was collected and stored in desiccator at room temperature (25°C) and protected from light until further analyses.

2.4 Characterization of nanocapsule suspension and fluidized bed granules

2.4.1 Characterization of nanocapsule suspension

The nanocapsule suspensions were characterized by photon correlation spectroscopy (PCS). The ȥ-average diameter and zeta potential were evaluated using a Zetasizer Nano ZS (Nanoseries®, Malvern Instruments, UK), diluting previously the samples in ultrapure water (1:500) and in 10 mmol L^{-1} NaCl aqueous solution, respectively. The dilution media were filtered (0.45 µm) before analyses. The pH values of the suspensions were determined using a calibrated potentiometer (Digimed, DM-22, Campo Grande, Brazil). The experiments were carried out in triplicate of batches.

2.4.2 Characterization of fluidized bed granules

Process yield (%) was calculated by the ratio between the weight of the powder obtained and all solid components of the formulation. Loss on drying (%) of granulated powder was determined using an infrared moisture analyzer (Ohaus MB45, Parsippany, USA). About 1 g of sample was spread uniformly in the sample holder, heated to 105°C for 1 min.

The particle size distribution and geometric mean diameter were measured by laser diffraction (Mastersizer 2000, Malvern, UK) equipped with a dry powder disperser (Scirocco 2000, Malvern, UK). An air pressure of 3 bar and a feed rate of 75% were used for the analysis.

Morphological analyses of fluidized bed granules before and after their redispersion in water were carried out by scanning electron microscopy (SEM; JEOL, JSM 6060, Tokyo, Japan) at the *Centro de Microscopia e Microanálises*-UFRGS (Porto Alegre, Brazil). A double-adhesive carbon tape was placed on an aluminum stub and the powder spread on the carbon tape. In order to analyze the redispersed granules in water, the sample was deposited on silicon wafer and covered with water for 5 min, which was removed using absorbent paper. The stubs were put in a desiccator to dry overnight under vacuum. Then, they were gold sputtered and examined a microscope operating at 10 kV voltage.

2.4.2.1 Flow properties of the fluidized bed granules

The bulk density (ρ_{bulk}) was determined by filling the granules (about 4.00 g) into a 25-mL graduated cylinder without tapping. The tapped density (ρ_{tap}) was determined using

a tap densitometer (JEL, J. Engelsmann AG, Ludwigshafen am Rhein, Germany) at 1,250 taps until reaching a constant volume. The densities were then calculated by dividing the weight of granules (g) with the respective volume (mL). The Carr's compressibility index (CI) and Hausner's ratio (HR) were determined from the bulk and tapped densities as shown in Eq. (1) and Eq. (2), respectively.

$$CI = \frac{\rho_{tap} - \rho_{bulk}}{\rho_{tap}} \times 100 \quad (1)$$

$$HR = {}^{\rho_{tap}}/_{\rho_{bulk}} \quad (2)$$

The cohesion and caking tests were performed on texture analyzer with powder flow analyzer attachment (TA.XTplus, Stable Micro Systems, Godalming, UK). A fixed powder volume of 140 mL was poured into the cylindrical vessel prior to the testing. Before starting these tests, two powder conditioning cycles were accomplished through the rotor is moved down at a speed of 50 mm.s^{-1} and an angle of 178°, and then back up through the powder at 50 mm.s^{-1} in the same angle to remove any stress history from the powder and to normalize the powder column after filling. In the cohesion test, the rotating blade moves down at 50 mm.s^{-1} and moves up at 50 mm.s^{-1} at path angle of 170°. The area under force *vs* distance curve (cohesion coefficient, g.mm) is calculated and divided by the weight of the sample (g) to obtain the cohesion index (mm). In the caking test, the rotating blade moves down through powder column at 20 mm.s^{-1} at path angle of 20° until reaching a force of 750 g. Then the rotor upwards at 10 mm.s^{-1} and an angle of 45°. This is repeated for five compactation cycles. At the end, the rotor slices through the compacted cake recording the mean force (mean cake strength, g) and work required to get it flowing freely (cake strength, g.mm).

2.4.3 Reconstitution of the fluidized bed granules

2.4.3.1 Aqueous redispersibility of fluidized bed granules

The aqueous redispersibility of the fluidized bed granules containing nanocapsules was evaluated after the redispersion of the powder in 2 mL of ultrapure water with the aid of a vortex, reaching a concentration of 3 mg.mL^{-1} (12x higher than in the original nanocapsule suspension). Laser diffraction analyses were performed to obtain the particle size distribution of the redispersed granules. In the first step of the experiment, the suspension was centrifuged at 7,280 *x* g for 10 min after which 1.5 mL of the

supernatant, containing dissolved excipient and redispersed nanocapsules, was withdrawn. The supernatant was then replaced with same volume of ultrapure water without stirring, and centrifuged again. These steps were repeated five times to ensure that all the redispersed nanocapsules and excipient were removed. After the last centrifugation, the supernatant was discarded, and the remaining sediment was dried at 40°C until constant weight for 72 h. In each step, an aliquot of the supernatant was withdrawn for laser diffraction analysis. This procedure was adapted from Kho et al. (2010). The measurements were performed in triplicate. The percentage of redispersibility (%R) of the fluidized bed granules was calculated from the initial mass of powder and the mass of the final sediment of the non-redispersed aggregates.

2.4.3.2 Characterization of redispersed fluidized bed granules

The pH values of the redispersed granules in water were determined using a potentiometer (Digimed, DM-22, Campo Grande, Brazil). In order to assay the drug content of the granules before and after reconstitution, these samples were dispersed in the mobile phase, kept under ultrasound for 60 min, centrifuged at 1,597 x g for 20 min, and filtered (0.45 µm) before HPLC analysis, according to a validated analytical method. The system consisted of a Shimadzu LC-20A system (LC-20AT pump), CBM-20A system controller, SPD-M20A photodiode-array detector, SIL-20A auto-sampler (Tokyo, Japan) and a Phenomenex C18 column (150 mm x 4.6 mm, 5 µm, Gemini). The mobile phase was composed of acetonitrile:water (50:50 v/v). The injected volume was 20 µL at an isocratic flow rate of 1.0 $mL.min^{-1}$ and the detection wavelength was 210 nm. The particle size distribution was measured by laser diffraction (Mastersizer 2000, Malvern, UK). The viscosities of the redispersed granules were carried out at 25 ± 1°C, using a rotational viscosimeter (LVDV II + Pro model, Brookfield, USA) with a spindle ULA. The measurements (n = 3) were performed at 0.1 rpm for 60 s and obtained by plotting the shear stress as a function of the shear rate.

2.5 In vitro drug release from fluidized bed granules

In vitro phenytoin release studies from redispersed fluidized bed granules (3 $mg.mL^{-1}$ of drug) were carried out in simulated intestinal fluid (SIF), using a dialysis membrane method at 37°C, and ensuring sink conditions. Each formulation was placed in a dialysis bag (10 kDa molecular weight cutoff, Sigma Aldrich, Brazil). Aliquots (2 mL) were collected and replaced with fresh medium at predetermined time intervals. The

samples were centrifuged at 7,280 x g for 10 min before filtering (0.45 µm) to avoid membrane saturation by aggregates of pancreatin. Thereafter, the samples were analyzed by HPLC, according to the method previously described. A solution of phenytoin (3 $mg.mL^{-1}$) was prepared in ethanol: water (60:40 v/v) to evaluate the diffusion profile of the non-encapsulated drug. The experiments were performed in triplicate.

2.6 In vivo experiments

2.6.1 Animals

Adult C57BL/6 mice (25-35 g, 30 – 90 day-old) of both genders were used in the experiments. Animals were maintained at controlled temperature (24 ± 1°C), at relative humidity (55%), under a 12:12 h light-dark cycle, with free access to water and food. *In vivo* studies were carried out in accordance with National guidelines of the Council for Control of Animal Experiments (CONCEA), U.S. Public Health Service's Policy on Humane Care and Use of Laboratory Animals (PHS Policy), and with the approval by the Ethics Committee for Animal Research of the Federal University of Santa Maria (protocol # 3273040416).

2.6.2 Behavioral seizure evaluation

The granules were reconstituted in water at a concentration of 3 $mg.mL^{-1}$ and administered by gavage (p.o.) in mice in the dose of 30 $mg.kg^{-1}.day^{-1}$ (n=5/group). Animals were treated with water (vehicle), non-encapsulated phenytoin (PH) redispersed in water (3 $mg.mL^{-1}$), redispersed granules containing unloaded nanocapsules (FB-LNC), granules containing phenytoin-loaded nanocapsules (FB-LNC_{PH3}), and granules containing phenytoin (FB-PH_3). Two hours thereafter, pilocarpine was injected (300 $mg.kg^{-1}$, i.p.) to induce seizures following standard procedures (BORGES et al., 2003; FUNCK et al., 2014), and the animals were observed for 60 min. Seizure severity was scored according to modified method (RACINE, 1972). Stages 1-3 were recognized as myoclonic seizures and stages 4–6 as generalized seizures. During the experiment, we recorded the latency to myoclonic seizures, latency to generalized seizures, survival time, and seizure severity.

2.7 Statistical analysis

Data were expressed as mean ± standard deviation and analyzed by one-way ANOVA for multiple groups followed by Tukey post hoc test and Student's *t*-test for comparison of two groups. Seizure latencies were analyzed by the Kruskal-Wallis followed by post hoc analyses with the Mann-Whitney test. Significance was determined for p values < 0.05.

3. Results and Discussion

3.1 Nanocapsule suspensions

Lipid-core nanocapsules coated by chitosan were selected for this study due to their good redispersion properties from fluid bed granules, as previously reported by our group (ANDRADE et al., 2018). Phenytoin-loaded nanocapsules (LNC_{PH}) produced for this study had a z-average of 162 ± 2 nm and low polydispersity index (0.15 ± 0.02), demonstrating the good homogeneity of the system; a positive zeta potential (+16.3 ± 1.32 mV) due to chitosan coating; an encapsulation efficiency close to 95%; and a drug content of 0.225 $mg.mL^{-1}$, as expected. Moreover, the acetic acid used to dissolve the chitosan was responsible for the acid pH (3.99 ± 0.03) of the suspensions. Phenytoin-loaded nanocapsules were stable for 21 days of storage protected from light at room temperature.

3.2 Fluidized bed granules

3.2.1 Physicochemical characterization

The granules were obtained by a fluid bed granulation process, using a mixture of highly soluble maltodextrin and phenytoin as substrate, and nanocapsule suspension as the binder system. In order to evaluate the role of the nanocapsule suspension in the granule properties, granules containing only non-encapsulated phenytoin, or a combination of non-encapsulated and encapsulated phenytoin were produced. To increase the drug loading in the granules, phenytoin was initially mixed to maltodextrin trough a geometric dilution technique composing the substrate of the process. This substrate was fluidized for 20 min to ensure that there are no clumping or agglomeration of powder during the process (BOSE et al., 2012). Thereafter, the nanocapsule suspension or water was sprayed onto the fluidized bed. The granulation

process parameters are gathered in Table 1. The granules had good yields (73-82%), drug content near to 4 $mg.g^{-1}$, and moisture content lower than 5%. This parameter was monitored to determine the granulation end-point (BRIENS; BOJARRA, 2010; FAURE; YORK; ROWE, 2001). Furthermore, it was observed that only granules prepared with nanocapsules, as binder, showed particle size within the expected size range for the technique (0.1-2 mm) (PARIKH, 2005). However, both granules (FB-PH and FB-LNC_{PH}) had narrow size distribution (SPAM values < 2), demonstrating the good homogeneity of the formed agglomerates. Particles with narrow size distribution mean particles with a homogeneous distribution of the binder (IVESON et al., 2001). Compared with the raw maltodextrin (D[4,3] = 50 µm) both granules showed bigger mean particle size. This reflects the growth of the granule with an initial nucleation phase, where the liquid binder is brought into contact with a dry powder bed, followed by granule compaction and growth (IVESON et al., 2001). Fluidized bed granules containing phenytoin-loaded nanocapsules (FB-LNC_{PH}) showed bigger mean particle size than those containing only phenytoin (FB-PH) ($p < 0.05$), showing that nanocapsules improved the agglomeration by the formation of solid bridges between the particles, acting as a good binder. On the other hand, FB-PH were produced with a small volume of water, in which the particles easily tend to clump together, possibly originating a weak granulated material. Farber and co-workers (2005) reported that solid bridges are not formed or are weak, when mannitol and lactose granules were produced with water as a binder, resulting in granules with poor mechanical properties.

Table 1. Granulation process parameters and physicochemical characterization of fluidized bed granules containing phenytoin (FB-PH), and granules containing phenytoin-loaded nanocapsules (FB-LNC_{PH})(n = 3).

Formulation	Yield (%)	Moisture content (%)	D[4,3] µm	SPAN	Drug content ($mg.g^{-1}$)
FB-PH	78 ± 4	3.03 ± 0.65	76 ± 1	1.78 ± 0.12	4.16 ± 0.37
FB-LNC_{PH}	76 ± 3	2.87 ± 0.52	122 ± 14*	1.85 ± 0.18	3.96 ± 0.03

* significant at $p < 0.05$.

In a next step, SEM analyses were performed to evaluate the morphology of the fluidized bed granules as well as the recovery of nanocapsules after their redispersion in water. Fig. 1A shows the presence of solid bridges in FB-LNC$_{PH}$ as well as pores on their surface (black arrows in Fig. 1A2). This may be occurred due to the immersion of the smaller particles into the larger particle in the nucleation phase, producing nuclei with saturated pores (IVESON et al., 2001) as well as due to the shear forces in the fluidized bed, which can originate more porous and less dense granules (JOSHI et al., 2017). On the other hand, the granules prepared with water as binder (FB-PH) did not present bridges between the particles (Fig. 1B1), confirming that these granules are formed by weak inter-particles forces, as discussed earlier. Moreover, the presence of primary particles in the granulation end-point (Fig. 1B2) suggests non-uniformity of the finished product, one of the most reported problems during fluid bed granulation (JOSHI et al., 2017). FB-PH had size around 75 µm and can be considered ‘small granules’, consisting of large ungranulated primary feed particles (IVESON et al., 2001).

Regarding the recovery of nanocapsules after their redispersion in water, Fig. 1C1 shows the presence of free nanocapsules (see black arrows), soluble maltodextrin/phenytoin agglomerates and nanocapsules/maltodextrin microagglomerates after adding water to FB-LNC$_{PH}$. On the other hand, FB-PH were not fully solubilized in contact with water, as remaining material can be observed attached to the silica wafer (Fig. 1C2). Therefore, it may be suggested that FB-LNC$_{PH}$ disintegrated after water penetration through the pores, followed by the release of the nanocapsules embedded and adsorbed on their surface/bridges to the aqueous medium. These results corroborates with those reported by Andrade et al. (2018).

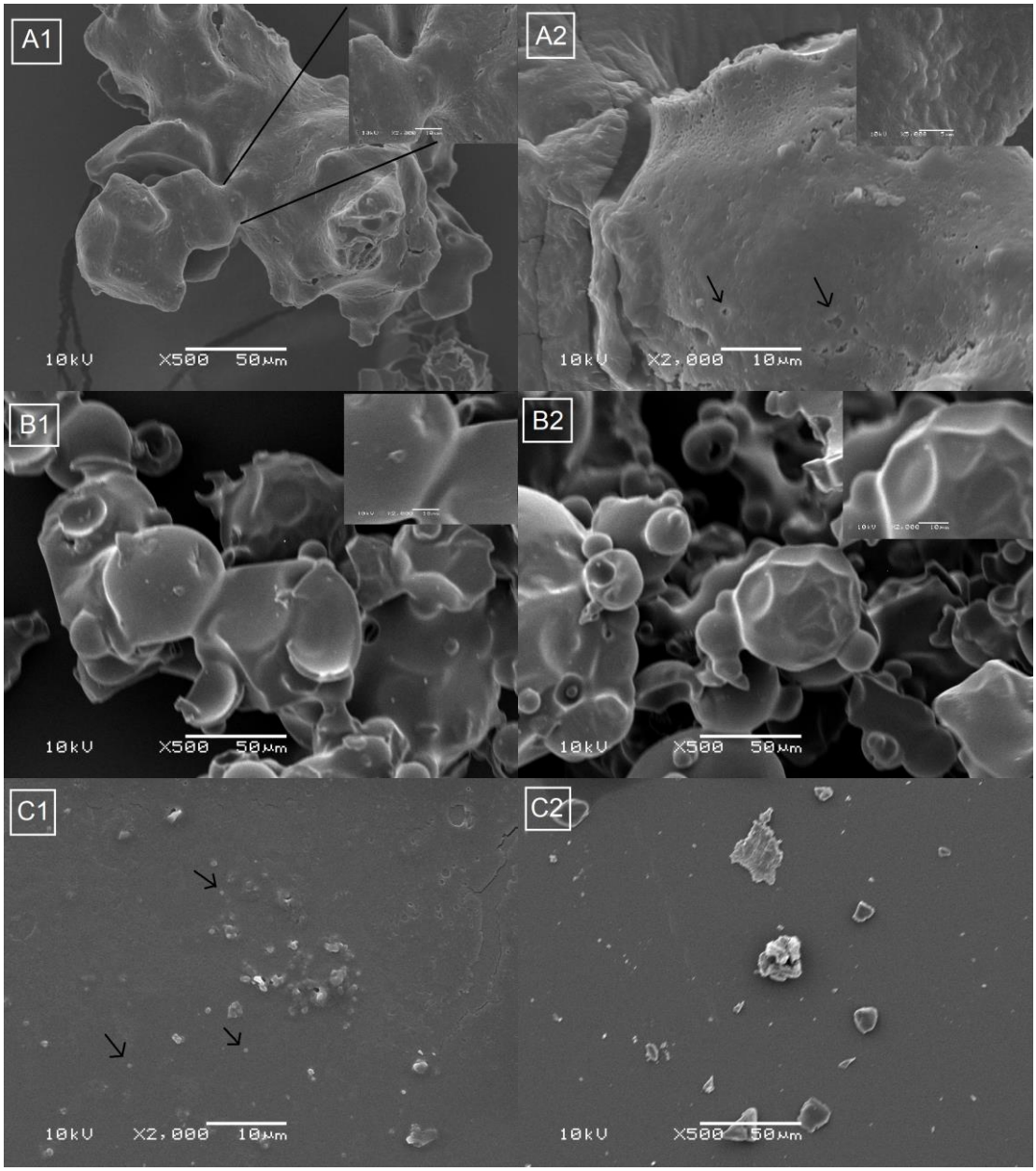

Fig. 1. SEM images of particles after granulation process. (A1, A2) fluidized bed granules containing phenytoin-loaded nanocapsules (FB-LNC$_{PH}$); (B1, B2) fluidized bed granules containing phenytoin (FB-PH); (C1) redispersed granules containing phenytoin-loaded nanocapsules and (C2) redispersed granules containing phenytoin. (A, B) Further details of the particles were shown at the top right corner in each image. The black arrows indicate pores on the granule surface (A2) and nanocapsules released in the aqueous medium (C1).

3.2.2 Flow properties

Fluidized bed granulation technique has been also used to improve flow properties of powders, ensuring the desired characteristics of the final product (i.e., moisture content, granule size, density, flowability, and friability) (JOSHI et al., 2017). The flow characterization by different methods ensure a complete understanding of the powder flow properties (LETURIA et al., 2014). On this basis, a powder rheometer with force-displacement transducer was used to measure the cohesivity and caking ability of the granules, allowing quick and reproducible measurements. Cohesiveness is the tendency of the powder particles to clump together and agglomerate and caking is the tendency of a powder to form large agglomerates (hard cake) during storage and transport (SHAH; TAWAKKUL; KHAN, 2008).

The flow properties of the granules are shown in Table 2, represented by the Carr's index (CI) and Hausner's ratio (HR), which are compendial flow powder measurements (USP, 2009) as well as the cohesion index and cake strength, as non-compendial powder flow parameters. FB-LNC$_{PH}$ had passable flow properties ($21 < CI < 25$; $1.26 < HR < 1.34$) while raw maltodextrin and FB-PH presented poor flow ($26 < CI < 31$; $1.35 < HR < 1.45$). Higher Hausner's ratio values indicate cohesive powders. This characteristic was confirmed by the cohesion index values measured for maltodextrin, FB-PH and FB-LNC$_{PH}$ (>14 for cohesive powders; classification proposed by Stable Micro Systems Ltd.). In this regard, FB-LNC$_{PH}$ showed an intermediate flow behavior with a relative cohesive nature. This finding can be explained due to the more sensitive to changes in flow rate by cohesive materials (LETURIA et al., 2014). Under the action of the low stress (i.e. in the case of the tapping test), some powders have a free to intermediate flow, as reported by Fatah (2009), but their cohesive character is detectable only under high stress (i.e. shearing tests). In the conditioning cycle (cohesion test), the blade gently displaces the powder to establish a uniform state. However, in the test cycle, the blade moves down, forcing the powder to flow around the blade, generating a localized high stress region near to the blade (LETURIA et al., 2014). Sometimes, powders cohesivity makes more difficult their flowability. However, moderate cohesivity is desirable in filling operations that can cause fine powders to flow off (SHAH; TAWAKKUL; KHAN, 2008). In relation to the caking test, the area under the curve, highlighted by gray colored AUC within zone between 1 and 2 (Fig. 2A), is integrated in the force-displacement, representing the work done to move the blade through powder column. For FB-PH, the distance traveled by the blade was

recorded each time 750 g of force was reached, and the cycles did not overlay because after each cycle a lower distance until reaching the required force was necessary. Moreover, the FB-PH had higher cake strength and mean cake strength compared to those of raw maltodextrin ($p < 0.05$). This finding explains their great segregation potential, which may result in variability in sachets filling for pharmaceutical powders (IVESON et al., 2001; SHAH; TAWAKKUL; KHAN, 2008). Although the cohesive nature of a powder determines the caking tendency, this did not occur for FB-LNC_{PH}, which did not form a cake under the standard test conditions. Fig. 2B shows a constant increase in force ending with a sharp spike up to the compaction force (750 g) over each compaction cycle. Therefore, it was not possible to calculate the cake strength and mean cake strength for FB-LNC_{PH}, suggesting a higher resistance to deformation compared with FB-PH. Fiel et al. (2011) demonstrated that the LNC are more rigid than conventional polymeric nanocapsules due to rigidity of the polymer wall and lipid core. A material that deforms plastically does not fully recover once the applied stress is removed, leading higher contact area, and hence higher adhesion forces that may conduce to cake formation (ZAFAR et al., 2017).

Table 2. Flow properties for raw material (maltodextrin, MD), fluidized bed granules containing phenytoin (FB-PH), and granules containing phenytoin-loaded nanocapsules (FB-LNC_{PH})(n = 3).

Formulation	Carr's index	Hausner's ratio	Cohesion index (mm)	Cake strength (g.mm)	Mean cake strength (g)
MD	26 ± 2	1.35 ± 0.04	21 ± 1	597 ± 134	54 ± 5
FB-PH	31 ± 2	1.86 ± 0.04	16 ± 1	1719 ± 129*	110 ± 8*
FB-LNC_{PH}	21 ± 3	1.26 ± 0.04	17 ± 2	-	-

* significant at $p < 0.05$ compared with MD.

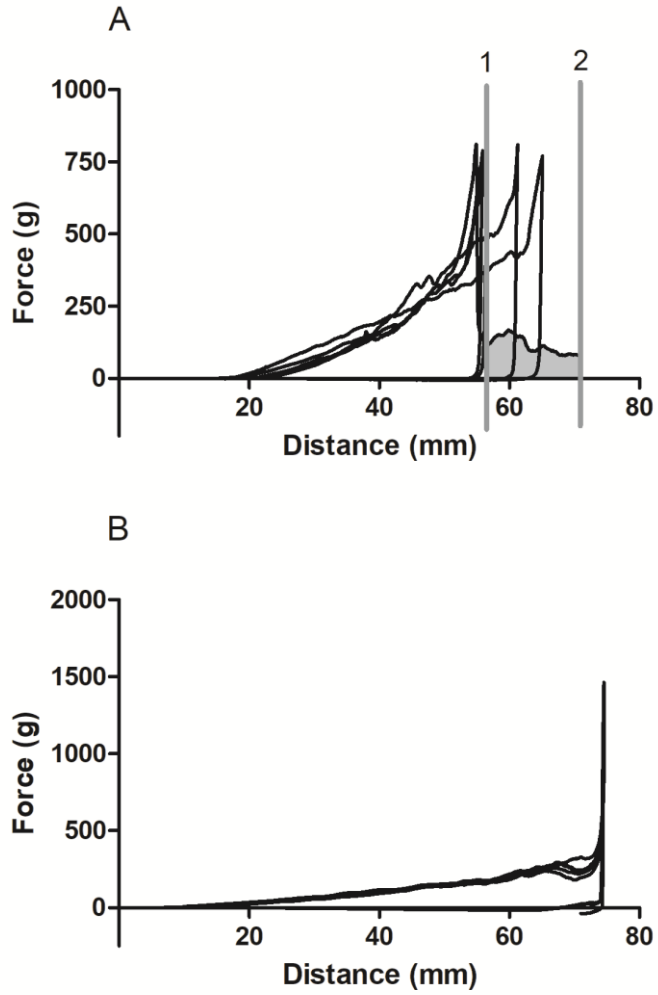

Fig. 2. Force-displacement profile for fluidized bed granules containing phenytoin (A) and granules containing phenytoin-loaded nanocapsules (B) in a caking strength test on texture analyzer (n = 5).

3.3 Reconstituted fluidized bed granules

3.3.1 Physicochemical characterization and redispersibility studies

Fluidized bed granules were reconstituted in water to reach the concentration of 3 $mg.mL^{-1}$ (named as FB-PH_3 and FB-LNC_{PH3}). The redispersibility indicates the percentage of nanoaggregates that are redispersible in an aqueous medium, evaluating the particles aggregation. FB-PH_3 were solubilized in the aqueous medium and it was not possible to calculate their redispersibility. On the other hand, FB-LNC_{PH3} showed a good redispersibility (90 ± 3%) with similar volume-weight mean particle size ($p > 0.05$) at the beginning and end of the experiment (data not shown). This finding

can be explained by the high solubility of maltodextrin in water (1 g.mL^{-1}) (ROWE; SHESKEY; OWEN, 2012) as well as the hydrophilic chitosan coating of the nanocapsules, which allows hydrogen bonding with water, facilitating the redispersion (MADY; DARWISH, 2010). According to Kho et al. (2010), the granules composition on the particle surface (in terms of hydrophobicity) influences the particle wetting, and hence the aqueous redispersion. The complete physicochemical characteristics of the reconstituted powders are presented in Table 3.

Table 3. Physicochemical characterization of the redispersed granules containing phenytoin (FB-PH_3) and granules containing phenytoin-loaded nanocapsules (FB-LNC_{PH3}) at concentration 3 mg.mL^{-1}.

Formulation	D[4,3] µm	SPAN	Drug content (mg.mL^{-1})	pH
FB-PH_3	23 ± 7^a	2.39 ± 0.38^a	2.88 ± 0.15^a	5.11 ± 0.09^a
FB-LNC_{PH3}	0.91 ± 0.06^b	2.83 ± 0.16^a	2.86 ± 0.10^a	4.72 ± 0.04^b

Different letters, in column, means statistically different values ($p < 0.05$).

FB-PH_3 showed particle size around 23 µm while FB-LNC_{PH3} presented a nanometric profile with mean particle size around 914 nm ($p < 0.05$). The bigger particle size for FB-PH_3 can be due to its higher solid content, which can decrease the wetting of the particles, leading to the formation of agglomerates (BHAKAY; DAVÉ; BILGILI, 2013). On the other hand, the mean size of the FB-LNC_{PH3} in the nanoscale can be explained by the granules disintegration after water penetration, releasing the nanocapsules as observed in SEM images (Fig. 1C1). Besides that, both granules presented drug content near to the expected concentration. Regarding the pH of the redispersed suspension, a lower pH was observed for FB-LNC_{PH3} compared with FB-PH_3, which is explained by the remaining acetic acid used in the chitosan coating of the nanocapsules, whose boiling point (118°C) is above the process temperature. However, low concentrations of acetic acid (0.002%) in the formulation do not cause major problems since this compound is one of the simplest carboxylic acids, being rapidly metabolized in the body (NCBI, 2017).

3.4 In vitro drug release studies

In this step, the influence of the binder (nanocapsules) of the granulation process was evaluated on the *in vitro* drug release profiles. Fig. 3 shows the drug release profiles from redispersed granules (FB-PH_3 and FB-LNC_{PH3}). Both formulations showed a slower drug release compared with phenytoin diffusion from an ethanolic solution at the same concentration (S-PH_3), which was completely diffused after 72 h. This behavior shows the good solubility of phenytoin in the intestinal fluid and under the experimental conditions used in this study and the slower drug release behavior from both granules. In addition, FB-LNC_{PH3} showed a faster release behavior than FB-PH_3 after 24 h. Different factors could be influencing these different release profiles from the granules, like the viscosity of the redispersion, the particle size and the presence of nanocapsules in the formulation. In order to evaluate the influence of the viscosity, rheological studies were carried out for FB-PH_3 and FB-LNC_{PH3}, which showed viscosity values of 56 ± 17 cP and 1295 ± 316 cP, respectively. These viscosities correspond to the highest shear stress in each non-newtonian rheological profile. Higher viscosities would mean slower drug release profiles. Therefore, the influence of the viscosity on the faster release behavior from FB-LNC_{PH3} can be refuted. On the other hand, nanocapsules may act as a drug diffusion barrier of the non-encapsulated (90% of total phenytoin) and encapsulated phenytoin (10%), considering their arrangement around the maltodextrin/phenytoin agglomerates, as discussed in *section 3.2.1*. However, the impact on the release control by this factor may be considered low taking into account that only 10% of the total drug in the system is nanoencapsulated. Regarding the particle size, after 24 h, the FB-LNC_{PH3} microagglomerates were probably broken, increasing the drug release rate. On the other hand, large agglomerates of the FB-PH_3 were not easily broken, as previously discussed by the SEM analysis, making difficult the phenytoin release. Bhakay and co-workers (2013) observed that the physical mixture containing micronized griseofulvin particles had a large particle size after redispersion, slowing down the drug dissolution rate when compared to nanocomposite particles produced with stabilizers (hydroxypropyl cellulose, sodium dodecyl sulfate and mannitol). Therefore, the faster drug release behavior promoted by FB-LNC_{PH3} can be explained by the best granules redispersion behavior compared with FB-PH_3.

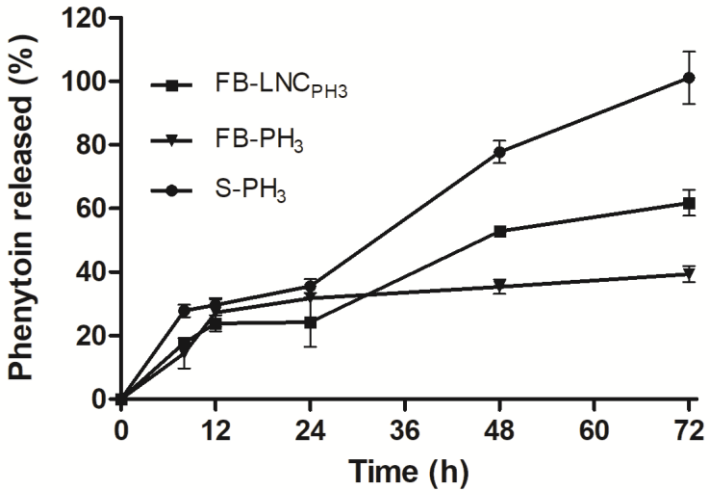

Fig. 3. *In vitro* drug release from redispersed granules containing nanocapsules (FB-LNC_{PH3}), granules containing phenytoin (FB-PH_3), and phenytoin ethanolic solution (S-PH_3) in the concentration of 3 mg.mL^{-1}.

3.5 In vivo experiments

In order to evaluate the influence of the nanocapsules on the *in vivo* performance, the pilocarpine-induced seizures model was used as it resembles human temporal lobe epilepsy (BORGES et al., 2003). This animal model was firstly described by Turski et al. (1983) and is characterized by chemical induction of the seizures from the excitability caused by alterations in the calcium and potassium ions. Moreover, muscarinic receptors are activated, producing a typical pattern of action (i.e. salivation) (TAWFIK, 2011). An acute model of induction of seizures was used to evaluate the anticonvulsant efficacy of the redispersed fluidized bed granules. The granules were reconstituted in water, according to the procedure in section *2.4.3.1,* reaching a concentration of 3 mg.mL^{-1}. The redispersed granules containing unloaded nanocapsules (FB-LNC) showed similar properties (0.905 ± 0.04 µm; pH 4.77 ± 0.07) to those of FB-LNC_{PH3} ($p > 0.05$).

The formulations were administered by gavage in mice (n = 5/group) at a dose of 30 mg.kg^{-1}, which was based on phenytoin pharmacokinetics parameters reported in the literature (MARKOWITZ et al., 2010; OHMORI et al., 1997; ROWLAND; BINKERD; HENDRICKX, 1990). The following groups were evaluated: 1) mice treated with water (vehicle), 2) mice treated with non-encapsulated phenytoin (PH) suspension in water,

3) mice treated with redispersed granules containing nanocapsules, 4) mice treated with redispersed granules containing unloaded nanocapsules, and 5) mice treated with redispersed granules containing only non-encapsulated phenytoin.

Fig. 4 shows the anticonvulsant effect for all groups on the pilocarpine-induced seizures. The group treated with the non-encapsulated phenytoin suspension did not show anticonvulsant effect when compared to the vehicle (control). On the other hand, both groups treated with the redispersed granules containing phenytoin resulted in significant increase ($p < 0.05$; Fig. 4A) on the latency to myoclonic seizures in comparison to group treated with water (vehicle). It can be suggested that the mucoadhesion properties of these granules could improve drug bioavailability and hence its anticonvulsant effect. However, a better performance by the nanoencapsulated phenytoin in the FB-LNC_{PH3} granules against myoclonic jerks was not observed, probably due to low concentration (0.4 $mg.g^{-1}$) in relation to the total drug concentration in the granules. In relation to latency to generalized seizures (Fig. 4B), redispersed granules containing nanocapsules (FB-LNC_{PH3}) showed superior anticonvulsant activity compared with placebo granules ($p < 0.05$), whereas a slight increase was observed in comparison with the vehicle, the non-encapsulated PH suspension and the granules containing only non-encapsulated phenytoin (FB-PH_3). No anticonvulsant effect was observed against generalized seizures for PH suspension. Wang et al. (2016) also observed no significant increase in latency to generalized seizures for the group treated with phenytoin in solution. However, phenytoin-loaded electroresponsive nanoparticles showed higher latency to generalized seizures. Regarding the survival time, the fluidized bed granules increased the survival time (Fig. 4C) and those containing nanocapsules subtly alleviated the severity of seizures (Fig. 4D). It interesting to note that only 10% of the encapsulated phenytoin into granules generated a promising anticonvulsant effect. Studies have been reported that lipid-core nanocapsules administered by intravenous and oral route can act as drug shuttles through the blood brain barrier, promoting its vectorization to the brain (CARREÑO et al., 2016; RODRIGUES et al., 2016). This can be confirmed by no significant antiepileptic action of the placebo granules. Moreover, the low amount of nanoencapsulated drug was enough to provide good technological properties to granules.

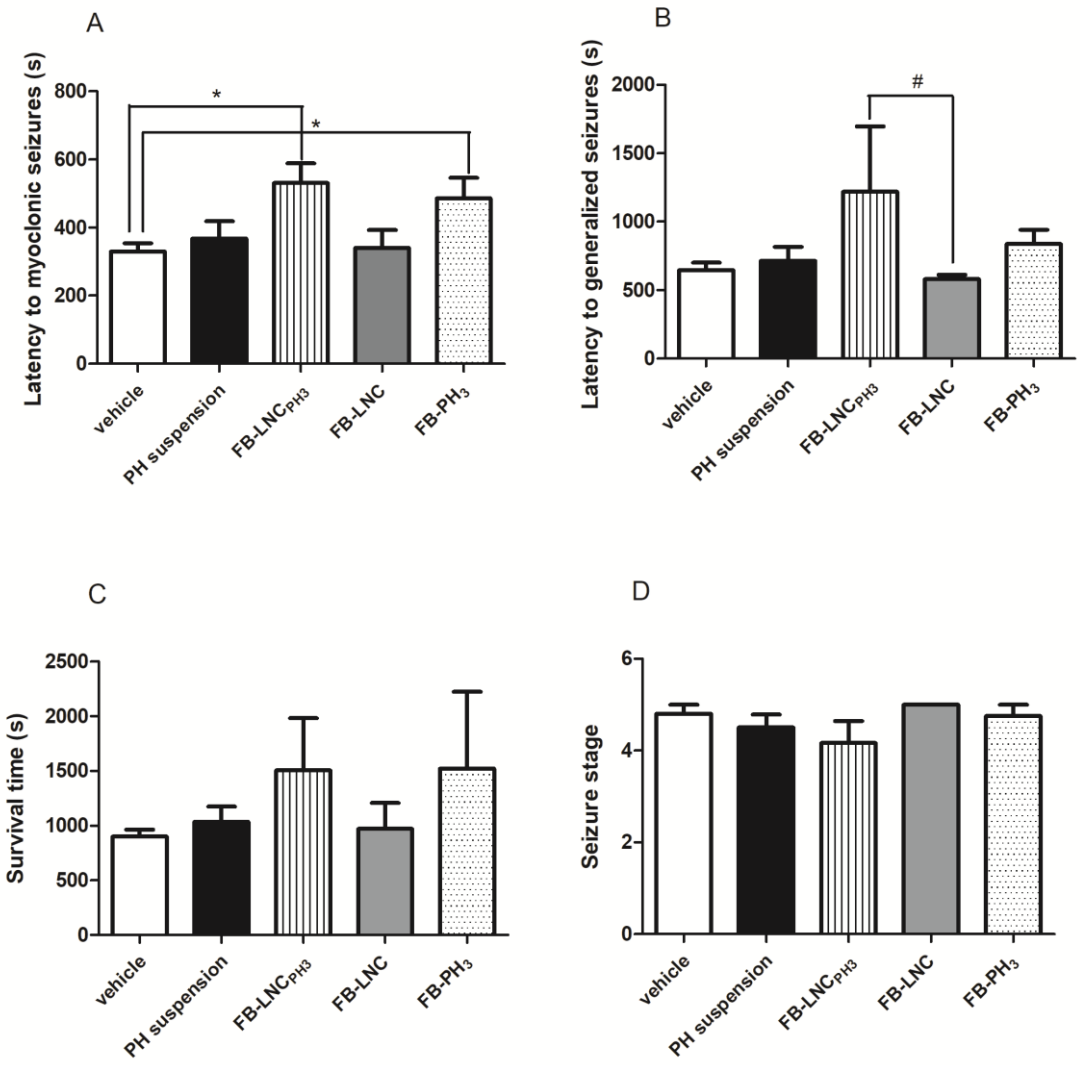

Fig. 4. The *in vivo* anticonvulsant effect of the phenytoin at dose of 30 $mg.kg^{-1}$ from redispersed granules in the pilocarpine-induced seizures model (n=5). The effect of non-encapsulated phenytoin (PH suspension), redispersed granules containing unloaded nanocapsules (FB-LNC), granules containing phenytoin-loaded nanocapsules (FB-LNC_{PH3}), and granules containing phenytoin (FB-PH_3) on the latency to myoclonic seizures (A), on the latency to generalized seizures (B), survival time of the animals (C), and seizure stage (D). * $p < 0.05$, compared to vehicle; $^{\#}$ $p < 0.05$, compared to placebo granules.

4. Conclusion

Nanocapsule suspension, as a binder, improves the technological properties of fluidized bed granules, which formed solid bridges between the particles responsible for a better flow and no caking of the powder during the storage. Moreover, after

reconstitution in water, these granules had good aqueous redispersibility, recovering the nanometric characteristics of the original suspensions. The granules control the drug release behavior, depending on the presence of the nanocapsules and the redispersibility profile. Moreover, the granules containing phenytoin-nanocapsules showed an increase on latency to myoclonic and generalized seizures compared with the non-encapsulated drug in suspension. Therefore, considering the technological properties and the *in vivo* performance, redispersed granules containing nanocapsules presented a promising approach in the anticonvulsant therapy. Further studies will be performed to increase the nanoencapsulated drug loading into fluidized bed granules.

5. Declaration of interest

The authors report no conflicts of interest.

6. Acknowledgments

The authors acknowledge Cristália Produtos Químicos e Farmacêuticos Ltda for gentle donation of phenytoin. The authors thank the financial support of CNPq/Brazil, CAPES/Brazil and FAPERGS. E.G.O. thanks CAPES for the doctoral's fellowship.

References

ANDRADE, D. F. et al. Fluid bed granulation as an innovative process to produce dry redispersible nanocapsules: Influence of cationic coating of particles. **Powder Technology**, v. 326, p. 25–31, 2018.

BATCHELOR, H.; APPLETON, R.; HAWCUTT, D. B. Comparing paediatric intravenous phenytoin doses using physiologically based pharmacokinetic (PBPK) modelling software. **Seizure**, v. 33, p. 8–12, 2015.

BENDER, E. A. et al. Hemocompatibility of poly(ε-caprolactone) lipid-core nanocapsules stabilized with polysorbate 80-lecithin and uncoated or coated with chitosan. **International Journal of Pharmaceutics**, v. 426, n. 1–2, p. 271–279, 2012.

BHAKAY, A.; DAVÉ, R.; BILGILI, E. Recovery of BCS Class II drugs during aqueous redispersion of core-shell type nanocomposite particles produced via fluidized bed coating. **Powder Technology**, v. 236, p. 221–234, 2013.

BORGES, K. et al. Neuronal and glial pathological changes during epileptogenesis in the mouse pilocarpine model. **Experimental Neurology**, v. 182, p. 21–34, 2003.

BOSE, S. et al. Application of spray granulation for conversion of a nanosuspension into a dry powder form. **European Journal of Pharmaceutical Sciences**, v. 47, n. 1, p. 35–43, 2012.

BRIENS, L.; BOJARRA, M. Monitoring Fluidized Bed Drying of Pharmaceutical Granules. **AAPS PharmSciTech**, v. 11, n. 4, p. 1612–1618, 2010.

BURGGRAEVE, A. et al. Process analytical tools for monitoring, understanding, and control of pharmaceutical fluidized bed granulation: A review. **European Journal of Pharmaceutics and Biopharmaceutics**, v. 83, n. 1, p. 2–15, 2013.

CARREÑO, F. et al. Pharmacokinetic Investigation of Quetiapine Transport across Blood-Brain Barrier Mediated by Lipid Core Nanocapsules Using Brain Microdialysis in Rats. **Molecular Pharmaceutics**, v. 13, n. 4, p. 1289–1297, 2016.

CÉ, R. et al. Colloids and Surfaces A: Physicochemical and Engineering Aspects Chitosan-coated dapsone-loaded lipid-core nanocapsules: Growth inhibition of clinical isolates, multidrug-resistant Staphylococcus aureus and Aspergillus ssp. **Colloids and Surfaces A: Physicochemical and Engineering Aspects**, v. 511, p. 153–161, 2016.

DELEU, D.; AARONS, L.; AHMED, I. A. Estimation of population pharmacokinetic parameters of free-phenytoin in adult epileptic patients. **Archives of Medical Research**, v. 36, n. 1, p. 49–53, 2005.

DIMER, F. A. et al. Nanoencapsulation Improves Relative Bioavailability and Antipsychotic Effect of Olanzapine in Rats. **Journal of Biomedical Nanotechnology**, v. 11, p. 1482–1493, 2015.

FARBER, L.; TARDOS, G. I.; MICHAELS, J. N. Micro-mechanical properties of drying material bridges of pharmaceutical excipients. **International Journal of Pharmaceutics**, v. 306, n. 1–2, p. 41–55, 2005.

FATAH, N. Study and comparison of micronic and nanometric powders: Analysis of physical, flow and interparticle properties of powders. **Powder Technology**, v. 190, n. 1–2, p. 41–47, 2009.

FAURE, A.; YORK, P.; ROWE, R. C. Process control and scale-up of pharmaceutical wet granulation processes: a review. **European Journal of Pharmaceutics and Biopharmaceutics**, v. 52, p. 269–277, 2001.

FIEL, L. A. et al. Diverse deformation properties of polymeric nanocapsules and lipid-core nanocapsules. **Soft Matter**, v. 7, n. 16, p. 7240, 2011.

FRIEDRICH, R. B. et al. Drying polymeric drug-loaded nanocapsules: the wet granulation process as a promising approach. **Journal of Nanoscience and Nanotechnology**, v. 10, n. 1, p. 616–621, 2010.

FUNCK, V. R. et al. Long-term decrease in Na+,K+-ATPase activity after pilocarpine-induced status epilepticus is associated with nitration of its alpha subunit. **Epilepsy Research**, v. 108, n. 10, p. 1705–1710, 2014.

HOFFMEISTER, C. R. et al. Hydrogels containing redispersible spray-dried melatonin-loaded nanocapsules: a formulation for transdermal-controlled delivery. **Nanoscale Research Letters**, v. 7, n. 1, p. 251, 2012.

IVESON, S. M. et al. Nucleation, growth and breakage phenomena in agitated wet granulation processes: A review. **Powder Technology**, v. 117, n. 1–2, p. 3–39, 2001.

JOSHI, S. et al. To study and understand the process of wet granulation by fluidized bed granulation technique. **International Journal of Research in Pharmacy and Chemistry**, v. 7, n. 3, p. 232–238, 2017.

KESHANI, S. et al. Spray drying: An overview on wall deposition, process and modeling. **Journal of Food Engineering**, v. 146, p. 152–162, 2015.

KHO, K. et al. Aqueous re-dispersibility of spray-dried antibiotic-loaded polycaprolactone nanoparticle aggregates for inhaled anti-biofilm therapy. **Powder Technology**, v. 203, n. 3, p. 432–439, 2010.

LETURIA, M. et al. Characterization of flow properties of cohesive powders: A comparative study of traditional and new testing methods. **Powder Technology**, v. 253, p. 406–423, 2014.

MADY, M. M.; DARWISH, M. M. Effect of chitosan coating on the characteristics of DPPC liposomes. **Journal of Advanced Research**, v. 1, n. 3, p. 187–191, 2010.

MARKOWITZ, G. J. et al. The pharmacokinetics of commonly used antiepileptic drugs in immature CD1 mice. **Neuroreports**, v. 21, n. 6, p. 452–456, 2010.

MEGIDDO, I. et al. Health and economic benefits of public financing of epilepsy treatment in India: An agent-based simulation model. **Epilepsia**, v. 57, n. 3, p. 464–474, 2016.

NANDIYANTO, A. B. D.; OKUYAMA, K. Progress in developing spray-drying methods for the production of controlled morphology particles: From the nanometer to submicrometer size ranges. **Advanced Powder Technology**, v. 22, n. 1, p. 1–19, 2011.

NATIONAL CENTER FOR BIOTECHNOLOGY INFORMATION. **PubChem Compound Database; CID=176**. Disponível em: <https://pubchem.ncbi.nlm.nih.gov/compound/176>. Acesso em: 21 dez. 2017.

OHMORI, H. et al. Effects of low-dose phenytoin administered to newborn mice on developing cerebellum. **Neurotoxicology and Teratology**, v. 19, n. 3, p. 205–211, 1997.

PARIKH, D. M. Introduction. In: PARIKH, D. M. (Ed.). . **Handbook of Pharmaceutical Granulation Technology**. 2. ed. New York: Taylor & Francis, 2005. p. 1–6.

RACINE, R. J. Modification of seizure activity by electrical stimulation: II. Motor seizure. **Electroencephalography and Clinical Neurophysiology**, v. 32, p. 281–294, 1972.

RIBEIRO, R. F. et al. Spray-dried powders improve the controlled release of antifungal tioconazole-loaded polymeric nanocapsules compared to with lyophilized products. **Materials Science and Engineering C**, v. 59, p. 875–884, 2016.

RODRIGUES, S. F. et al. Lipid-core nanocapsules act as a drug shuttle through the blood brain barrier and reduce glioblastoma after intravenous or oral administration. **Journal of Biomedical Nanotechnology**, v. 12, n. 5, p. 986–1000, 2016.

ROWE, R. C.; SHESKEY, P. J.; OWEN, S. C. **Handbook of Pharmaceutical Excipients**. 5. ed. London: Pharmaceutical Press, 2012.

ROWLAND, J. R.; BINKERD, P. E.; HENDRICKX, A. G. Developmental toxicity and pharmacokinetics of oral and intravenous phenytoin in the rat. **Reproductive Toxicology**, v. 4, p. 191–202, 1990.

SCHAFFAZICK, S. R. et al. Freeze-drying polymeric colloidal suspensions: Nanocapsules, nanospheres and nanodispersion. A comparative study. **European Journal of Pharmaceutics and Biopharmaceutics**, v. 56, n. 3, p. 501–505, 2003.

SHAH, R. B.; TAWAKKUL, M. A.; KHAN, M. A. Comparative Evaluation of Flow for Pharmaceutical Powders and Granules. **AAPS PharmSciTech**, v. 9, n. 1, p. 250–258, 2008.

TAWFIK, M. K. Coenzyme Q10 enhances the anticonvulsant effect of phenytoin in pilocarpine-induced seizures in rats and ameliorates phenytoin-induced cognitive impairment and oxidative stress. **Epilepsy and Behavior**, v. 22, n. 4, p. 671–677, 2011.

TEWA-TAGNE, P.; BRIANÇON, S.; FESSI, H. Spray-dried microparticles containing polymeric nanocapsules: Formulation aspects, liquid phase interactions and particles characteristics. **International Journal of Pharmaceutics**, v. 325, n. 1–2, p. 63–74, 2006.

TURSKI, W. A. et al. Limbic seizures produced by pilocarpine in rats: behavioural, electroencephalographic and neuropathological study. **Behavioural Brain Research**, v. 9, p. 315–335, 1983.

UNITED STATES PHARMACOPEIAL CONVENTION. **USP 32 NF 27**. 2. ed. Rockville: United States Pharmacopeial Convention, 2009.

VENTURINI, C. G. et al. Formulation of lipid core nanocapsules. **Colloids and Surfaces A: Physicochemical and Engineering Aspects**, v. 375, n. 1–3, p. 200–208, 2011.

WANG, Y. et al. Electroresponsive Nanoparticles Improve Antiseizure Effect of Phenytoin in Generalized Tonic-Clonic Seizures. **Neurotherapeutics**, v. 13, n. 3, p. 603–613, 2016.

ZAFAR, U. et al. A review of bulk powder caking. **Powder Technology**, v. 313, p. 389–401, 2017.

6 CAPÍTULO 3

APRESENTAÇÃO

O terceiro capítulo desta tese avaliou o efeito do uso de nanocápsulas de fenitoína na formação dos grânulos de fenitoína, obtidos em leito fluidizado, sobre as suas propriedades físico-químicas e mucoadesivas. O estudo foi conduzido para buscar elucidar o mecanismo de formação dos grânulos e aspectos que podem estar relacionados à atividade anticonvulsivante superior *in vivo*, discutida no Capítulo 2. Estes grânulos foram formados a partir um substrato (maltodextrina + fenitoína) e de nanocápsulas de fenitoína como aglutinante, sendo avaliados em relação à uniformidade de dose, índice de crescimento, recuperação das propriedades nanométricas após redispersão aquosa, liberação do fármaco *in vitro* e ação mucoadesiva sobre a mucosa intestinal. Um modelo da estrutura dos grânulos foi proposto a partir das análises morfológicas por Microscopia Eletrônica de Varredura (MEV) no intuito de compreender melhor a influência da sua composição e do processo de granulação nas suas características finais. Este artigo está em fase de redação para posterior submissão a periódico científico de circulação internacional.

.

Fluid bed granules containing drug-loaded nanocapsules: granule growth and mucoadhesion studies

Edilene Gadelha de Oliveira[a], Rafaela Santos de Oliveira[a], Kelly Cristine Zatta[b], Adriana Raffin Pohlmann[c], Sílvia Stanisçuaski Guterres[a], Ruy Carlos Ruver Beck[a*]

[a] Programa de Pós-Graduação em Ciências Farmacêuticas, Universidade Federal do Rio Grande do Sul, Porto Alegre, RS, Brazil

[b] Programa de Pós-Graduação em Nanotecnologia, Universidade Federal do Rio Grande do Sul, Porto Alegre, RS, Brazil

[c] Departamento de Química Orgânica, Instituto de Química, Universidade Federal do Rio Grande do Sul, Porto Alegre, RS, Brazil

*Author to whom correspondence should be addressed: Prof R.C.R. Beck; Departamento de Produção e Controle de Medicamentos, Universidade Federal do Rio Grande do Sul, Avenida Ipiranga, 2952, 90610-000, Porto Alegre, RS, Brazil; Phone +55 51 33085215; E-mail: ruy.beck@ufrgs.br

ABSTRACT

Understanding the granulation process and monitoring its parameters are important tools to improve the granule characteristics. The aim of this study was to evaluate the effect of using polymeric nanocapsules as binder to produce fluid bed granules on their growth as well as their mucoadhesion properties after aqueous redispersion. Granules were produced by fluid bed using maltodextrin/phenytoin as substrate and a suspension of phenytoin-loaded nanocapsules (PH-LNC) as binder. The granules (PH-LNC_G) showed good dose uniformity. A linear correlation between particle size and the volume of the sprayed suspension was obtained, with a granule growth index (135%), dependent on the volume of the binder added to the powder bed. A schematic model of the granules structure was proposed from SEM images, where the nanocapsules are covering the granule surface and forming the solid bridges. Redispersed granules containing nanocapsules (PH-LNC_{RG}) in water recovered the nanometric properties of the original suspension. They showed a similar release up to 12 h compared with the nanocapsules, followed by a faster phenytoin release, suggesting that the nanocapsule barrier surrounding the granules could be responsible for controlling the release at the first stage. Washability studies showed a higher amount of drug washed after 5 h from PH-LNC (95 ± 10%) than from PH-LNC_{RG} (42 ± 1%), which showed a 8-fold increase in the amount of permeated drug. The required work to detach the PH-LNC_{RG} from the intestinal mucosa was higher than that required for phenytoin solution (PH_S) ($p < 0.05$) due to the distance travelled by probe for redispersed granules (38 ± 8 mm) was greater than for PH_S (30 ± 3 mm). The higher mucoadhesive effect of the PH-LNC_{RG} occurred due a combined effect of nanocapsules and maltodextrin through the interaction between amino groups of chitosan and sialic acid residues on mucosa as well as the wetting of the maltodextrin that facilitates the mucosa dehydration, and hence the retention of drug. Therefore, the nanocapsules have an important role in the granule design as a mucoadhesive system.

Keywords: granules, nanocapsules, maltodextrin, phenytoin, mucoadhesion.

1. Introduction

Granulation is defined as a process of converting small particles in larger agglomerates in which the original particles can be still distinguished (BURGGRAEVE et al., 2013; JOSHI et al., 2017; VENGATESON; MOHAN, 2016). Understanding the granulation behavior contributes to predict and to improve the granule properties (BURGGRAEVE et al., 2013; PARIKH, 2005). Many studies have been focused on granule growth (CHEN et al., 2017; NIEUWMEYER; VAN DER VOORT MAARSCHALK; VROMANS, 2008; VAN DEN DRIES; VROMANS, 2002) and binder distribution (SMIRANI-KHAYATI et al., 2009). The granule growth in the wet granulation involves the nucleation phase, coalescence and breakage. These mechanisms occur simultaneously in the fluid bed (BURGGRAEVE et al., 2013). In general, the granules are evaluated regarding their flow properties (BACHER et al., 2008; SHAH; TAWAKKUL; KHAN, 2008), drug content uniformity (VAN DEN DRIES; VROMANS, 2002), and dissolution behavior (KINOSHITA et al., 2017).

The use of nanocapsules in the granulation process has been explored by our research group as a strategy to obtain solid dosage forms from liquid nanocapsules suspension. Friedrich and co-workers (2010) reported the production of granules containing dexamethasone-loaded nanocapsules by wet granulation. This approach improved the physicochemical stability of the formulation, which showed a good recovery of nanocapsules after granules redispersion in water. More recently, fluidized bed granules containing unloaded lipid-core nanocapsules were produced (ANDRADE et al., 2018), reporting the important role of the chitosan coating of the nanocapsules to obtain water-redispersible granules. Oliveira et al. (data not published) developed fluidized bed granules containing phenytoin-loaded nanocapsules, demonstrating their good technological properties and superior anticonvulsant activity. Further studies are necessary to elucidate the mechanism of the granule growth and evaluate if their mucoadhesion behavior could explain the best performance *in vivo*.

The main advantage of a mucoadhesive system is to extend the residence time, enhancing drug absorption in the gastrointestinal tract (NETSOMBOON; BERNKOP-SCHNÜRCH, 2016). Therefore, the interaction between the formulation and the mucus plays an important role in the drug oral bioavailability. The mucoadhesion is the state in which two materials adhere to each other through interfacial forces for a period of time (MANSURI et al., 2016). The mucus is a barrier to exogenous substances that needs to be overcome by drug to reach the underlying epithelium (GROO et al., 2013).

Fonseca and co-workers (2014) proposed a mucoadhesive system nasal administration of nanoencapsulated olanzapine. An increase the retention of drug on the nasal mucosa by electrostatic interaction between cationic amphiphilic methacrylic copolymer-functionalized poly(ε-caprolactone) nanocapsules and mucin chains was reported. Chaves et al. (2017) reported a higher retention time on the mucosa and higher amount of permeated drug through porcine sublingual mucosa by the encapsulation of carvedilol in polymeric nanocapsules, as an approach to carvedilol sublingual administration. In addition, Frank et al. (2017) demonstrated an increase the penetration and adhesion of imiquimod in vaginal tissue using chitosan-coating polymeric nanocapsules, as suspension or hydrogel.

In this scenario, the current study aims to assess the nanometric properties of redispersed granules containing phenytoin-loaded nanocapsules, evaluating the impact of the presence of the nanostructured material on the granule growth and on their mucoadhesion properties, assessing if the mucoadhesive behavior could explain the superior anticonvulsant effect of the redispersed granules containing phenytoin (PH), which was chosen as model drug because is a good candidate for nanoencapsulation. It has a narrow therapeutic index, which requires plasma monitoring (DELEU; AARONS; AHMED, 2005), and causes severe adverse effects such as hypotension and cardiac arrhythmias (BATCHELOR; APPLETON; HAWCUTT, 2015).

2. Materials and Methods

2.1 Materials

Poly(ε-caprolactone) (PCL) (MW = 80,000 g.mol^{-1}), sorbitan monostearate, low molar weight chitosan (MW = 50,000-190,000 g.mol^{-1}; 75-85% deacetylation) and pancreatin (porcine pancreas) were supplied by Sigma Aldrich (São Paulo, Brazil). Polysorbate 80 was acquired from Vetec (Rio de Janeiro, Brazil), soybean lecithin (Lipoid® S75) was obtained from Lipoid (Ludwigshafen, Germany), and grape seed oil from Delaware (Porto Alegre, Brazil). Maltodextrin (dextrose equivalent 9 – 15%) was supplied by Fagron (São Paulo, Brazil). Phenytoin was kindly donated by Cristália (São Paulo, Brazil). All other reagents and solvents were analytical or pharmaceutical grade.

2.2 Preparation and characterization of nanocapsule suspension

Suspensions of phenytoin-loaded nanocapsules (PH-LNC) were produced by the interfacial deposition of preformed polymer method (JÄGER et al., 2009; VENTURINI et al., 2011). Poly(ε-caprolactone) (1.00 g), sorbitan monostearate (0.385 g), grape seed oil (1.65 mL), and phenytoin (0.025 g) were dissolved in acetone at 40°C, while lecithin (0.60 g) was solubilized in ethanol. These organic phases were mixed and injected into an aqueous solution containing polysorbate 80 (0.77 g). Afterwards, acetone was eliminated under reduced pressure in rotavapor. The final volume was adjusted to 100 mL. The chitosan coating (0.6% w/v) of the nanocapsules was prepared using 1% acetic acid solution, kept under magnetic stirring overnight at 25°C. These suspensions were characterized by photon correlation spectroscopy (PCS) and electrophoretic mobility using a Zetasizer Nano ZS (Nanoseries®, Malvern Instruments, UK) to obtain the ȥ-average diameter and zeta potential values, respectively. The samples were diluted in filtered ultrapure water and in 10 mmol L^{-1} NaCl solution, respectively. The pH of the formulations was determined in a calibrated potentiometer (Digimed, DM-22, Campo Grande, Brazil). To assess the drug content, the samples were dispersed in acetonitrile, sonicated for 30 min, and centrifuged at 1,597 x g for 20 min before HPLC analysis.

2.3 Production of fluidized bed granules containing phenytoin-loaded nanocapsules

Fluidized bed granules were produced by granulation of a mixture of maltodextrin and phenytoin (substrate) with a suspension of PH-LNC, as binder, sprayed from the top down onto the fluidized bed (MiniGlatt, Glatt Air Techniques Inc., Binzen, Germany). The suspensions were used within their stability time (21 days). Nanocapsule suspensions were sprayed at a constant rate of 0.1 $g.min^{-1}$, using the following conditions: air flow (10-13 $m^3.h^{-1}$), atomizing air pressure (0.7 bar), and fluidization air temperature (80ºC). Maltodextrin and phenytoin (1:0.004 w/w), used as the substrate (100 g), were mixed for 20 min in a previous step of the granulation. The granules obtained were called as $PH\text{-}LNC_G$. Moreover, for the mucoadhesion studies, granules containing phenytoin (PH_G) were produced using only water as the binder system in order to evaluate the influence of the nanocapsules. After spraying the suspension, the powder was collected, storage in desiccator, protected from light, for further analyses.

2.4 Physicochemical characterization of fluidized bed granules containing phenytoin-loaded nanocapsules

2.4.1 Granule dose uniformity

An amount of powder (10 g) was randomly distributed in four quadrants. The powder sampling was collected in the anticlockwise in each quadrant with 78 cm^2 of area. The minimum number of samples (n) was calculated from $n = \sqrt{N}$, where N is the batch size in grams (GIL, 2010). Taking into account a batch of approximately 110 g, three samples of each quadrant (n = 12) were collected in an equivalent amount of powder with a theoretical drug content of 4 $mg.g^{-1}$. A validated analytical method by High Performance Liquid Chromatography (Shimadzu LC-20A system; SPD-M20A photodiode-array detector; Phenomenex C18 column, 150 mm x 4.6 mm) with following parameters was used: injection volume of 20 µL, flow rate of 1 $mL.min^{-1}$, and detection wavelength of 210 nm. The samples were dispersed in the mobile phase (acetonitrile:water 50:50), sonicated for 60 min, centrifuged at 1,597 x g for 20 min, and filtered (0.45 µm Millipore®) before HPLC analysis.

2.4.2 Growth behavior

Fluidized bed granules were produced as described in *section 2.3*. During the spraying of the nanocapsule suspension, the process was stopped after each 50 mL of the suspension was sprayed, followed by the sampling of about 1.5 g of the granules for particle size distribution analysis by laser diffraction (Mastersizer 2000, Malvern, UK) equipped with a dry powder disperser (Scirocco 2000, Malvern, UK) and for morphological analyses by scanning electron microscopy (SEM; JEOL, JSM 6060, Tokyo, Japan) at the *Centro de Microscopia e Microanálises* - UFRGS (Porto Alegre, Brazil). The samples were placed on double-sided carbon adhesive tape under aluminium stubs, gold sputtered and visualized in a microscope operating at 10 kV. The growth index (*GI*) was evaluated by Eq. (1) adapted from Chen et al. (2017).

$$GI\ (\%) = \frac{dm - d0}{d0}\ x\ 100 \qquad (1)$$

where d_0 and d_m are the initial diameter and mean diameter at specific sprayed suspension volume, respectively.

2.4.3 Redispersion behaviour

Fluidized bed granules were reconstituted in water to reach the same drug concentration of the original nanocapsules (0.225 mg.mL^{-1}). Redispersed granules containing phenytoin-loaded nanocapsules (PH-LNC$_{RG}$) were characterized by photon correlation spectroscopy (PCS) and electrophoretic mobility using a Zetasizer Nano ZS (Nanoseries®, Malvern Instruments, UK), as described in *section 2.2*. The pH of the formulations was determined in a calibrated potentiometer (Digimed, DM-22, Campo Grande, Brazil). To assess the drug content, redispersed granules were placed on mobile phase (acetonitrile:water 50:50), sonicated for 60 min. Then, the samples were centrifuged (1,597 x g for 20 min), and filtered supernatant before HPLC analysis (*section 2.4.1*). The experiments were carried out in triplicate of batches. For SEM analysis, the granules were deposited on silicon wafer, and covered with ultrapure water. After 5 min, the liquid was removed using an absorbent paper. Thereafter, the samples were gold sputtered, and the stubs were placed on a desiccator overnight before microscopic analysis at 10 kV. Morphological analyses were carried out by scanning electron microscopy (SEM; JEOL, JSM 6060, Tokyo, Japan) at the *Centro de Microscopia e Microanálises* - UFRGS (Porto Alegre, Brazil).

2.5 *In vitro* drug release studies

In vitro drug release studies from redispersed granules and the original nanocapsule suspension were performed on dialysis bags (10 kDa molecular weight cutoff, Sigma Aldrich, Brazil) closed with clamps and submerged in 80 mL of simulated intestinal fluid (pH 7.5 ± 1.0) at 37°C under sink conditions. At predetermined times, aliquots of 2 mL were withdrawn and replaced with fresh medium. The samples were centrifuged at 7,280 x g for 10 min for avoiding membrane saturation by pancreatin aggregates before filtering (Millipore® 0.45 µm), and analysed by HPLC. The diffusion profile of an ethanolic solution of phenytoin (PH$_S$) at concentration of 0.225 mg.mL^{-1} was also evaluated. Each dialysis experiment was performed in triplicate. Calibration curves in simulated intestinal fluid (n = 3) were made to determine the drug concentration, showing linearity (r = 0.998) in the range of 0.1 to 12.5 µg.mL^{-1}.

2.6 Mucoadhesion studies

2.6.1 Preparation of porcine mucosa of the small intestine

Small intestinal mucosa samples were obtained from 3 pigs immediately after slaughter at local slaughterhouse (Porto Alegre, Brazil). The underlying connective tissues were removed to isolate the mucosal membrane, which were subsequently washed with running water from lumen to remove non-digested food and lastly with cold ultrapure water. The porcine intestinal mucosa was cut into pieces (16 cm^2) with thickness around 0.8 mm, and frozen at -20°C until use in the mucoadhesion experiments (maximum storage time: 30 days). The intestinal mucosa was thawed for approximately 15 min at room temperature before the experiment.

2.6.2 Washability study

The mucoadhesive ability of phenytoin ethanolic solution (PH_S), phenytoin-loaded nanocapsules (PH-LNC), their redispersed granules (PH-LNC_{RG}), and redispersed granules containing phenytoin (PH_{RG}) was evaluated in washability studies (n = 3) (CHAVES et al., 2017; CONTRI et al., 2014). A simulated fluid intestinal (pH 7.5 ± 1.0) was fluxed at 0.7 $mL.min^{-1}$ by the action of a pump (Gilson; Minipuls 3, France) over the modified manual Franz diffusion cells (area of 0.9 cm^2), which were maintained under magnetic stirring at 37°C for 5 h of the experiment. Initially, the formulations (200 µL) were placed in contact with the mucosa for 30 min to allow the interaction between them. At predetermined time intervals, the outgoing fluid was collected and analysed by HPLC. Samples containing non-encapsulated phenytoin (PH_S and PH_{RG}) were diluted, centrifuged, and filtered to the HPLC assay, while PH-LNC and PH-LNC_{RG} were submitted to an extraction process, as described in *sections 2.2 and 2.4.1*, respectively. At the end of the experiment, the permeated drug to the receptor compartment was filtered (0.45 µm, Millipore®) as well as phenytoin from intestinal mucosa was extracted with acetonitrile, vortexed, sonicated for 30 min and filtered. Both samples were analysed by HPLC. The analytical method used to assay the drug in the mucosa showed specificity, good linearity (r = 0.998, n = 3) in the range of 4.95 – 19.2 $µg.mL^{-1}$, adequate intra-day (3.36%) and inter-day precision (4.33%). The recoveries were between 71.27% (PH_{RG}) and 96.41% (PH-LNC_{RG}). Limit of quantification (LoQ) and limit of detection (LoD) were 3.2 and 0.95 $µg.mL^{-1}$, respectively.

2.6.3 Mucoadhesion measurements

Mucoadhesion measurements were carried out using a texture analyser (TA.XT plus, Stable Micro Systems, Goldaming, UK) with adhesion apparatus (A/MUC). The intestinal tissues (approximately 5 cm^2) were cut, hydrated for 30 - 60 s with simulated intestinal fluid at 37°C, and attached to the cylindrical probe (1.2 cm^2) by double-face tape (Scotch® 9400, 12 mm x 30 m). Each formulation was placed on the sample holder. Experimental conditions such as the contact time, applied force and probe speed were selected based on preliminary tests. Three batches of intestinal mucosas were used for each sample. The following parameters were used to compare the different formulations: the upper platform was moved down near to the formulation at a constant speed 2 $mm.s^{-1}$ until a compressive force of 0.2 N during 900 s (contact time) at 0.05 $mm.s^{-1}$ was reached. The probe was removed at 2 $mm.s^{-1}$ and the maximum detachment force (N) and work of adhesion (N.mm), represented by the area under the force versus distance curve, were calculated. In order to confirm the reproducibility of the experiment, 6 measurements were performed for each formulation.

2.7 Statistical analysis

The data were expressed in mean ± standard deviation (SD). One-way ANOVA was carried out for multiple groups comparison using the post-hoc Turkey test, while test *t* Student was used to compare two groups. A level of $p < 0.05$ was considered statistically significant.

3. Results and discussion

3.1 Granule dose homogeneity

The real-time quality assessment of a product is an efficient way to control the granulation process, allowing to adjust parameters to tailor the product properties (BURGGRAEVE et al., 2013). Granules containing phenytoin-loaded nanocapsules ($PH\text{-}LNC_G$) were produced through a single-step process in a fluid bed (granulation and drying). They were obtained using maltodextrin/phenytoin as substrate and phenytoin-loaded nanocapsules as a liquid binder to achieve a total drug content of about 4 $mg.g^{-1}$. A volume of nanocapsule suspension (200 mL) was sprayed onto the powder bed. The phenytoin-loaded nanocapsules (PH-LNC) had z-average diameter

of 162 ± 2 nm with low polydispersity index (0.15 ± 0.02), and zeta potential of 16 ± 1 mV. Their drug content was close to 0.225 $mg.mL^{-1}$ and their pH was of 4.00 ± 0.03. Dose uniformity of the fluidized bed granules was assessed by HPLC. An amount of powder equivalent to 10% mass of batch size was randomly distributed in four quadrants. Three samples of each quadrant (n = 12) were collected and analysed by HPLC. Fig. 1 shows the phenytoin content in all quadrants, which were close to the expected concentration (4 $mg.g^{-1}$) with a relative standard deviation (RSD) of 1.66%. FDA recommends RSD < 5% to ensure good powder blends homogeneity (FDA, 2003). These results can be explained by the ability of fluid bed granulation to provide a more uniform drug distribution in the final product (FAURE; YORK; ROWE, 2001; PARIKH, 2005), even when compared to high shear granulators that can lead to in-homogeneity of drug due to granule breakage phenomena (VAN DEN DRIES et al., 2003; VAN DEN DRIES; VROMANS, 2002).

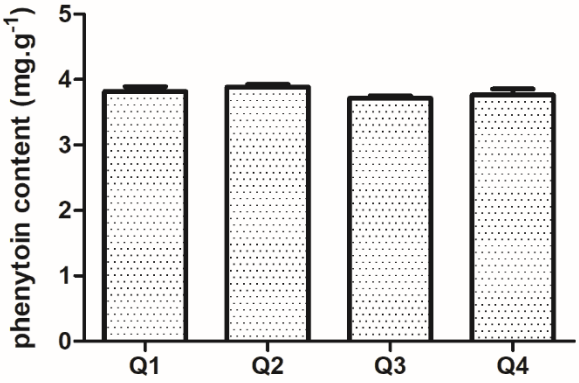

Fig. 1. Phenytoin content ($mg.g^{-1}$) of the fluidized bed granules containing nanocapsules (PH-LNC_G) distributed in each quadrant (Q) (n = 3).

3.2 Granule growth behavior

In order to obtain a better understanding of the mechanism of granule formation and to monitor the quality of the final product, a granule growth study was carried out. The effect of the volume of nanocapsule suspension sprayed during the granulation process on the mean particle size was evaluated (Fig. 2A). A linear correlation (r = 0.9863) between the suspension volume and granule size was found. Smirani-Khayati et al. (2009) also established a linear relationship between granule size and binding liquid transfer coefficient, using water as binder.

Considering the high amount of maltodextrin in the mixture (phenytoin + maltodextrin), representing more than 99% of the substrate, the growth of the granule size was compared to this raw material. In our study, the granule growth index increased 135% in relation to maltodextrin primary particles, reaching a D_{50} of 106 µm (SPAN = 1.786) at the end-point of the granulation. The narrow granule size distribution can be explained by similar amount of binder in all particles (IVESON et al., 2001). The spreading the binder in the powder bed is crucial to the granulation process (FAURE; YORK; ROWE, 2001). In the current study, a uniform final product was obtained with agglomerates particles, suggesting a good covering the binder. It is known that the particle agglomeration mechanism is mainly controlled by the binder droplet size, the contact with the powder bed and the humidity (FAURE; YORK; ROWE, 2001). Chen and co-workers (2017) proposed that the particle growth could be controlled by agglomeration at the early stages and layering at the end of the process.

The granulation process involves collisions between wetted particles as well as with the equipment wall resulting in large granules and excessive fines, one of the most common problem faced during the fluid bed granulation (BURGGRAEVE et al., 2013; NIEUWMEYER; VAN DER VOORT MAARSCHALK; VROMANS, 2008). Nieuwmeyer et al. (2008) defined that fines corresponds to particles < 100 µm, which depend on granule moisture content, size and composition. Radar charts of the granules at the end of the process (Fig. 2B) show only 10% of particles (d0.1(v)) having a particle size smaller than 100 µm, demonstrating that the granules obtained had low amount of fines. Moreover, the maintenance of an asymmetric shape in all radar charts (Fig. 2B) suggests a controlled granule growth. A reasonable balance of binding and breakup forces during fluid bed granulation provides a controlled agglomeration and granule growth, decreasing the production of fines (PARIKH, 2005).

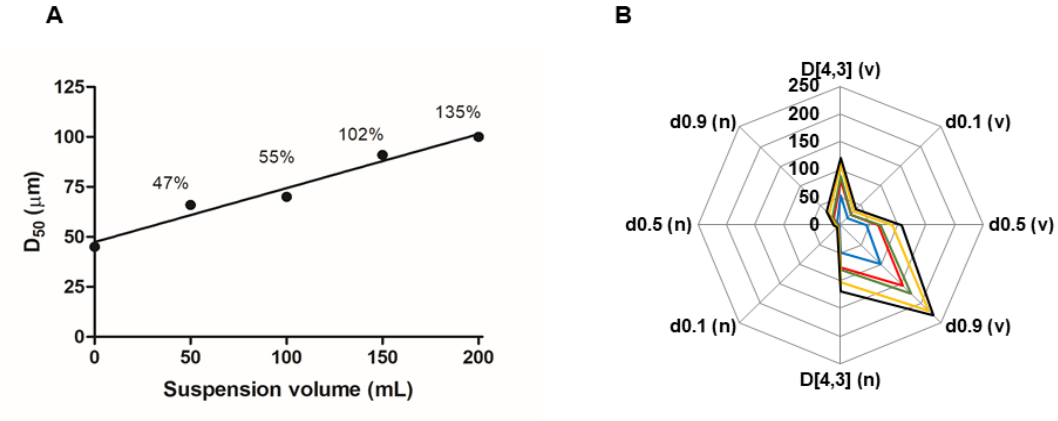

Fig. 2. Correlation between the particle size (µm) measured by laser diffraction after spraying the nanocapsule suspension volume and the granule growth index (%). (B) Radar charts built from particle size distribution data of the fluidized bed granules obtained by laser diffraction. Particle size distribution plots of raw maltodextrin primary particles (blue), granules produced using a sprayed suspension volume of 50 mL (red), 100 mL (green), 150 mL (yellow), and 200 mL (black). D[4,3] (v) – mean diameter based on volume-weight; d0.1 (v) – diameter based on volume at percentile 10; d0.5 (v) – diameter based on volume at percentile 50; d0.9 (v) – diameter based on volume at percentile 90; D[4,3] (n) – mean diameter based on number-weight; d0.1 (v) – diameter based on number at percentile 10; d0.5 (v) – diameter based on number at percentile 50; d0.9 (v) – diameter based on number at percentile 90 under the distribution curve.

In order to improve this discussion, SEM analyses were carried out. Fig. 3 shows the granule growth from the primary particles of maltodextrin (raw material) and after the addition of the binder (nanocapsule suspension). At the early stage, a mixture of primary particles (maltodextrin and phenytoin) collides with each other. Then, the binder is sprayed, and its droplets are deposited onto the particles in a wetting zone (BURGGRAEVE et al., 2013; PARIKH, 2005). After reaching a spraying volume of 50 mL of the suspension, the coexistence of primary particles and initial nuclei/granules can be observed, suggesting an insufficient amount of binder for wetting the particles. After spraying 100 mL of suspension, no primary particles were found, while well-defined bridges between the granules (around 100 µm) could be visualized. The evidence of the formation of granules with the same amount of binder (blank

nanocapsules) was shown by SEM images by our group (ANDRADE et al., 2018), which showed good flow properties. Almost at the same time, primary particles disappear, suggesting that the binder is homogeneously distributed in the powder bed, according to Smirani--Khayati et al. (2009).

At the end stage, an increase of binder volume promoted an increase in the granule size. This growth stage involves the coalescence and consolidation of the particles, originating large agglomerates (BURGGRAEVE et al., 2013; CHEN et al., 2017). Initially, the particles are held together by liquid bridges that contain a solute material, that subsequently solidifies by the solvent removal, originating solid bridges (PARIKH, 2005; ZAFAR et al., 2017). At the end-point of the granulation, the granules, with a moisture content lower than 5%, showed ‘pop-corn’ – type appearance due to the low deformability during granule collisions that occur in fluid bed granulation, as showed by Parikh (2005).

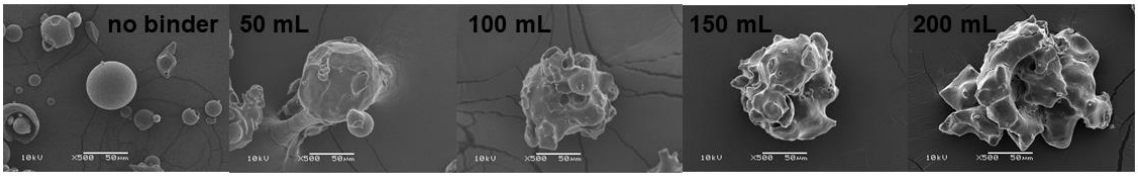

Fig. 3. SEM images of the primary particles (maltodextrin), and granule growth from spraying nanocapsule suspension (50 to 200 mL) at 500x magnification.

According to Iveson and co-workers (2001), the nucleation mechanism depends on binder droplet size. The nucleation will occur by the distribution of small binder drops on the particle surface, which will start to coalescence. A uniform wetting and a controlled nucleation depend on the degree of binder dispersion in the powder bed. The SEM images of the granules before (Fig. 4A) and after redispersion in water (Fig. 4B) showed that nanocapsules are adsorbed on the granule surface and on solid bridges and that after redispersion they are released in water together with some maltodextrin/phenytoin/nanocapsules agglomerates. Based on the literature and these data, a schematic illustration of the granule structure was proposed (Fig. 4C). In this model, the granules are covered by nanocapsules in their extension during the nucleation and growth phase.

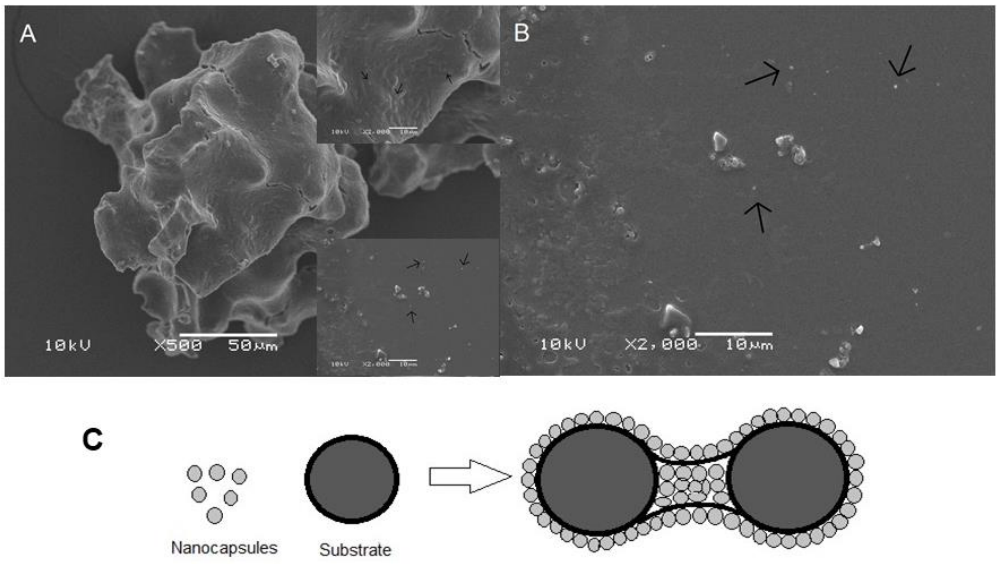

Fig. 4. SEM images of (A) fluidized bed granules, (B) recovered nanocapsules after granules reconstitution in water and (C) schematic illustration of the proposed granule structure. The black arrows indicate the presence of nanocapsules on the surface (top right corner) and on solid bridges granule (bottom right corner).

3.3 Characterization of the redispersed granules

A drying process, such as freeze-drying, spray-drying, and fluidized bed drying, can affect the redispersibility of powders, influencing the recovery of nanoparticles (BHAKAY et al., 2014). Therefore, to evaluate the recovery of the nanometric properties, the granules (PH-LNC_G) were reconstituted in water at the same concentration of their original nanocapsule suspension. The redispersed granules (PH-LNC_{RG}) showed a ζ-average diameter of 208 ± 42 nm similar to that observed for nanocapsules ($p > 0.05$), and a polydispersity index of 0.46 ± 0.07 due to the presence of agglomerates in the aqueous medium, as can be visualized in Fig. 4B. The zeta potential (+16 ± 3 mV) of the redispersed granules remained unchanged after the granulation process, indicating no destabilization of the chitosan coating during the granule formation. The drug content for PH-LNC_{RG} was similar to the expected concentration (0.225 $mg.mL^{-1}$). Besides that, the highest pH of the redispersed granules (5.10 ± 0.13), compared to original suspension, is due to the presence of maltodextrin and the acetic acid removal by evaporation, which was used to dissolve the chitosan. Therefore, redispersion of the granules recovered nanocapsules with similar properties compared with the original suspension, excepting the pH value.

3.4 *In vitro* drug release

The granulation process has been used to improve powder flow properties, drug content uniformity and to tailor the dissolution behavior (BURGGRAEVE et al., 2013; SMIRANI-KHAYATI et al., 2009). Fig. 5 shows that phenytoin was fully diffused from ethanolic solution (PH_S) after 4 h. On the other hand, a controlled release profile up to 48 h was shown by the redispersed granules (PH-LNC_{RG}) and their original nanocapsules (PH-LNC). Up to 12 h, similar drug release behavior was observed for the redispersed granules and the original nanocapsules suspension. After that, the redispersed granules showed a faster drug release compared with the original suspension, as expected due to the presence of a large amount (90%) of non-encapsulated phenytoin in the substrate. The similar release behaviour at the earlier stage can be explained by the release of the phenytoin from the nanocapsules on the surface of the granules, which are barrier that difficult the release of the non-encapsulated drug from the inner granule compartment. Although there is a low amount of encapsulated phenytoin is the granules (10%), the release of this drug is expected to last a long time and depends on its diffusion from the oil core to the intestinal fluid. This phenomenon is predictable taking into account the phenytoin log D of 2.52, which allows to classify its mechanism of encapsulation in polymeric nanocapsules as type III (OLIVEIRA et al., 2013), in which part of the drug is absorbed on the polymeric wall and the other part is dispersed in the oil core. On the other hand, the faster drug release from the redispersed granules after 12 h can be explained by the breakup of the agglomerates, releasing the nanocapsules to the medium and increasing the dissolution of the non-encapsulated phenytoin of the granules.

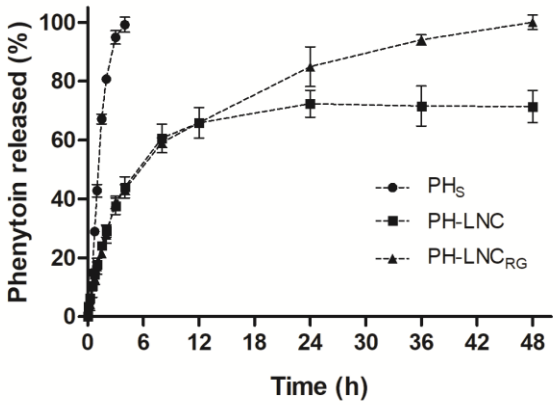

Fig. 5. Drug release profiles of phenytoin solution (PH_S), phenytoin-loaded nanocapsules (PH-LNC) and redispersed granules containing phenytoin-loaded nanocapsules (PH-LNC_{RG}) in simulated intestinal fluid (n = 3).

3.5 *In vitro* mucoadhesion

In vitro mucoadhesion studies are useful for screening mucoadhesive systems, elucidating their adhesion mechanisms (IVARSSON; WAHLGREN, 2012; SRIAMORNSAK; WATTANAKORN; TAKEUCHI, 2010). In this work, the mucoadhesion studies were carried out using two methods (washability and tensile test). The porcine intestinal mucosa model was chosen because it is the closest to human intestinal mucus (GROO et al., 2013). Based on the small intestinal volume of about 130 mL and its transit time of 3 - 4 h (MUDIE; AMIDON; AMIDON, 2009), a simulated intestinal fluid flow of 42 $mL.h^{-1}$ was used in the washability studies. This flow allows evaluating the adhesion of the formulations to porcine intestinal mucosa under action of a simulated intestinal flux. The previous contact time of the formulation with the mucosa was 30 min since interaction equilibrium is rapidly reached (10 min) (BARRATT et al., 2001).

Fig. 6 shows that the phenytoin was fully washed after 5 h of applying the solution (PH_S) or the PH-LNC. No statistical difference was found between these two groups ($p > 0.05$). On the other hand, the amount of drug washed from PH-LNC after 5 h (95 ± 10%) was higher ($p < 0.05$) than from PH-LNC_{RG} (42 ± 1%), evidencing an important role of the granulation process on the mucoadhesion. Moreover, the effect of mucosa adherence on drug permeation was also evaluated assaying the amount of drug that reached the receptor medium during the experiment. A 8-fold increase in the permeated drug amount from PH-LNC_{RG} was observed when compared to the original nanocapsule suspension ($p < 0.05$). This result can be explained by the improved interaction between the redispersed granules and the intestinal mucosa, which can occur due to the presence of maltodextrin and the nanocapsules. To confirm this hypothesis, granules without nanocapsules were prepared, using water as binder, followed by their redispersion in water. Redispersed granules containing phenytoin (PH_{RG}) retained lower drug amount than PH-LNC_{RG} at interval time of 3 to 5 h ($p < 0.05$), although their amount of drug retained was higher than that showed by the PH-LNC. These results suggest a combined mucoadhesive effect promoted by the nanocapsules and the maltodextrin. However, the amount of permeated drug was

similar for PH-LNC$_{RG}$ and PH$_{RG}$ (25 ± 5% and 27 ± 11%, respectively) as well as the amount of drug remained on the mucosa surface (11 ± 6% and 18 ± 7%, respectively) ($p > 0.05$).

Based on these results, the structure of the granules has an important role on their aqueous redispersion, as previously discussed, and on their mucoadhesion properties. Two mechanisms may be involved in this effect. The chitosan on the nanocapsules surface interacts with mucin by electrostatic interaction between its amino groups and sialic acid residues on mucosa (MANSURI et al., 2016; VIEIRA et al., 2018). Moreover, maltodextrins are polysaccharides that have water absorption ability (PYCIA et al., 2016) and these wetting properties could facilitate the dehydration of the mucosa, resulting in retention of drug (CARRERAS; CANALES; MELERO, 2016) and channelling of it through tight junctions. Besides that, carboxyl groups in maltodextrin chemical structure could interact with mucus by hydrogen bonding (MANSURI et al., 2016). These mucoadhesion mechanisms have also been discussed by other authors. Sriamornsak and co-workers (2010) evaluated the mucoadhesion of pectin (polysaccharide) by atomic force microscopy and suggested that its mucoadhesive property could be due to the absorption mechanism on the mucin molecules or electrostatic repulsion between pectin and mucin. Vieira et al. (2018) demonstrated the higher *in vitro* mucoadhesion of chitosan-coated solid lipid nanoparticles than uncoated lipid nanoparticles due to electrostatic interaction between mucus and chitosan.

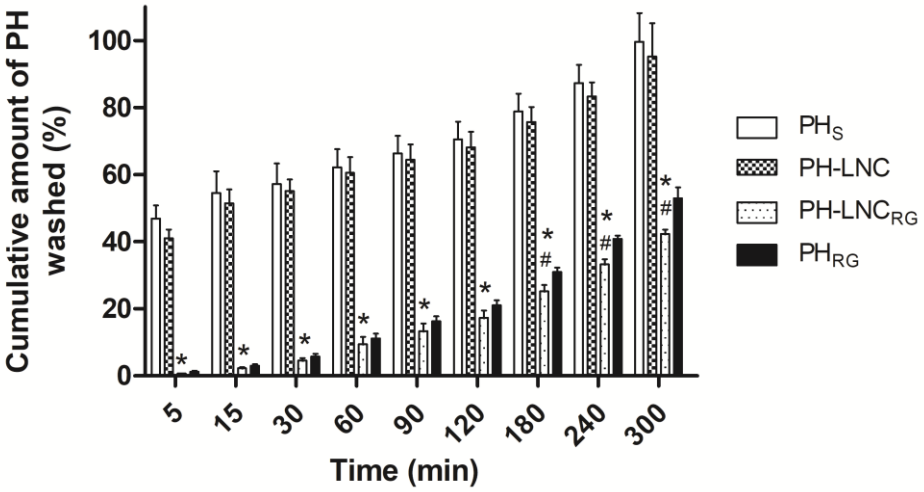

Fig. 6. Washability profiles (n = 3) of phenytoin solution (PH_S), phenytoin-loaded nanocapsules (PH-LNC), redispersed granules containing phenytoin-loaded nanocapsules ($PH\text{-}LNC_{RG}$), and phenytoin granules (PH_{RG}). *$PH\text{-}LNC_{RG}$ versus PH-LNC ($p < 0.0001$) and $^{\#}$ $PH\text{-}LNC_{RG}$ versus PH_{RG} ($p < 0.05$) (test *t* - Student).

Tensile methods (i.e. texture analyser or tensiometer) have been also investigated for the measurement of mucoadhesive strength (MANSURI et al., 2016). Tensile testing measures the force requires to cause detachment between a mucoadhesive formulation and a mucosal membrane (COOK et al., 2017). In this study, tensile measurements were carried out in order to further investigate the differences observed in the washability studies, as discussed above. A compressive force of 0.2 N was used, considering the mechanical axial force values (0 – 0.9 N) in the steady-state of the small intestine obtained from Sokolis' work (2017). According to Fig. 7, the required work to detach the redispersed granules ($PH\text{-}LNC_{RG}$) from the intestinal mucosa was higher than that required for PH_S ($p < 0.05$), as the distance travelled by probe for $PH\text{-}LNC_{RG}$ (38 ± 8 mm) was greater than for phenytoin solution (30 ± 3 mm). However, no statistical differences were found among the groups PH_S, PH-LNC, and PH_{RG} ($p > 0.05$). In the washability study, it was observed a significative mucoadhesive effect for PH_{RG} than PH_S, unlike the tensile test. This could be explained by the differences between the methods such as longer contact time and intestinal flow passage through the mucosa. On the other hand, a significant mucoadhesive effect occurs when nanocapsules and maltodextrin act together on intestinal mucosa, as shown in the washability test. Therefore, the best mucoadhesive properties of the redispersed granules containing nanocapsules depend on the design of fluid bed granule composition, regarding the importance of the nanocapsules as binder system. These findings could explain why the granules showed a superior anticonvulsivant activity *in vivo*, as suggested by Oliveira et al. (data not published).

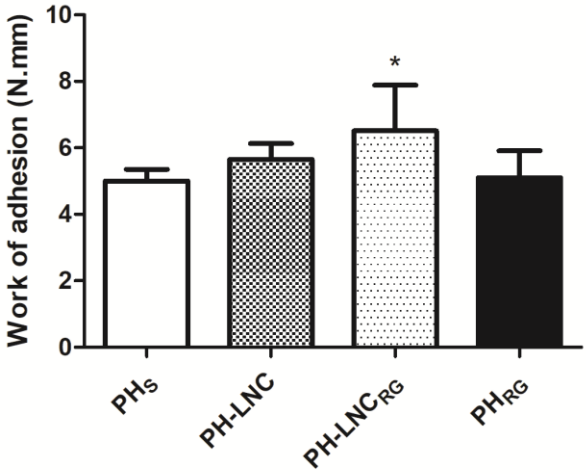

Fig. 7. Effect of phenytoin solution (PH_S), phenytoin-loaded nanocapsules (PH-LNC), redispersed granules containing phenytoin-loaded nanocapsules ($PH\text{-}LNC_{RG}$), and granules containing phenytoin (PH_{RG}) on work of adhesion against porcine intestinal mucosa (n = 6). * statistical difference ($p < 0.05$) between PH_S and $PH\text{-}LNC_{RG}$.

4. Conclusion

Fluidized bed granules containing phenytoin-loaded nanocapsules have granule growth behavior dependent on the volume of the binder sprayed to the maltodextrin/phenytoin bed. Nanocapsules were responsible for a controlled agglomeration of the particles. Homogenous granules were produced, whose redispersion in water led to the release of nanocapsules from the solid bridges and the granule surface, recovering the nanometric properties of the original suspension. The presence of nanocapsules surrounding the granules acted as a diffusion barrier for the release of the non-encapsulated drug from their inner compartment. Moreover, the redispersed granules improved the phenytoin adherence on the porcine intestinal mucosa due to a combined effect of the nanocapsules and maltodextrin, highlighting the important role of a nanostructured material on formation of the fluidized bed granules designed as mucoadhesive systems.

5. Declaration of interest

The authors report no conflicts of interest.

6. Acknowledgments

The authors thank Cristália Produtos Químicos e Farmacêuticos Ltda for gentle donation the pharmaceutical active (phenytoin) and Ouro do Sul slaughterhouse for porcine intestinal mucosa. The authors acknowledge the financial support of CNPq/Brazil, CAPES/Brazil and FAPERGS. E.G.O. thanks CAPES for her PhD fellowship.

References

ANDRADE, D. F. et al. Fluid bed granulation as an innovative process to produce dry redispersible nanocapsules: Influence of cationic coating of particles. **Powder Technology**, v. 326, p. 25–31, 2018.

BACHER, C. et al. Compressibility and compactibility of granules produced by wet and dry granulation. **International Journal of Pharmaceutics**, v. 358, p. 69–74, 2008.

BARRATT, G. et al. Polymeric Micro- and Nanoparticles as Drug Carriers. In: DUMITRIU, S. (Ed.). . **Polymeric Biomaterials**. 2. ed. New York: Marcel Dekker Inc., 2001. p. 753–783.

BATCHELOR, H.; APPLETON, R.; HAWCUTT, D. B. Comparing paediatric intravenous phenytoin doses using physiologically based pharmacokinetic (PBPK) modelling software. **Seizure**, v. 33, p. 8–12, 2015.

BENDER, E. A. et al. Hemocompatibility of poly(ε-caprolactone) lipid-core nanocapsules stabilized with polysorbate 80-lecithin and uncoated or coated with chitosan. **International Journal of Pharmaceutics**, v. 426, n. 1–2, p. 271–279, 2012.

BHAKAY, A. et al. Redispersible fast dissolving nanocomposite microparticles of poorly water-soluble drugs. **International Journal of Pharmaceutics**, v. 461, n. 1–2, p. 367–379, 2014.

BURGGRAEVE, A. et al. Process analytical tools for monitoring, understanding, and control of pharmaceutical fluidized bed granulation: A review. **European Journal of Pharmaceutics and Biopharmaceutics**, v. 83, n. 1, p. 2–15, 2013.

CARRERAS, J. J.; CANALES, P.; MELERO, A. Mucoadhesion of Polymeric Drug Delivery Systems : Polymeric Nanoparticles and its Interactions with the Intestinal Barrier. **JSM Nanotechnology & Nanomedicine**, v. 4, p. 1–5, 2016.

CHAVES, P. DOS S. et al. Carvedilol-loaded nanocapsules: Mucoadhesive properties and permeability across the sublingual mucosa. **European Journal of Pharmaceutics and Biopharmaceutics**, v. 114, p. 88–95, 2017.

CHEN, X. et al. Study on the fluidized bed granulation of fine-grained rutile concentrate. **Powder Technology**, v. 315, p. 53–59, 2017.

CONTRI, R. V. et al. Combined effect of polymeric nanocapsules and chitosan hydrogel on the increase of capsaicinoids adhesion to the skin surface. **Journal of Biomedical Nanotechnology**, v. 10, n. 5, p. 820–830, 2014.

COOK, S. L. et al. Mucoadhesion: A food perspective. **Food Hydrocolloids**, v. 72, p. 281–296, 2017.

DELEU, D.; AARONS, L.; AHMED, I. A. Estimation of population pharmacokinetic parameters of free-phenytoin in adult epileptic patients. **Archives of Medical Research**, v. 36, n. 1, p. 49–53, 2005.

FAURE, A.; YORK, P.; ROWE, R. C. Process control and scale-up of pharmaceutical wet granulation processes: a review. **European Journal of Pharmaceutics and Biopharmaceutics**, v. 52, p. 269–277, 2001.

FONSECA, F. N. et al. Mucoadhesive amphiphilic methacrylic copolymer-functionalized poly(Ɛ-caprolactone) nanocapsules for nose-to-brain delivery of olanzapine. **Journal of Biomedical Nanotechnology**, v. 11, n. 8, p. 1472–1481, 2014.

FOOD AND DRUG ADMINISTRATION. **Guidance for Industry. Powder Blends and Finished Dosage Units - Stratified In-Process Dosage**. Disponível em: <http://www.fda.gov/OHRMS/DOCKETS/98fr/03d-0493-gdl0001.pdf>. Acesso em: 6 fev. 2017.

FRANK, L. A. et al. The use of chitosan as cationic coating or gel vehicle for polymeric nanocapsules: Increasing penetration and adhesion of imiquimod in vaginal tissue. **European Journal of Pharmaceutics and Biopharmaceutics**, v. 114, p. 202–212, 2017.

FRIEDRICH, R. B. et al. Drying polymeric drug-loaded nanocapsules: the wet granulation process as a promising approach. **Journal of Nanoscience and Nanotechnology**, v. 10, n. 1, p. 616–621, 2010.

GIL, E. S. **Controle físico-químico de qualidade de medicamentos**. 3. ed. São Paulo: Pharmabooks, 2010.

GROO, A. C. et al. Fate of paclitaxel lipid nanocapsules in intestinal mucus in view of their oral delivery. **International Journal of Nanomedicine**, v. 8, p. 4291–4302, 2013.

IVARSSON, D.; WAHLGREN, M. Comparison of in vitro methods of measuring mucoadhesion: Ellipsometry, tensile strength and rheological measurements. **Colloids and Surfaces B: Biointerfaces**, v. 92, p. 353–359, 2012.

IVESON, S. M. et al. Nucleation, growth and breakage phenomena in agitated wet granulation processes: A review. **Powder Technology**, v. 117, n. 1–2, p. 3–39, 2001.

JÄGER, E. et al. Sustained release from lipid-core nanocapsules by varying the core viscosity and the particle surface area. **Journal of Biomedical Nanotechnology**, v. 5, n. 1, p. 130–140, 2009.

JOSHI, S. et al. To study and understand the process of wet granulation by fluidized bed granulation technique. **International Journal of Research in Pharmacy and Chemistry**, v. 7, n. 3, p. 232–238, 2017.

KINOSHITA, R. et al. Effects of wet-granulation process parameters on the dissolution and physical stability of a solid dispersion. **International Journal of Pharmaceutics**, v. 524, n. 1–2, p. 304–311, 2017.

MANSURI, S. et al. Mucoadhesion: A promising approach in drug delivery system. **Reactive and Functional Polymers**, v. 100, p. 151–172, 2016.

MUDIE, D. M.; AMIDON, G. L.; AMIDON, G. E. Physiological Parameters for Oral Delivery and In vitro Testing. **Molecular Pharmaceutics**, v. 49, n. 18, p. 1841–1850, 2009.

NETSOMBOON, K.; BERNKOP-SCHNÜRCH, A. Mucoadhesive vs. mucopenetrating particulate drug delivery. **European Journal of Pharmaceutics and Biopharmaceutics**, v. 98, p. 76–89, 2016.

NIEUWMEYER, F.; VAN DER VOORT MAARSCHALK, K.; VROMANS, H. The consequences of granulate heterogeneity towards breakage and attrition upon fluid-bed drying. **European Journal of Pharmaceutics and Biopharmaceutics**, v. 70, n. 1, p. 402–408, 2008.

OLIVEIRA, C. P. et al. An algorithm to determine the mechanism of drug distribution in lipid-core nanocapsule formulations. **Soft Matter**, v. 9, n. 4, p. 1141, 2013.

PARIKH, D. M. Introduction. In: PARIKH, D. M. (Ed.). . **Handbook of Pharmaceutical Granulation Technology**. 2. ed. New York: Taylor & Francis, 2005. p. 1–6.

PYCIA, K. et al. Maltodextrins from chemically modified starches. Selected physicochemical properties. **Carbohydrate Polymers**, v. 146, p. 301–309, 2016.

SHAH, R. B.; TAWAKKUL, M. A.; KHAN, M. A. Comparative Evaluation of Flow for Pharmaceutical Powders and Granules. **AAPS PharmSciTech**, v. 9, n. 1, p. 250–258, 2008.

SMIRANI-KHAYATI, N. et al. Binder liquid distribution during granulation process and its relationship to granule size distribution. **Powder Technology**, v. 195, n. 2, p. 105–112, 2009.

SOKOLIS, D. P. Experimental study and biomechanical characterization for the passive small intestine: Identification of regional differences. **Journal of the Mechanical Behavior of Biomedical Materials**, v. 74, p. 93–105, 2017.

SRIAMORNSAK, P.; WATTANAKORN, N.; TAKEUCHI, H. Study on the mucoadhesion mechanism of pectin by atomic force microscopy and mucin-particle method. **Carbohydrate Polymers**, v. 79, n. 1, p. 54–59, 2010.

VAN DEN DRIES, K. et al. Granule breakage phenomena in a high shear mixer; influence of process and formulation variables and consequences on granule homogeneity. **Powder Technology**, v. 133, n. 1–3, p. 228–236, 2003.

VAN DEN DRIES, K.; VROMANS, H. Relationship between inhomogeneity phenomena and granule growth mechanisms in a high-shear mixer. **International Journal of Pharmaceutics**, v. 247, n. 1–2, p. 167–177, 2002.

VENGATESON, U.; MOHAN, R. Experimental and modeling study of fluidized bed granulation: Effect of binder flow rate and fluidizing air velocity. **Resource-Efficient Technologies**, v. 2, p. S124–S135, 2016.

VENTURINI, C. G. et al. Formulation of lipid core nanocapsules. **Colloids and Surfaces A: Physicochemical and Engineering Aspects**, v. 375, n. 1–3, p. 200–208, 2011.

VIEIRA, A. C. C. et al. Mucoadhesive chitosan-coated solid lipid nanoparticles for better management of tuberculosis. **International Journal of Pharmaceutics**, v. 536, p. 478–485, 2018.

ZAFAR, U. et al. A review of bulk powder caking. **Powder Technology**, v. 313, p. 389–401, 2017.

7 DISCUSSÃO GERAL

7 DISCUSSÃO GERAL

O presente estudo propõe o desenvolvimento de pós e grânulos contendo nanocápsulas de fenitoína, avaliando a recuperação das suas propriedades nanométricas para obtenção de formulações adequadas para uso oral. A fenitoína foi escolhida, pois é um fármaco bastante utilizado no tratamento de crises parciais e generalizadas em crianças e adultos (MEGIDDO et al., 2016). Seu estreito índice terapêutico, graves efeitos adversos como arritmias cardíacas e efeitos neurológicos (BATCHELOR; APPLETON; HAWCUTT, 2015) e a recorrência das crises epilépticas, realçam a importância da investigação de formulações mais seguras e eficazes como alternativa ao tratamento convencional. Neste contexto, os sistemas nanotecnológicos podem ser uma boa estratégia para melhorar a atividade de fármacos que atuam no SNC (DIMER et al., 2015; RODRIGUES et al., 2016; ZANOTTO-FILHO et al., 2013), assim como já relatado para outras substâncias ativas (BERNARDI et al., 2012; GUTERRES et al., 2001; PAESE et al., 2009).

Inicialmente, foram desenvolvidas nanocápsulas de núcleo lipídico através do método de deposição interfacial do polímero pré-formado (FESSI et al., 1989). Estas nanoestruturas são formadas por um núcleo oleoso, contendo monoestearato de sorbitano, envolvidas por uma camada polimérica e estabilizadas por moléculas de polissorbato 80 (JÄGER et al., 2009; VENTURINI et al., 2011). Inicialmente, foram testados diferentes óleos e polímeros. No entanto, o óleo de semente de uva foi o mais adequado devido à boa solubilidade do fármaco no núcleo oleoso (0,16 mg/mL).

O óleo de semente de uva é composto por 90% de ácido graxos insaturados, majoritariamente o ácido linoleico (58-78%), seguido pelo ácido oleico (3-15%). Na sua constituição, são ainda encontrados compostos ativos como tocoferóis e outros componentes fenólicos, que contribuem para sua ação antioxidante, os quais dependem da origem e condições de processamento. O ponto de volatilização deste óleo é, aproximadamente, 190 a 230 °C, facilitando a sua manipulação em processos que requerem calor (BAIL et al., 2008). Ismail e colaboradores (2015) demonstraram que o óleo de semente de uva tem um efeito neuroprotetor contra lesão cerebral induzida por CCl_4 em ratos irradiados com raios-γ. Este efeito foi atribuído a sua capacidade de sequestrar radicais livres, regular a expressão de enzimas, como xantina oxidase (XO) e óxido nítrico sintase induzida (iNOS), e suprimir a resposta inflamatória.

A presença de moléculas de polissorbato 80 e lecitina na interface partícula-água aumentou a estabilidade da suspensão de nanocápsulas, originando partículas com perfil exclusivamente nanométrico e estreita distribuição de tamanho. Além disso, a poli(ε-caprolactona) (PCL) também auxiliou na sua estabilidade. Este polímero possui características de biocompatibilidade, biodegradabilidade (SINHA et al., 2004), e tem sido bastante utilizado em sistemas de liberação controlada (CORADINI et al., 2014; POHLMANN et al., 2013). As nanocápsulas de núcleo lipídico também foram revestidas com quitosana, que em trabalhos anteriores, foi demonstrada a sua hemocompatibilidade (BENDER et al., 2012) e melhora na atividade antimicrobiana de fármacos (CÉ et al., 2016). Além disso, as propriedades de mucoadesão (KHOR; LIM, 2003) e facilidade em atravessar barreiras biológicas (PREGO et al., 2005) da quitosana conferem às nanocápsulas a possibilidade de interagir com superfícies biológicas, aumentando a biodisponibilidade de fármacos utilizados pela via oral.

No capítulo 1, as nanocápsulas de núcleo lipídico foram desenvolvidas pelo método de deposição interfacial do polímero pré-formado e caracterizadas por diferentes técnicas de análise. As distribuições de tamanho de partícula das formulações pelas técnicas de Difração a Laser e Espalhamento de Luz Dinâmico, bem como a validação do método analítico para quantificação da fenitoína em Cromatografia Líquida de Alta Eficiência (CLAE) estão presentes nos Apêndices A e B desta tese, respectivamente.

As suspensões apresentaram aspecto homogêneo branco leitoso, tamanho nanométrico (158 a 168 nm), com estreita distribuição de tamanho, forma esférica e uma “impressão digital” obtida pela distribuição do tamanho de partícula das formulações em gráficos de radar. As nanocápsulas de fenitoína não-revestidas (PHT-LNC) mostraram um potencial zeta negativo, pH (6,5) e teor de fármaco de 0,25 mg/mL, enquanto que as nanocápsulas de fenitoína revestidas com quitosana (PHT-CS-LNC) apresentaram potencial zeta positivo, pH (4,0) e teor de 0,23 mg/mL, ambas com eficiência de encapsulação em torno de 95%, e estabilidade físico-química de 21 dias.

Os pós foram obtidos a partir da técnica de secagem por aspersão (*spray-drying*), utilizando os dois tipos de nanocápsulas. O desenvolvimento destes pós seguiu o fluxograma de otimização (Figura 4). Caso fosse obtido um pó adesivo (*sticky*) ou não redispersível ao final do processo, então uma nova concentração de adjuvante deveria ser testada. Um pó redispersível foi considerado otimizado após a

recuperação do perfil nanométrico da suspensão original. Diante disso, diferentes concentrações do adjuvante de secagem foram testadas. A maltodextrina foi escolhida como adjuvante, pois é um excipiente solúvel em água, aprovado pelo FDA, adequado para formulação adulta e pediátrica (BOUREZG et al., 2012; ROWE; SHESKEY; OWEN, 2012) e para a redispersão de pós contendo nanocápsulas (HOFFMEISTER et al., 2012; TEWA-TAGNE; BRIANÇON; FESSI, 2007).

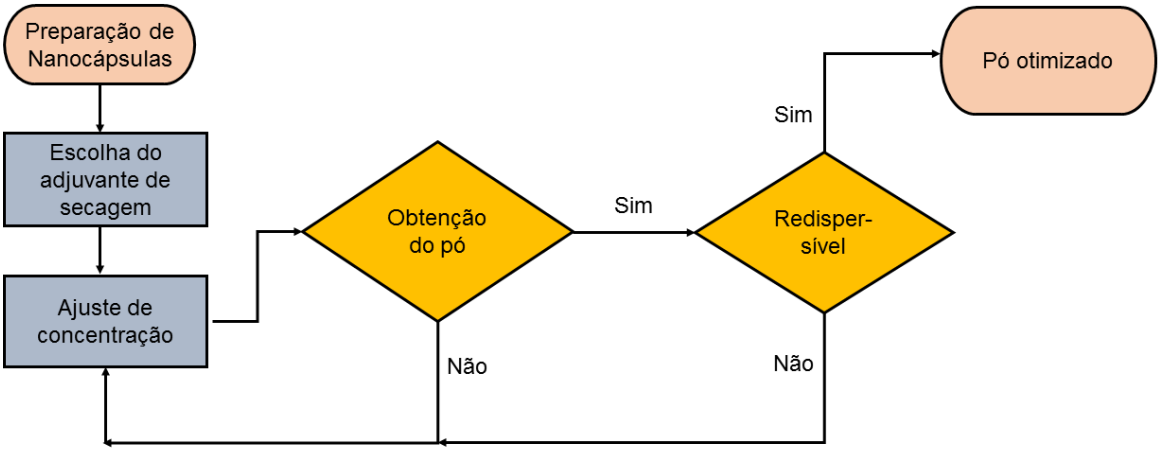

Figura 5 – Fluxograma de otimização do pó contendo nanocápsulas de núcleo lipídico.

Inicialmente, as nanocápsulas foram secas utilizando maltodextrina na concentração de 5% (m/v). Uma melhor redispersão foi observada com os pós contendo nanocápsulas revestidas com quitosana em relação àquelas sem revestimento, sugerindo que a carga de superfície tem um papel importante na redispersão dos pós. Para manter a estabilidade de sistemas coloidais, após o processo de secagem por aspersão, repulsões estéricas e eletrostáticas necessitam superar as forças atrativas (exemplo: van der Waals) entre as partículas (HONG et al., 2014).

No intuito de se obter um pó mais concentrado para posteriores estudos *in vivo*, uma quantidade mínima de excipiente de secagem foi necessária. Então, uma concentração menor de maltodextrina (1,75% m/v) foi testada, obtendo-se um pó não adesivo e redispersível contendo nanocápsulas com revestimento catiônico. Entretanto, não foi possível a secagem de nanocápsulas não-revestidas com essa concentração de adjuvante, pois o material ficou bastante aderido às paredes da torre de secagem. Isso pode ter ocorrido devido à quantidade insuficiente de adjuvante que

deveria proteger a estrutura das nanocápsulas de um estresse térmico (MÜLLER et al., 2000; TEWA-TAGNE; BRIANÇON; FESSI, 2006).

A partir desses resultados, os pós contendo nanocápsulas de fenitoína revestidas com quitosana (SD-PHT-CS-LNC) foram escolhidos para os estudos subsequentes. Estes pós foram obtidos com sucesso devido ao alto rendimento do processo (70%), à baixa água residual (< 2%) e ao teor próximo ao teórico (3,96 mg/g). Além disso, a manutenção do perfil granulométrico e da concentração de fármaco no pó durante 90 dias demostrou a boa estabilidade físico-química das nanocápsulas na forma sólida. Por outro lado, os pós mostraram um grande diâmetro de partícula (> 100 µm), com ampla distribuição de tamanho, apresentando-se como microaglomerados esféricos (índice de esfericidade = 0,75), em forma de cachos de uva. Contudo, após a redispersão em água, houve uma diminuição em cerca de 100x (~ 1 µm) o seu tamanho original e as nanocápsulas foram liberadas para o meio aquoso a partir da superfície destes microaglomerados.

Posteriormente, os pós foram reconstituídos em água ultrapura para se obter a concentração de fármaco de 0,25 mg/mL, demostrando uma parcial redispersibilidade (67 ± 4%) em meio aquoso em relação à suspensão original, bem como a recuperação de suas propriedades nanométricas. Estes apresentaram diâmetro médio de 345 ± 01 nm, índice de polidispersão de 0,36 ± 0,04, potencial zeta positivo (+20 ± 04 mV) e teor de fármaco (0,25 mg/mL). O pH em torno de 6,0 pode ser explicado devido à presença de grupos hidroxila da maltodextrina em meio aquoso. Quanto à estabilidade do pó reconstituído, houve manutenção das propriedades do mesmo após 24 horas, permanecendo estável durante esse período de armazenamento.

Os gráficos de radar das nanocápsulas de fenitoína revestidas com quitosana, baseados em suas distribuições de tamanho de partícula, em fluido gástrico simulado (SGF) e fluido intestinal simulado (SIF) ao longo do tempo (0, 1, 2 e 3 horas), apresentaram-se sobreponíveis. O mesmo comportamento foi observado para o pó reconstituído. O tamanho de partícula deve ser monitorado nestes fluidos no intuito de avaliar a degradação dos sistemas lipídicos (CARRIÈRE, 2016; KLINKESORN; MCCLEMENTS, 2009). A partir destes resultados, pode-se concluir que, tanto as nanocápsulas revestidas com quitosana, quanto seu pó redispersível apresentaram boa estabilidade gastrointestinal.

Embora estas formulações apresentem adequadas propriedades físico-químicas, é importante avaliar o impacto do processo de secagem por aspersão no

perfil de liberação do fármaco em um fluido gastrointestinal. A liberação do fármaco não encapsulado no meio gástrico (85%) foi mais baixa que em meio intestinal (100%) porque sua solubilidade é menor em pH ácido. No entanto, esta solubilidade dependente do pH foi superada através da nanoencapsulação da fenitoína. Diante disso, o perfil de liberação do fármaco a partir de nanocápsulas foi mais lento em relação ao da fenitoína não encapsulada em SGF e SIF e similar àquele obtido a partir do pó reconstituído em ambos os meios. A partir desses resultados, conclui-se que o processo de secagem foi responsável pela manutenção do controle de liberação da fenitoína a partir das nanocápsulas.

Os estudos *in vivo* foram realizados em colaboração com o Prof. Dr. Mauro Schneider Oliveira, do Laboratório de Psicofarmacologia e Neurotoxicidade, localizado no Departamento de Fisiologia e Farmacologia da Universidade Federal de Santa Maria (UFSM) e previamente aprovados pelo Comitê de Ética em Pesquisa Animal da mesma instituição (protocolo # 3273040416). Eles foram conduzidos de acordo com o Conselho Nacional de Controle de Experimentação Animal (CONCEA).

Um modelo agudo de indução de crises epilépticas por pilocarpina foi utilizado em camundongos adultos C57BL/6 de ambos os sexos, o qual têm sido bastante estudado pela semelhança com a epilepsia do lobo temporal em humanos (BORGES et al., 2003; CAVALHEIRO et al., 1991; CURIA et al., 2008). No comportamento pré-convulsivo nos camundongos, foi observada salivação, padrão típico da ação da pilocarpina, a qual ocasiona ativação de receptores muscarínicos, e consequentemente, de fosfolipase C, produzindo diacilglicerol (DAG) e inositol trifosfato (IP_3), levando a alterações nos íons sódio e potássio, promovendo um aumento da excitabilidade (FERNANDES; MAZZACORATTI; CAVALHEIRO, 2010; TAWFIK, 2011).

Durante os experimentos, foi registrado o tempo de latência das crises mioclônicas, das crises generalizadas, e duração do tempo destas crises generalizadas, de acordo com a escala de Racine (1972): 0. Nenhuma alteração no comportamento; 1. Movimento facial, hiperatividade; 2. cabeça balançando, tremor; 3. clônus unilateral do antebraço; 4. Clônus e *rearing* (número de levantamentos verticais) de membros anteriores bilaterais; 5. clônus bilaterais com perda de postura; 6. crises tônico-clônicas generalizadas, *status eplilepticus* ou morte. As fases 1-3 foram reconhecidas como crises mioclônicas e as fases 4-6 como crises generalizadas.

Inicialmente, os animais foram tratados pela via intraperitoneal (i.p.) com salina (grupo controle), suspensão de fenitoína em salina (grupo 1), suspensão de nanocápsulas não-revestidas contendo fenitoína (grupo 2), suspensão de nanocápsulas não-revestidas sem fenitoína (grupo 3), suspensão de nanocápsulas revestidas com quitosana contendo fenitoína (grupo 4), suspensão de nanocápsulas revestidas com quitosana sem fenitoína (grupo 5), na dose de 2,5 mg/kg (n = 5). Após 30 minutos, a pilocarpina foi injetada por via i.p. (300 mg/kg) de acordo com procedimentos padronizados (BORGES et al., 2003; FUNCK et al., 2014). Os animais foram observados por 60 minutos em relação à escala de Racine (1972). Os resultados destes experimentos estão presentes no Apêndice C desta tese.

Foi observado um aumento na latência para crises mioclônicas no grupo tratado com a dispersão de fenitoína (PHT) e no grupo tratado com nanocápsulas de fenitoína não-revestidas (PHT-LNC), comparando à salina. Por outro lado, não foi encontrada diferença estatística entre as nanocápsulas revestidas (PHT-CS-LNC) e a dispersão de fenitoína. Na latência e duração das crises generalizadas, também não foram observadas diferenças para todos os grupos. Estes resultados preliminares sugerem que a baixa concentração de fármaco na formulação (0,25 mg/mL), e consequentemente, uma menor dose atingida, pode ter contribuído para o limitado efeito anticonvulsivante da fenitoína. Além disso, a farmacocinética não-linear da fenitoína é outro fator que aumenta a variabilidade da resposta biológica.

Estudos apontam que doses mais altas de fenitoína (30-200 mg/kg) são utilizadas para atingir altas concentrações plasmáticas pela via oral que podem chegar à níveis terapêuticos (ALVARIZA et al., 2014; BURSTEIN et al., 1999). Diante disso, os pós contendo nanocápsulas foram reconstituídos em água no intuito de se obter uma formulação mais concentrada (1 mg/mL) do que a forma de suspensão e, portanto, atingir a maior dose possível de fenitoína (10 mg/kg/dia). Além disso, os pós contendo nanocápsulas com e sem fenitoína (1 mg/mL) apresentaram características nanométricas semelhantes às da suspensão original (0,25 mg/mL).

As formulações foram administradas por gavagem nos animais durante 7 dias para atingir a concentração terapêutica no estado de equilíbrio da fenitoína. Após 60 minutos da última administração oral, foi injetada a pilocarpina para induzir as crises convulsivas. Os animais foram divididos em quatro grupos, os quais foram tratados com água (controle) (1), suspensão de fenitoína não encapsulada (PHT) em água (2), pó redispersível contendo nanocápsulas catiônicas sem fármaco (SD-CS-LNC) (3) e

pó redispersível contendo nanocápsulas catiônicas de fenitoína (SD-PHT-CS-LNC) (4). Em relação ao efeito das formulações sobre as crises induzidas por pilocarpina, foi observado um aumento da latência para crises generalizadas no grupo tratado com pó redispersível contendo nanocápsulas de fenitoína catiônicas, quando comparado ao fármaco não encapsulado ($p < 0,05$) e ao pó contendo nanocápsulas catiônicas sem fenitoína ($p < 0,05$). Além disso, o pó redispersível reduziu a severidade das crises e aumentou o tempo de sobrevivência dos animais.

Os resultados *in vivo* deste capítulo corroboram com os dados publicados por Wang e colaboradores (2016), que desenvolveram nanopartículas não-eletroresponsivas e eletroresponsivas utilizando modelo de pilocarpina em ratos para avaliar o efeito anticonvulsivante. Os autores observaram que a solução de fenitoína não aumentou o tempo de latência para crises generalizadas, comparado ao controle, enquanto que as nanopartículas eletroresponsivas apresentaram uma maior latência para estas crises em relação às nanopartículas não eletroresponsivas.

Portanto, o pó redispersível contendo nanocápsulas de fenitoína apresentaram um efeito anticonvulsivante superior em relação ao fármaco não encapsulado. Esta boa performance *in vivo* pode ser correlacionada à ação da fenitoína nanoencapsulada, pois o grupo tratado com pó redispersível com nanocápsulas sem fármaco não apresentou efeito anticonvulsivante.

No capítulo 2 desta tese, os grânulos contendo nanocápsulas de fenitoína revestidas foram obtidos em leito fluidizado (Mini-Glatt, Glatt Air Techniques Inc., Ransey, NJ, USA). A escolha da maltodextrina, como substrato, e das nanocápsulas revestidas, como aglutinante, foi baseada nos resultados de experimentos iniciais que foram publicados por Andrade e colaboradores (2018). Os autores desenvolveram grânulos contendo nanocápsulas de núcleo lipídico brancas através da técnica de leito fluidizado. Eles demonstraram que o revestimento catiônico melhorou a redispersão aquosa dos grânulos, facilitando a recuperação das propriedades nanométricas da suspensão original. Este artigo se encontra no Apêndice D desta tese.

No desenvolvimento dos grânulos contendo nanocápsulas de fenitoína (FB-LNC_{PH}), foi utilizado um volume de 200 mL de suspensão de nanocápsulas (aglutinante) e uma mistura de maltodextrina e fenitoína (1:0,004), como substrato, para aumentar o teor de fármaco nos grânulos. Além disso, os grânulos contendo somente fenitoína (FB-PH) também foram produzidos para avaliar a influência das nanoestruturas no processo de granulação. Como a quantidade de fármaco na mistura

é baixa, então a técnica de diluição geométrica foi escolhida para misturar inicialmente os componentes. Além disso, a produção de grânulos de maior tamanho de partícula foi possível após a combinação da diluição geométrica com a mistura simples no próprio leito fluidizado. Isso porque na diluição geométrica ocorre uma trituração do pó com o uso do gral e pistilo, diminuindo o tamanho das partículas primárias e, consequentemente, aumentando a área superficial. Dessa forma, há mais pontos de contato que permitem a formação de grânulos maiores e mais fortes (PARIKH, 2005).

Os grânulos apresentaram bom rendimento (73-82%), com umidade abaixo de 5%, e teor próximo ao esperado (4 mg/g). Considerando que a granulação em leito fluidizado permite a obtenção de partículas com tamanho entre 100 e 2000 µm, somente os grânulos contendo nanocápsulas apresentaram diâmetro médio dentro deste intervalo (D[4,3] = 122 µm). Por outro lado, ambos os grânulos (FB-PH and FB-LNC_{PH}) tiveram estreita distribuição de tamanho (SPAN < 2), demonstrando a boa homogeneidade dos grânulos obtidos. O aumento de tamanho dos mesmos em relação à maltodextrina pura (D[4,3] = 50 µm) reflete o seu crescimento com uma fase de nucleação inicial, seguida por uma compactação do grânulo e crescimento (IVESON et al., 2001). Os grânulos FB-LNC_{PH} apresentaram um tamanho maior que os grânulos FB-PH (D[4,3] = 75 µm), sugerindo que as nanocápsulas melhoram a aglomeração das partículas pela formação de pontes sólidas, atuando como aglutinante, enquanto que grânulos obtidos com água tendem a formar aglomerados fracos com ausência destas pontes.

A partir das análises de MEV, foi possível confirmar a presença de pontes sólidas nos grânulos contendo nanocápsulas bem como poros em sua superfície. As forças de cisalhamento no processo de granulação em leito fluidizado pode originar grânulos porosos e menos densos (JOSHI et al., 2017). Por outro lado, os grânulos preparados com água não apresentaram pontes entre as partículas, confirmando que estes são formados por forças fracas. Além disso, a presença de partículas primárias no ponto final de granulação sugere a não-uniformidade do produto (JOSHI et al., 2017).

A presença de nanocápsulas e aglomerados de maltodextrina/fenitoína/ nanocápsulas demonstrou a boa recuperação das nanoestruturas após a redispersão em água dos grânulos FB-LNC_{PH}. Por outro lado, os grânulos FB-PH não foram solubilizados completamente, sendo observado material remanescente nas microfotografias. Portanto, sugere-se que os grânulos FB-LNC_{PH} desintegram após a

penetração da água através dos poros, seguido pela liberação das nanocápsulas adsorvidas na superfície/pontes sólidas dos grânulos.

As propriedades de fluidez, coesividade e *caking* dos grânulos foram avaliadas através de diferentes métodos. O fluxo foi avaliado pelo índice de Carr e pela razão de Hausner (métodos farmacopeicos), enquanto que o teste de coesão (não-farmacopeico) avalia a tendência das partículas de se aglomerarem. Neste ensaio, a amostra é submetida a dois ciclos de condicionamento para nivelar a coluna de pó. Em seguida, o teste é pausado e o nível de enchimento deverá ser verificado, sendo removido o excesso de pó (ou adicionado). No ciclo de condicionamento, a lâmina (*blade*) desliza suavemente através do pó para estabelecer um estado uniforme. No entanto, no ciclo de teste, a lâmina move-se para baixo, forçando o pó a fluir ao seu redor, gerando uma região de alto estresse (LETURIA et al., 2014). A área sob a curva é o trabalho necessário para mover a pá através da coluna de pó. Em relação aos resultados dos índices de fluxo e de coesão, os grânulos FB-LNC_{PH} apresentaram fluidez aceitável com relativa coesividade, enquanto que a maltodextrina e os grânulos FB-PH mostraram um fluxo pobre e um alto índice de coesão.

O teste de *caking* (método não-farmacopeico) avalia a tendência do pó de formar grandes aglomerados ou *hard cake* (bolo duro) durante o armazenamento e estocagem. O teste inicia com 2 ciclos de condicionamento semelhante ao teste de coesão. A lâmina nivela a coluna de pó e mede sua altura, movendo-se para baixo e compactando suavemente o pó a uma força pré-definida (normalmente 750 g). Quando esta força é alcançada, mede-se a altura do bolo (*cake*). Em seguida, corta-se o *cake* de volta ao topo da coluna com o mínimo de perturbação, antes da recompactação. Este processo é repetido em um número programado de ciclos. Uma vez que o *cake* tenha sido formado no final do ciclo, a lâmina corta-o e mede a força necessária para isso. Esta força é registrada como a *cake strength*, sendo o trabalho necessário para cortar o bolo (g.mm) e a *mean cake strength* é a força média para cortar o bolo em gramas. A força média do *cake* é uma medida útil, uma vez que remove a influência da altura do mesmo no cálculo.

Quanto aos resultados deste ensaio, uma força maior foi necessária para cortar o *cake* (*cake strength*) formado a partir dos grânulos FB-PH em relação à maltodextrina pura. Este achado explica a potencial segregação do pó, a qual pode resultar em variabilidade no enchimento de sachês com pós farmacêuticos (SHAH; TAWAKKUL; KHAN, 2008). Por outro lado, os grânulos FB-LNC_{PH} não formaram o

cake sob as condições padronizadas no teste. Desta forma, não foi possível calcular o *cake strength* e *mean cake strength*, sugerindo uma alta resistência à deformação. Isso pode ocorrido devido à rigidez das nanocápsulas de núcleo lipídico (FIEL et al., 2011) presentes nestes grânulos.

Após avaliar as propriedades de fluxo dos grânulos, estes foram reconstituídos em água na concentração de 1, 3 e 5 mg/mL, e avaliados quanto às suas características físico-químicas. Os grânulos contendo nanocápsulas, reconstituídos na concentração de 1 mg/mL (FB-LNC$_{PH1}$), mostraram uma boa redispersibilidade (87 ± 4%), tamanho de partícula de 660 ± 17 nm, teor de fármaco próximo ao esperado (0,97 ± 0,04 mg/mL) e pH de 4,73 ± 0,03. Além disso, os grânulos contendo nanocápsulas, reconstituídos na concentração de 3 mg/mL (FB-LNC$_{PH3}$), apresentaram uma boa redispersibilidade (90 ± 3%), um tamanho nanométrico (914 ± 58 nm), teor próximo ao esperado (2,86 ± 0,10 mg/mL) e pH de 4,72 ± 0,04. Não foi possível avaliar a redispersibilidade dos grânulos contendo nanocápsulas na concentração de 5 mg/mL (FB-LNC$_{PH5}$) devido ao aspecto viscoso da formulação. Por outro lado, o tamanho médio de partícula encontrado foi em torno de 1,00 ± 0,08 µm, o teor próximo ao esperado (5,04 ± 0,23 mg/mL) e pH de 4,75 ± 0,01.

Somente os resultados dos grânulos redispersos (3 mg/mL) foram discutidos no capítulo 2 devido à melhor performance *in vivo* em experimentos iniciais com estas concentrações. Portanto, os grânulos redispersos contendo nanocápsulas sem fármaco (FB-LNC) foram produzidos e reconstituídos na concentração equivalente à 3 mg/mL de fenitoína, apresentando propriedades (905 ± 40 nm; pH 4,77 ± 0,07) semelhantes àquelas do FB-LNC$_{PH3}$. Além disso, os grânulos contendo somente fenitoína foram também reconstituídos para 3 mg/mL (FB-PH$_3$) e mostraram um tamanho de partícula em torno de 23 µm, teor de fármaco próximo ao esperado e um pH próximo a 5,00. A diferença do tamanho de partícula entre os grânulos com e sem nanocápsulas pode ser explicada pela desintegração dos mesmos que, após penetração da água, liberam as nanoestruturas para o meio aquoso, enquanto que, para os grânulos de fenitoína, a alta quantidade de sólidos diminui a molhabilidade das partículas, levando à formação de microaglomerados.

Os perfis de liberação do fármaco *in vitro* foram avaliados a partir dos grânulos redispersos (FB-PH$_3$ and FB-LNC$_{PH3}$) e a partir de uma solução etanólica de fenitoína (3 mg/mL). Ambas as formulações apresentaram uma liberação do fármaco mais lenta que a fenitoína em solução. Após 24 horas, os grânulos redispersos FB-LNC$_{PH3}$

mostraram uma liberação mais rápida que FB-PH_3. Isso pode ter ocorrido devido à quebra dos aglomerados de maltodextrina/fenitoína/nanocápsulas, aumentando a taxa de dissolução do fármaco, enquanto que os grânulos FB-PH_3 não são facilmente desfeitos. Portanto, a melhor redispersão dos grânulos contendo nanocápsulas pode explicar o comportamento de liberação mais rápida da fenitoína.

Estes grânulos redispersos foram também avaliados quanto à atividade anticonvulsivante em modelo de crises induzidas por pilocarpina em camundongos. Como discutido anteriormente, os grânulos foram reconstituídos nas concentrações 1, 3 e 5 mg/mL, atingindo as doses de 10, 30 e 50 mg/kg de fenitoína, respectivamente, considerando o volume máximo administrado (10 mL/kg). Um maior efeito anticonvulsivante foi observado para o grupo de animais, no qual administrou-se a dose de 30 mg/kg por gavagem. Estes resultados preliminares estão presentes no Apêndice C desta tese. Desta forma, estudos posteriores foram realizados, utilizando esta dose de fármaco. Os animais foram divididos em grupos: 1) água (veículo), 2) suspensão de fenitoína não encapsulada em água, 3) grânulos redispersos contendo nanocápsulas, 4) grânulos contendo somente fenitoína não encapsulada e 5) grânulos redispersos contendo nanocápsulas sem fármaco.

O grupo tratado com a fenitoína não encapsulada não mostrou efeito anticonvulsivante quando comparado ao veículo. No entanto, ambos os grânulos redispersos aumentaram a latência para crises mioclônicas, comparando ao grupo controle. Isso pode ter ocorrido devido às propriedades de mucoadesão dos grânulos, o que poderia melhorar a biodisponibilidade do fármaco e, consequentemente, seu efeito anticonvulsivante. Contudo, não foi observada uma melhor performance dos grânulos redispersos FB-LNC_{PH3} contra crises mioclônicas, quando comparado aos grânulos FB-PH_3, possivelmente devido à baixa quantidade de fármaco nanoencapsulado (0,4 mg/g), em relação ao fármaco total (4 mg/g).

Em relação às crises generalizadas, os grânulos redispersos FB-LNC_{PH3} mostraram uma atividade anticonvulsivante superior comparada àquela dos grânulos contendo nanocápsulas sem fármaco, enquanto que houve um ligeiro aumento em relação ao veículo, à suspensão de fenitoína não encapsulada e aos grânulos redispersos contendo fenitoína. Além disso, os grânulos redispersos FB-LNC_{PH3} apresentaram um aumento de tempo de sobrevivência e aliviaram a severidade das crises dos animais. Diante destes achados, estes grânulos mostraram um efeito anticonvulsivante promissor, considerando que somente 10% da fenitoína está na

forma encapsulada. No entanto, mais estudos serão realizados no intuito de aumentar a quantidade de fármaco nanoencapsulado presente nos grânulos.

No terceiro capítulo desta tese, avaliou-se o impacto da presença das nanocápsulas no crescimento do grânulo e nas suas propriedades mucoadesivas, o que poderia explicar o melhor efeito anticonvulsivante *in vivo* dos grânulos redispersos contendo nanocápsulas. Inicialmente, os grânulos contendo nanocápsulas foram avaliados quanto à uniformidade de dose, os quais apresentaram uma boa homogeneidade do pó em relação à concentração de fármaco esperada (4 mg/g) com um desvio padrão relativo de 1,66%. Estes resultados sugerem que os grânulos obtidos no processo de mistura/granulação são homogêneos.

Outra forma de monitorar a qualidade do produto final é o estudo sobre o mecanismo de formação destes grânulos. Diante disso, o efeito do volume de suspensão de nanocápsulas pulverizado sobre o tamanho de partícula foi avaliado durante o processo de granulação. Posteriormente, uma correlação linear (r = 0,9863) foi encontrada entre estes dois parâmetros. Além disso, o crescimento do grânulo foi comparado à maltodextrina pura, a qual representa mais de 99% de quantidade de sólidos na mistura constituída por maltodextrina e fenitoína. Houve um crescimento de 135% em relação às partículas primárias de maltodextrina, atingindo um D_{50} de 106 µm (SPAN = 1,786) no ponto final da granulação. Esta estreita distribuição do tamanho de partícula pode ser explicada pela quantidade uniforme de aglutinante distribuída em todas as partículas (IVESON et al., 2001).

Os gráficos de radar dos grânulos mostraram que 10% de suas partículas possuem tamanho menor que 100 µm ao final do processo, demonstrando a baixa quantidade de finos (NIEUWMEYER; VAN DER VOORT MAARSCHALK; VROMANS, 2008). A manutenção da forma assimétrica em todos os gráficos de radar sugere um crescimento controlado do grânulo. Um equilíbrio entre as forças de ligação e de quebra durante a granulação fornece um controle da aglomeração e crescimento do grânulo, diminuindo a produção de finos (PARIKH, 2005).

O crescimento do grânulo pode ser visualizado a partir das imagens de MEV. No estágio inicial, uma mistura de partículas primárias (maltodextrina e fenitoína) colidem entre si. Em seguida, as gotículas do aglutinante são depositadas sobre estas partículas (BURGGRAEVE et al., 2013). Após atingir o volume de suspensão pulverizado de 50 mL, as partículas primárias e os núcleos iniciais foram observados, sugerindo que a quantidade de aglutinante é insuficiente para molhar as partículas.

Com o aumento do volume de suspensão para 100 mL, não foram encontradas partículas primárias, enquanto que as pontes sólidas entre os grânulos foram visualizadas. O aglutinante vai sendo distribuído uniformemente pelo leito do pó ao mesmo tempo que partículas primárias desaparecem (SMIRANI-KHAYATI et al., 2009). No estágio final, o aumento do volume da suspensão de nanocápsulas promoveu um aumento do tamanho do grânulo. A coalescência e a consolidação das partículas, bem como o crescimento do grânulo originam grandes aglomerados (BURGGRAEVE et al., 2013; CHEN et al., 2017). Inicialmente, as partículas se unem através de pontes líquidas que contêm um material solúvel que, posteriormente, solidifica após evaporação do solvente, originando as pontes sólidas (PARIKH, 2005; ZAFAR et al., 2017).

Um modelo esquemático da estrutura do grânulo foi proposto baseado na literatura e nas imagens de MEV. Este modelo demonstra que as nanocápsulas estão adsorvidas na superfície do grânulo e nas pontes sólidas em toda a sua extensão. Como discutido no capítulo 2, após redispersão em água, as nanocápsulas são liberadas em meio aquoso junto com aglomerados de maltodextrina/fenitoína/ nanocápsulas.

Os grânulos foram reconstituídos em água, na mesma concentração da suspensão de nanocápsulas (0,225 mg/mL). Os grânulos redispersos apresentaram propriedades nanométricas semelhantes à suspensão original, com exceção do valor de pH. Isso ocorreu devido à presença de maltodextrina e remoção do ácido acético por evaporação, o qual foi utilizado para dissolver a quitosana durante a produção das suspensões. Além disso, estes grânulos apresentaram estabilidade durante 90 dias em relação ao tamanho de partícula e ao teor, demonstrando a boa estabilidade físico-química das nanocápsulas na forma sólida.

Os grânulos redispersos também foram comparados à suspensão original quanto ao perfil de liberação do fármaco. A fenitoína, a partir de uma solução etanólica, difundiu completamente para o meio simulado intestinal após 4 horas. Por outro lado, a suspensão de nanocápsulas e seus grânulos redispersos mostraram um perfil de liberação controlado após 48 horas. O perfil de liberação do fármaco foi semelhante até 12 horas para os grânulos redispersos e a suspensão original. Isso pode ser explicado pela liberação gradual da fenitoína a partir das nanoestruturas na superfície dos grânulos, as quais atuam como uma barreira para a liberação do fármaco no compartimento interno do grânulo. Depois disso, os grânulos redispersos

apresentaram uma liberação do fármaco mais rápida comparada àquela da suspensão original. Nesse momento, os aglomerados são desfeitos, liberando as nanocápsulas e aumentando a dissolução da fenitoína não encapsulada. Além disso, este comportamento é esperado devido à grande quantidade de fenitoína não encapsulada (90%) presente nos grânulos.

Para avaliar a mucoadesão dos grânulos redispersos, foram escolhidos o método de lavabilidade e o teste de tensão em mucosa intestinal suína. No ensaio de lavabilidade, um fluxo de 0,7 mL/min de meio simulado intestinal foi utilizado para simular as condições *in vivo*. A fenitoína foi completamente lavada após 5 horas da aplicação de uma solução hidroalcoólica ou de uma suspensão de nanocápsulas de fenitoína. Por outro lado, a quantidade de fármaco lavado à partir da suspensão foi maior que àquela dos grânulos redispersos, evidenciando o papel importante da granulação no processo de mucoadesão. Além disso, foi observado um aumento de 8 vezes na quantidade de fármaco permeado a partir dos grânulos, quando comparado ao das nanocápsulas. Isso pode ser explicado pela melhor interação entre os grânulos redispersos e a mucosa intestinal, provavelmente em decorrência da presença de maltodextrina.

Para confirmar esta hipótese, os grânulos de fenitoína sem nanocápsulas foram preparados e redispersos em água. Estes retiveram uma quantidade maior de fármaco quando comparado à suspensão original. Contudo, uma menor quantidade de fenitoína ficou retida na mucosa, em relação àquela observada a partir de grânulos contendo nanocápsulas, durante o intervalo de tempo de 3 a 5 horas. Estes resultados sugerem um efeito mucoadesivo combinado das nanocápsulas e da maltodextrina. Baseado nestes resultados, a estrutura dos grânulos tem um importante papel na redispersão aquosa, como discutido anteriormente, e nas suas propriedades de mucoadesão. Dois mecanismos podem estar envolvidos neste processo. A quitosana das nanocápsulas interage com a mucina por interações eletrostáticas entre os seus grupos amino e os resíduos de ácido siálico da mucosa (MANSURI et al., 2016; VIEIRA et al., 2018). Além disso, as maltodextrinas são polissacarídeos que têm a habilidade de absorver água, o que poderia facilitar a desidratação da mucosa, resultando em retenção do fármaco (CARRERAS; CANALES; MELERO, 2016).

O teste de tensão, realizado em um texturômetro, mede a força necessária para ocasionar deslocamento entre uma formulação mucoadesiva e a mucosa. O trabalho requerido para deslocar a mucosa intestinal a partir dos grânulos foi maior do que

àquele a partir de uma solução de fenitoína. Isso ocorreu devido à uma maior distância percorrida pela sonda (*probe*) para os grânulos redispersos em relação à solução de fármaco. Diante disso, um efeito mucoadesivo significativo foi observado quando as nanocápsulas e a maltodextrina atuam juntas sobre a mucosa intestinal, corroborando com os resultados do teste de lavabilidade. Portanto, o *design* e a composição dos grânulos contendo nanocápsulas são responsáveis por suas melhores propriedades de mucoadesão, considerando a importância das nanoestruturas como sistema aglutinante. Além disso, estes achados poderiam explicar a promissora atividade anticonvulsivante *in vivo* destes grânulos redispersos, a qual foi demonstrada no capítulo 2.

8 CONCLUSÕES

8 CONCLUSÕES

Foram desenvolvidas nanocápsulas de núcleo lipídico contendo fenitoína com e sem revestimento de quitosana, que apresentaram boas propriedades nanométricas. No entanto, a suspensão de nanocápsulas revestidas com quitosana se mostrou mais promissora para o desenvolvimento de pós e grânulos para reconstituição aquosa no tocante à recuperação dessas características nanométricas. A composição destas formulações influenciou diretamente em suas propriedades físico-químicas e biológicas, melhorando a eficácia do fármaco em um modelo de atividade anticonvulsivante. Diante disso, as conclusões do trabalho foram divididas de acordo com os resultados obtidos nos três capítulos:

- Os pós para reconstituição foram obtidos com sucesso a partir da técnica de secagem por aspersão (*spray-drying*), com boa recuperação das características nanométricas da suspensão de nanocápsulas de fenitoína original após reconstituição em água. Os pós redispersíveis apresentaram boa estabilidade físico-química e gastrointestinal, apresentando uma liberação mais lenta do fármaco quando encapsulado, similar ao perfil das nanocápsulas, e uma melhora na ação anticonvulsivante *in vivo*.
- Os grânulos contendo nanocápsulas de fenitoína foram obtidos por leito fluidizado, apresentando boas propriedades de fluxo e de redispersibilidade após serem reconstituídos em água, liberando as nanoestruturas a partir dos aglomerados para o meio e aumentando a velocidade de liberação do fármaco, quando comparado àquele liberado a partir dos grânulos contendo somente fenitoína. Os grânulos redispersíveis, contendo apenas 10% do fármaco na sua forma nanoencapsulada, mostraram um promissor efeito anticonvulsivante.
- O uso de nanocápsulas de fenitoína foi determinante para o crescimento dos grânulos obtidos em leito fluidizado, os quais apresentaram uma boa uniformidade de dose. Um modelo esquemático da sua estrutura demonstrou que as nanocápsulas recobrem a superfície dos mesmos, inclusive as pontes sólidas. Esse arranjo possibilitou a recuperação das características nanométricas da suspensão original, bem como um perfil de liberação bifásico no qual se tem uma fase inicial mais lenta, seguida

por outra mais rápida. Além disso, a ação combinada de nanocápsulas e maltodextrina foi responsável pelo maior efeito mucoadesivo desta formulação, sugerindo que as nanocápsulas tiveram um papel importante no *design* dos grânulos e em suas características finais.

REFERÊNCIAS

ALVARIZA, S. et al. Pharmacological Reports Chronic administration of phenytoin induces efflux transporter overexpression in rats. **Pharmacological Reports**, v. 66, p. 946–951, 2014.

ANDRADE, D. F. et al. Fluid bed granulation as an innovative process to produce dry redispersible nanocapsules: Influence of cationic coating of particles. **Powder Technology**, v. 326, p. 25–31, 2018.

BAIL, S. et al. Characterisation of various grape seed oils by volatile compounds, triacylglycerol composition, total phenols and antioxidant capacity. **Food Chemistry**, v. 108, n. 3, p. 1122–1132, 2008.

BANERJEE, P. N.; FILIPPI, D.; HAUSER, W. A. The descriptive epidemiology of epilepsy - a review. **Epilepsy Research**, v. 85, n. 1, p. 31–45, 2009.

BASA, S. et al. Production and In Vitro Characterization of Solid Dosage form Incorporating Drug Nanoparticles. **Drug Development and Industrial Pharmacy**, v. 34, p. 1209–1218, 2008.

BATCHELOR, H.; APPLETON, R.; HAWCUTT, D. B. Comparing paediatric intravenous phenytoin doses using physiologically based pharmacokinetic (PBPK) modelling software. **Seizure**, v. 33, p. 8–12, 2015.

BATTINO, D. et al. Influence of aging on serum phenytoin concentrations: A pharmacokinetic analysis based on therapeutic drug monitoring data. **Epilepsy Research**, v. 59, n. 2–3, p. 155–165, 2004.

BECK, R. C. R. et al. Surface morphology of spray-dried nanoparticle-coated microparticles designed as an oral drug delivery system. **Brazilian Journal of Chemical Engineering**, v. 25, n. 2, p. 389–398, 2008.

BENDER, E. A. et al. Hemocompatibility of poly(ε-caprolactone) lipid-core nanocapsules stabilized with polysorbate 80-lecithin and uncoated or coated with chitosan. **International Journal of Pharmaceutics**, v. 426, n. 1–2, p. 271–279, 2012.

BENNEWITZ, M. F.; SALTZMAN, M. W. Nanotechnology for Delivery of Drugs to the Brain for Epilepsy. **Neurotherapeutics**, v. 6, n. 2, p. 323–336, 2009.

BERNARDI, A. et al. Indomethacin-loaded lipid-core nanocapsules reduce the damage triggered by Aβ1-42 in Alzheimer's disease models. **International Journal of Nanomedicine**, v. 7, p. 4927–4942, 2012.

BORGES, K. et al. Neuronal and glial pathological changes during epileptogenesis in the mouse pilocarpine model. **Experimental Neurology**, v. 182, p. 21–34, 2003.

BOSE, S. et al. Application of spray granulation for conversion of a nanosuspension into a dry powder form. **European Journal of Pharmaceutical Sciences**, v. 47, n. 1, p. 35–43, 2012.

BOUREZG, Z. et al. Colloids and Surfaces A: Physicochemical and Engineering Aspects Redispersible lipid nanoparticles of Spironolactone obtained by three drying methods. **Colloids and Surfaces A: Physicochemical and Engineering Aspects**, v. 413, p. 191–199, 2012.

BURGGRAEVE, A. et al. Process analytical tools for monitoring, understanding, and control of pharmaceutical fluidized bed granulation: A review. **European Journal of Pharmaceutics and Biopharmaceutics**, v. 83, n. 1, p. 2–15, 2013.

BURSTEIN, A. H. et al. Phenytoin pharmacokinetics following oral administration of phenytoin suspension and fosphenytoin solution to rats. **Epilepsy Research**, v. 34, n. 2–3, p. 129–133, 1999.

CALVO, P.; REMUNAN-LOPEZ, C. Development of positively charged colloidal drug carriers:chitosan-coated polyester nanocapsules and submicron-emulsions. **Colloid and Polymer Science**, v. 275, n. 1, p. 46–53, 1997.

CARRERAS, J. J.; CANALES, P.; MELERO, A. Mucoadhesion of Polymeric Drug Delivery Systems : Polymeric Nanoparticles and its Interactions with the Intestinal Barrier. **JSM Nanotechnology & Nanomedicine**, v. 4, p. 1–5, 2016.

CARRIÈRE, F. Impact of gastrointestinal lipolysis on oral lipid-based formulations and bioavailability of lipophilic drugs. **Biochimie**, v. 125, p. 297–305, 2016.

CAVALHEIRO, E. A. et al. Long-Term Effects of Pilocarpine in Rats: Structural Damage of the Brain Triggers Kindling and Spontaneous Recurrent Seizures. **Epilepsia**, v. 32, n. 6, p. 778–782, 1991.

CÉ, R. et al. Colloids and Surfaces A: Physicochemical and Engineering Aspects Chitosan-coated dapsone-loaded lipid-core nanocapsules: Growth inhibition of clinical isolates, multidrug-resistant Staphylococcus aureus and Aspergillus ssp. **Colloids and Surfaces A: Physicochemical and Engineering Aspects**, v. 511, p. 153–161, 2016.

CHEN, L. et al. Pluronic P105/F127 mixed micelles for the delivery of docetaxel against Taxol-resistant non-small cell lung cancer: Optimization and in vitro, in vivo evaluation. **International Journal of Nanomedicine**, v. 8, p. 73–84, 2013.

CHEN, X. et al. Study on the fluidized bed granulation of fine-grained rutile concentrate. **Powder Technology**, v. 315, p. 53–59, 2017.

CORADINI, K. et al. Co-encapsulation of resveratrol and curcumin in lipid-core nanocapsules improves their in vitro antioxidant effects. **European Journal of Pharmaceutics and Biopharmaceutics**, v. 88, p. 178–185, 2014.

CRUZ, L. et al. Diffusion and mathematical modeling of release profiles from nanocarriers. **International Journal of Pharmaceutics**, v. 313, n. 1–2, p. 198–205, 2006.

CURIA, G. et al. The pilocarpine model of temporal lobe epilepsy. **Journal of Neuroscience Methods**, v. 172, n. 2, p. 143–157, 2008.

DAVIES, J. A. Mechanisms of action of antiepileptic drugs. **Seizure**, v. 4, n. 4, p. 267–71, dez. 1995.

DELEU, D.; AARONS, L.; AHMED, I. A. Estimation of population pharmacokinetic parameters of free-phenytoin in adult epileptic patients. **Archives of Medical Research**, v. 36, n. 1, p. 49–53, 2005.

DESCAMPS, N. et al. Glass transition and flowability/caking behaviour of maltodextrin DE 21. **Journal of Food Engineering**, v. 119, p. 809–813, 2013.

DIMER, F. A. et al. Nanoencapsulation of olanzapine increases its efficacy in antipsychotic treatment and reduces adverse effects. **Journal of Biomedical Nanotechnology**, v. 10, n. 6, p. 1137–1145, 2014.

DIMER, F. A. et al. Nanoencapsulation Improves Relative Bioavailability and Antipsychotic Effect of Olanzapine in Rats. **Journal of Biomedical Nanotechnology**, v. 11, p. 1482–1493, 2015.

EMA. **Committee for Medicinal Products for Human Use (CHMP) Reflection Paper: Formulations of Choice for the Paediatric Population**. Disponível em: <http://www.ema.europa.eu/docs/en_GB/document_library/Scientific_guideline/2009/09/WC500003782.pdf>. Acesso em: 3 fev. 2017.

EMA. **Committee for Medicinal Products for Human Use (CHMP) Guideline on pharmaceutical development of medicines for paediatric use**. Disponível em: <http://www.ema.europa.eu/docs/en_GB/document_library/Scientific_guideline/2013/07/WC500147002.pdf>. Acesso em: 3 fev. 2017.

FANG, Z. et al. Pluronic P85-coated poly(butylcyanoacrylate) nanoparticles overcome phenytoin resistance in P-glycoprotein overexpressing rats with lithium-pilocarpine-induced chronic temporal lobe epilepsy. **Biomaterials**, v. 97, p. 110–121, 2016.

FAURE, A.; YORK, P.; ROWE, R. C. Process control and scale-up of pharmaceutical wet granulation processes: a review. **European Journal of Pharmaceutics and Biopharmaceutics**, v. 52, p. 269–277, 2001.

FERNANDES, M. J. S.; MAZZACORATTI, M. G. N.; CAVALHEIRO, E. A. Pathophysiological Aspects of Temporal Lobe Epilepsy and the Role of P2X Receptors. **The Open Neuroscience Journal**, v. 4, p. 35–43, 2010.

FESSI, H. et al. Nanocapsule formation by interfacial polymer deposition following solvent displacement. **International Journal of Pharmaceutics**, v. 55, n. 1, p. 1–4, 1989.

FIEL, L. A. et al. Diverse deformation properties of polymeric nanocapsules and lipid-core nanocapsules. **Soft Matter**, v. 7, n. 16, p. 7240, 2011.

FIGUEIRÓ, F. et al. Resveratrol-loaded lipid-core nanocapsules treatment reduces in vitro and in vivo glioma growth. **Journal of Biomedical Nanotechnology**, v. 9, n. 3, p. 516–526, 2013.

FONSECA, F. N. et al. Mucoadhesive amphiphilic methacrylic copolymer-functionalized poly(Ɛ-caprolactone) nanocapsules for nose-to-brain delivery of olanzapine. **Journal of Biomedical Nanotechnology**, v. 11, n. 8, p. 1472–1481, 2014.

FRIEDRICH, R. B. et al. Drying polymeric drug-loaded nanocapsules: the wet granulation process as a promising approach. **Journal of Nanoscience and Nanotechnology**, v. 10, n. 1, p. 616–621, 2010.

FRIEDRICH, R. B. et al. Skin penetration behavior of lipid-core nanocapsules for simultaneous delivery of resveratrol and curcumin. **European Journal of Pharmaceutical Sciences**, v. 78, p. 204–213, 2015.

FROZZA, R. L. et al. Characterization of trans-resveratrol-loaded lipid-core nanocapsules and tissue distribution studies in rats. **Journal of Biomedical Nanotechnology**, v. 6, n. 6, p. 694–703, 2010.

FUNCK, V. R. et al. Long-term decrease in Na+,K+-ATPase activity after pilocarpine-induced status epilepticus is associated with nitration of its alpha subunit. **Epilepsy Research**, v. 108, n. 10, p. 1705–1710, 2014.

GAILLARD, P. J.; BRINK, A.; DE BOER, A. G. Diphtheria toxin receptor-targeted brain drug delivery. **International Congress Series**, v. 1277, p. 185–198, 2005.

GOLDENBERG, M. M. Overview of Drugs Used For Epilepsy and Seizures Etiology, Diagnosis, and Treatment. **Pharmacy & Therapeutics**, v. 35, n. 7, p. 392–415, 2010.

GUTERRES, S. S. et al. Gastro-intestinal tolerance following oral administration of spray-dried diclofenac-loaded nanocapsules and nanospheres. **S.T.P. Pharma Sciences**, v. 11, p. 229–33, 2001.

GUTERRES, S. S.; BECK, R. C. R.; POHLMANN, A. R. Spray-drying technique to prepare innovative nanoparticulated formulations for drug administration: a brief overview. **Brazilian Journal of Physics**, v. 39, n. 1A, p. 205–209, 2009.

HAKIM, L. F. et al. Aggregation behavior of nanoparticles in fluidized beds. **Powder Technology**, v. 160, n. 3, p. 149–160, 2005.

HERVÉ, F.; GHINEA, N.; SCHERRMANN, J.-M. CNS delivery via adsorptive transcytosis. **The AAPS journal**, v. 10, n. 3, p. 455–72, 2008.

HOFFMEISTER, C. R. et al. Hydrogels containing redispersible spray-dried melatonin-loaded nanocapsules: a formulation for transdermal-controlled delivery. **Nanoscale Research Letters**, v. 7, n. 1, p. 251, 2012.

HONG, L. et al. Colloids and Surfaces A: Physicochemical and Engineering Aspects Impact of particle size and surface charge density on redispersibility of spray-dried powders. **Colloids and Surfaces A: Physicochemical and Engineering Aspects**, v. 459, p. 274–281, 2014.

ISKANDAR, F. Nanoparticle processing for optical applications - A review. **Advanced Powder Technology**, v. 20, n. 4, p. 283–292, 2009.

ISMAIL, A. F. M.; MOAWED, F. S. M.; MOHAMED, M. A. Protective mechanism of grape seed oil on carbon tetrachloride-induced brain damage in γ-irradiated rats. **Journal of Photochemistry and Photobiology B: Biology**, v. 153, p. 317–323, 2015.

IVESON, S. M. et al. Nucleation, growth and breakage phenomena in agitated wet granulation processes: A review. **Powder Technology**, v. 117, n. 1–2, p. 3–39, 2001.

JÄGER, E. et al. Sustained release from lipid-core nanocapsules by varying the core viscosity and the particle surface area. **Journal of Biomedical Nanotechnology**, v. 5, n. 1, p. 130–140, 2009.

JOSHI, S. et al. To study and understand the process of wet granulation by fluidized bed granulation technique. **International Journal of Research in Pharmacy and Chemistry**, v. 7, n. 3, p. 232–238, 2017.

JUNG, T. et al. Biodegradable nanoparticles for oral delivery of peptides: Is there a role for polymers to affect mucosal uptake? **European Journal of Pharmaceutics and Biopharmaceutics**, v. 50, n. 1, p. 147–160, 2000.

KHOR, E.; LIM, L. Y. Implantable applications of chitin and chitosan. **Biomaterials**, v. 24, n. 13, p. 2339–2349, 2003.

KLINKESORN, U.; MCCLEMENTS, D. J. Influence of chitosan on stability and lipase digestibility of lecithin-stabilized tuna oil-in-water emulsions. **Food Chemistry**, v. 114, n. 4, p. 1308–1315, 2009.

LABET, M.; THIELEMANS, W. Synthesis of polycaprolactone: a review. **Chemical Society Reviews**, v. 38, n. 12, p. 3484–3504, 2009.

LETURIA, M. et al. Characterization of flow properties of cohesive powders: A comparative study of traditional and new testing methods. **Powder Technology**, v. 253, p. 406–423, 2014.

LIPKIND, G. M.; FOZZARD, H. A. Molecular Model of Anticonvulsant Drug Binding to the Voltage-Gated Sodium Channel Inner Pore. **Molecular Pharmacology**, v. 78, n. 4, p. 631–638, 2010.

MANSURI, S. et al. Mucoadhesion: A promising approach in drug delivery system. **Reactive and Functional Polymers**, v. 100, p. 151–172, 2016.

MARCHIORI, M. C. L. et al. Spray-Dried Powders Containing Tretinoin-Loaded Engineered Lipid-Core Nanocapsules: Development and Photostability Study. **Journal of Nanoscience and Nanotechnology**, v. 11, n. 3, p. 1–9, 2012.

MEGIDDO, I. et al. Health and economic benefits of public financing of epilepsy treatment in India: An agent-based simulation model. **Epilepsia**, v. 57, n. 3, p. 464–474, 2016.

MINISTÉRIO DA SAÚDE. Portaria SAS/MS nº 492, de 23 de setembro de 2010. Ministério da Saúde, 2010. Revoga a Portaria SAS/MS nº 864, de 04 de novembro de 2002, que aprova o Protocolo Clínico e Diretrizes Terapêuticas da Epilepsia. **Diário Oficial da União**, n.184, Brasília-DF, 24 set., p.673, 2010.

MORA-HUERTAS, C. E.; FESSI, H.; ELAISSARI, A. Polymer-based nanocapsules for drug delivery. **International Journal of Pharmaceutics**, v. 385, n. 1–2, p. 113–142, 2010.

MÜLLER, C. R. et al. Preparation and characterization of spray-dried polymeric nanocapsules. **Drug development and industrial pharmacy**, v. 26, n. 3, p. 343–7, 2000.

NAFEE, N. et al. Relevance of the colloidal stability of chitosan/PLGA nanoparticles on their cytotoxicity profile. **International Journal of Pharmaceutics**, v. 381, n. 2, p. 130–139, 2009.

NANDIYANTO, A. B. D.; OKUYAMA, K. Progress in developing spray-drying methods for the production of controlled morphology particles: From the nanometer to submicrometer size ranges. **Advanced Powder Technology**, v. 22, n. 1, p. 1–19, 2011.

NIEUWMEYER, F.; VAN DER VOORT MAARSCHALK, K.; VROMANS, H. The consequences of granulate heterogeneity towards breakage and attrition upon fluid-bed drying. **European Journal of Pharmaceutics and Biopharmaceutics**, v. 70, n. 1, p. 402–408, 2008.

NIWA, T.; MIURA, S.; DANJO, K. Design of dry nanosuspension with highly spontaneous dispersible characteristics to develop solubilized formulation for poorly water-soluble drugs. **Pharmaceutical Research**, v. 28, n. 9, p. 2339–2349, 2011.

OURIQUE, A. F. et al. Redispersible liposomal-N-acetylcysteine powder for pulmonary administration: Development, in vitro characterization and antioxidant activity. **European Journal of Pharmaceutical Sciences**, v. 65, p. 174–182, 2014.

OYARZUN-AMPUERO, F. A. et al. Chitosan-coated lipid nanocarriers for therapeutic applications. **Journal of Drug Delivery Science and Technology**, v. 20, n. 4, p. 259–265, 2010.

PAESE, K. et al. Semisolid formulation containing a nanoencapsulated sunscreen: Effectiveness, in vitro photostability and immune response. **Journal of Biomedical Nanotechnology**, v. 5, n. 3, p. 240–246, 2009.

PARIKH, D. M. Introduction. In: PARIKH, D. M. (Ed.). . **Handbook of Pharmaceutical Granulation Technology**. 2. ed. New York: Taylor & Francis, 2005. p. 1–6.

PATEL, T. et al. Polymeric nanoparticles for drug delivery to the central nervous system. **Advanced Drug Delivery Reviews**, v. 64, n. 7, p. 701–705, 2012.

PERCY, S. R. **Improvement in drying and concentrating liquid substances by atomizing.** USA, 1872.

POHLMANN, A. R. et al. Poly(ϵ-caprolactone) microcapsules and nanocapsules in drug delivery. **Expert opinion on drug delivery**, v. 10, n. 5, p. 623–38, 2013.

PRASHANTH, H. K. V.; KITTUR, F. S.; THARANATHAN, R. N. Solid state structure of chitosan prepared under different N-deacetylating conditions. **Carbohydrate Polymers**, v. 50, n. 1, p. 27–33, 2002.

PREGO, C. et al. Transmucosal macromolecular drug delivery. **Journal of Controlled Release**, v. 101, p. 151–162, 2005.

PREGO, C. et al. Efficacy and mechanism of action of chitosan nanocapsules for oral peptide delivery. **Pharmaceutical Research**, v. 23, n. 3, p. 549–556, 2006.

PYCIA, K. et al. Maltodextrins from chemically modified starches. Selected physicochemical properties. **Carbohydrate Polymers**, v. 146, p. 301–309, 2016.

QUINTANAR-GUERRERO, D. et al. Preparation techniques and mechanisms of formation of biodegradable nanoparticles from preformed polymers. **Drug Development and Industrial Pharmacy**, v. 24, n. 12, p. 1113–28, 1998.

RACINE, R. J. Modification of seizure activity by electrical stimulation: II. Motor seizure. **Electroencephalography and Clinical Neurophysiology**, v. 32, p. 281–294, 1972.

REIS, C. P. et al. Nanoencapsulation I. Methods for preparation of drug-loaded polymeric nanoparticles. **Nanomedicine: Nanotechnology, Biology, and Medicine**, v. 2, n. 1, p. 8–21, 2006.

RHODES, M. Separation of particles from a gas: gas cyclones. In: MARTIN RHODES (Ed.). . **Introduction to Particle Technology**. 2. ed. Chichester: John Wiley, 2008. p. 247–264.

RIBEIRO, R. F. et al. Spray-dried powders improve the controlled release of antifungal tioconazole-loaded polymeric nanocapsules compared to with lyophilized products. **Materials Science and Engineering C**, v. 59, p. 875–884, 2016.

RODRIGUES, S. F. et al. Lipid-core nanocapsules act as a drug shuttle through the blood brain barrier and reduce glioblastoma after intravenous or oral administration. **Journal of Biomedical Nanotechnology**, v. 12, n. 5, p. 986–1000, 2016.

ROGAWSKI, M. A; LÖSCHER, W. The neurobiology of antiepileptic drugs. **Nature reviews. Neuroscience**, v. 5, n. 7, p. 553–564, 2004.

ROWE, R. C.; SHESKEY, P. J.; OWEN, S. C. **Handbook of Pharmaceutical Excipients**. 5. ed. London: Pharmaceutical Press, 2012.

SCHAFFAZICK, S. R. et al. Freeze-drying polymeric colloidal suspensions: Nanocapsules, nanospheres and nanodispersion. A comparative study. **European Journal of Pharmaceutics and Biopharmaceutics**, v. 56, n. 3, p. 501–505, 2003.

SHAH, R. B.; TAWAKKUL, M. A.; KHAN, M. A. Comparative Evaluation of Flow for Pharmaceutical Powders and Granules. **AAPS PharmSciTech**, v. 9, n. 1, p. 250–258, 2008.

SHORVON, S. The antiepileptic drugs. In: SHORVON, S. (Ed.). . **Handbook of Epilepsy Treatment**. 3 ed ed. Chichester: Wiley-Blackwell, 2010. p. 158–286.

SINGH, A.; VAN DEN MOOTER, G. Spray drying formulation of amorphous solid dispersions. **Advanced Drug Delivery Reviews**, v. 100, p. 27–50, 2016.

SINHA, V. R. et al. Poly-ε-caprolactone microspheres and nanospheres: An overview. **International Journal of Pharmaceutics**, v. 278, n. 1, p. 1–23, 2004.

SMIRANI-KHAYATI, N. et al. Binder liquid distribution during granulation process and its relationship to granule size distribution. **Powder Technology**, v. 195, n. 2, p. 105–112, 2009.

SOUZA, J. DE; FREITAS, Z. M. F.; STORPIRTIS, S. Modelos in vitro para determinação da absorção de fármacos e previsão da relação dissolução/absorção. **Revista Brasileira de Ciências Farmacêuticas**, v. 43, n. 4, p. 515–527, 2007.

TAWFIK, M. K. Coenzyme Q10 enhances the anticonvulsant effect of phenytoin in pilocarpine-induced seizures in rats and ameliorates phenytoin-induced cognitive impairment and oxidative stress. **Epilepsy and Behavior**, v. 22, n. 4, p. 671–677, 2011.

TEWA-TAGNE, P.; BRIANÇON, S.; FESSI, H. Spray-dried microparticles containing polymeric nanocapsules: Formulation aspects, liquid phase interactions and particles characteristics. **International Journal of Pharmaceutics**, v. 325, n. 1–2, p. 63–74, 2006.

TEWA-TAGNE, P.; BRIANÇON, S.; FESSI, H. Preparation of redispersible dry nanocapsules by means of spray-drying: Development and characterisation. **European Journal of Pharmaceutical Sciences**, v. 30, n. 2, p. 124–135, 2007.

UNVERFERTH, K. et al. Synthesis, anticonvulsant activity, and structure-activity relationships of sodium channel blocking 3-aminopyrroles. **Journal of Medicinal Chemistry**, v. 41, n. 1, p. 63–73, 1998.

VENTURINI, C. G. et al. Formulation of lipid core nanocapsules. **Colloids and Surfaces A: Physicochemical and Engineering Aspects**, v. 375, n. 1–3, p. 200–208, 2011.

VIEIRA, A. C. C. et al. Mucoadhesive chitosan-coated solid lipid nanoparticles for better management of tuberculosis. **International Journal of Pharmaceutics**, v. 536, p. 478–485, 2018.

WANG, Y. et al. Electroresponsive Nanoparticles Improve Antiseizure Effect of Phenytoin in Generalized Tonic-Clonic Seizures. **Neurotherapeutics**, v. 13, n. 3, p. 603–613, 2016.

WONG, H. L.; WU, X. Y.; BENDAYAN, R. Nanotechnological advances for the delivery of CNS therapeutics. **Advanced Drug Delivery Reviews**, v. 64, n. 7, p. 686–700, 2012.

WORLD HEALTH ORGANIZATION. **Epilepsy**. Disponível em: <http://www.who.int/mediacentre/factsheets/fs999/en/>. Acesso em: 12 out. 2016.

YAMAMOTO, H. et al. Engineering of poly(DL-lactic-co-glycolic acid) nanocomposite particles for dry powder inhalation dosage forms of insulin with the spray-fluidized bed granulating system. **Advanced Powder Technology**, v. 18, n. 2, p. 215–228, 2007.

YANG, H. Nanoparticle-mediated Brain-Specific Drug Delivery, Imaging, and Diagnosis. **Pharmaceutical Research**, v. 27, n. 9, p. 1759–1771, 2010.

YUSRAINI, E.; HARIYADI, P.; KUSNANDAR, F. Preparation and partial characterization of low dextrose equivalent (DE) maltodextrin from banana starch produced by enzymatic hydrolysis. **Starch**, v. 20, p. 312–321, 2013.

ZAFAR, U. et al. A review of bulk powder caking. **Powder Technology**, v. 313, p. 389–401, 2017.

ZANOTTO-FILHO, A. et al. Curcumin-loaded lipid-core nanocapsules as a strategy to improve pharmacological efficacy of curcumin in glioma treatment. **European Journal of Pharmaceutics and Biopharmaceutics**, v. 83, n. 2, p. 156–167, 2013.

ZHA, C.; BROWN, G. B.; BROUILLETTE, W. J. Synthesis and Structure - Activity Relationship Studies for Hydantoins and Analogues as Voltage-Gated Sodium Channel Ligands. **Journal of Medicinal Chemistry**, v. 47, n. 26, p. 6519–6528, 2004.

ZUGLIANELLO, C. et al. Redispersible spray-dried nanocapsules for the development of skin delivery systems: proposing a novel blend of drying adjuvants. **Soft Materials**, v. 16, n. 1, p. 20–30, 2018.

APÊNDICE A – Perfis de distribuição de tamanho de partícula e potencial zeta de nanocápsulas de núcleo lipídico

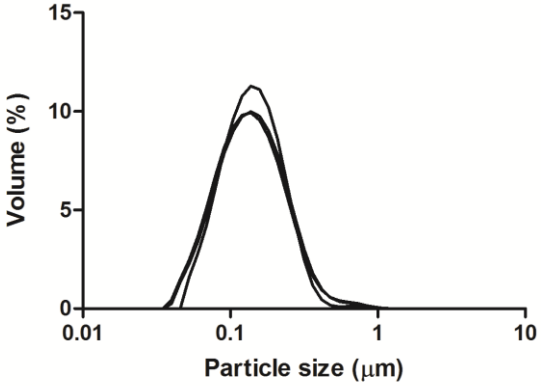

Figura 1 – Distribuição do tamanho de partícula obtido por Difração a Laser (DL) para nanocápsulas de núcleo lipídico de fenitoína não-revestidas (PHT-LNC). Cada gráfico mostra a triplicata de lotes.

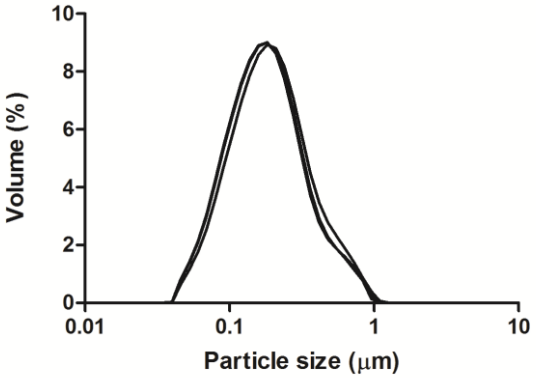

Figura 2 – Distribuição do tamanho de partícula obtido por Difração a Laser (DL) para nanocápsulas de núcleo lipídico de fenitoína revestidas com quitosana (PHT-CS-LNC). Cada gráfico mostra a triplicata de lotes.

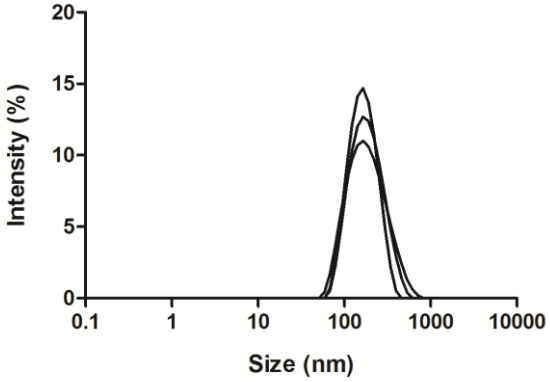

Figura 3 – Distribuição do tamanho de partícula obtido por Espalhamento de Luz Dinâmico para nanocápsulas de núcleo lipídico de fenitoína não-revestidas (PHT-LNC). Cada gráfico mostra a triplicata de lotes.

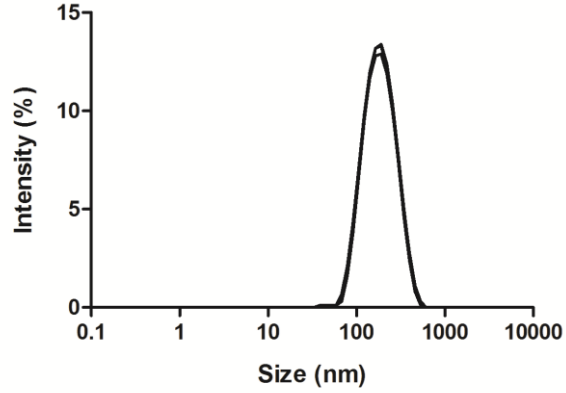

Figura 4 – Distribuição do tamanho de partícula obtido por Espalhamento de Luz Dinâmico para nanocápsulas de núcleo lipídico de fenitoína revestidas com quitosana (PHT-CS-LNC). Cada gráfico mostra a triplicata de lotes.

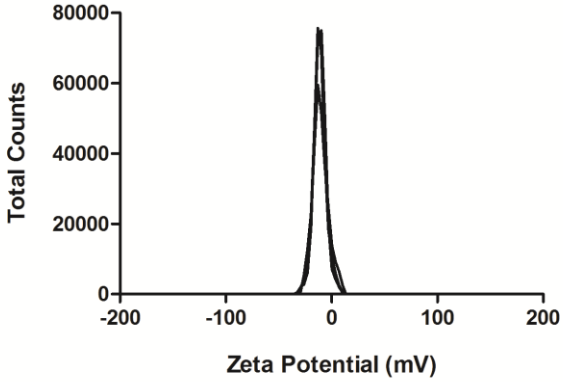

Figura 5 – Potencial zeta obtido a partir de mobilidade eletroforética para nanocápsulas de núcleo lipídico de fenitoína (PHT-LNC). Cada gráfico mostra a triplicata de lotes.

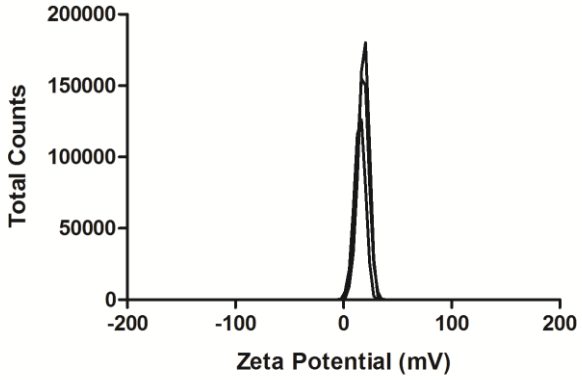

Figura 6 – Potencial zeta obtido a partir de mobilidade eletroforética para nanocápsulas de núcleo lipídico de fenitoína revestidas com quitosana (PHT-CS-LNC). Cada gráfico mostra a triplicata de lotes.

APÊNDICE B – Validação de metodologia analítica para quantificação de fenitoína a partir de suspensões de nanocápsulas e do pó contendo suspensão de nanocápsulas

O método utilizado para a quantificação de fenitoína foi desenvolvido e validado por Cromatografia Líquida de Alta Eficiência (CLAE), de acordo com as normas do ICH (1996). Utilizou-se o equipamento Shimadzu LC-20A (Tokyo, Japan), coluna C18 Phenomenex (150 mm x 4,6 mm; 0,5 µm). A fase móvel foi uma mistura de acetonitrila e água ultrapura (1:1, v/v). O volume de injeção foi de 20 µL em fluxo isocrático de 1,0 mL/min. O comprimento de onda utilizado foi 210 nm. A fenitoína apresentou tempo de retenção, aproximadamente 5,6 min, como observado na Figura 1.

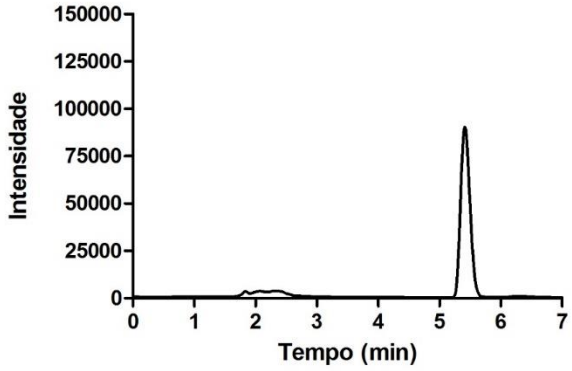

Figura 1 – Cromatograma referente à fenitoína a partir de uma suspensão de nanocápsulas na concentração de 10 µg/mL.

A especificidade do método foi avaliada a partir de uma suspensão de nanocápsulas brancas (Figura 2), de pós (Figura 3) e grânulos (Figura 4), contendo estas nanocápsulas, incluindo todos os possíveis componentes da matriz, exceto o fármaco. Foi observado que não há interferentes das formulações na quantificação da fenitoína pelo método proposto.

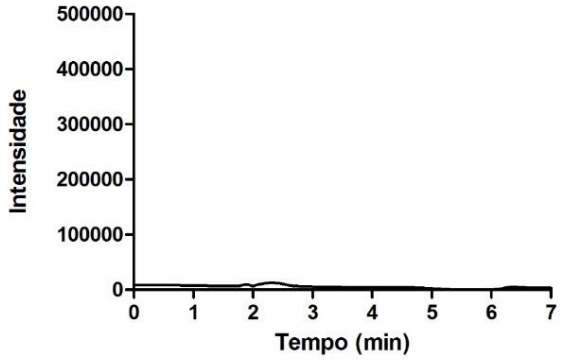

Figura 2 – Cromatograma referente à amostra de suspensão de nanocápsulas brancas revestidas com quitosana.

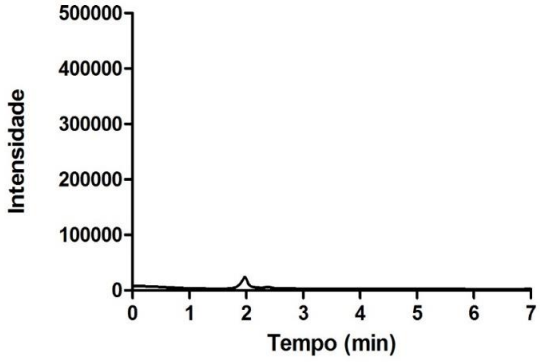

Figura 3 – Cromatograma referente à amostra de pó contendo suspensão de nanocápsulas brancas revestidas com quitosana.

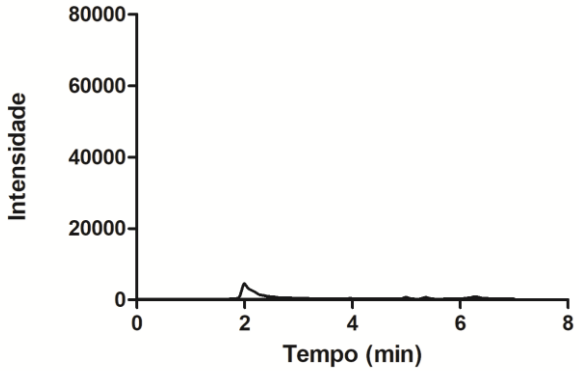

Figura 4 – Cromatograma referente à amostra de grânulos contendo suspensão de nanocápsulas brancas revestidas com quitosana.

Para avaliar a linearidade, foram obtidas 3 curvas analíticas a partir de uma solução estoque do fármaco em acetonitrila. As concentrações utilizadas foram 1,0; 5,0, 10, 15 e 20,0 µg/mL. A Figura 5 mostra a curva analítica da fenitoína através da correlação da área do pico e a sua concentração em µg/mL. Foi verificado que o intervalo de 1,0 a 20,0 µg/mL mostrou linearidade adequada para a quantificação do fármaco. Estes resultados foram submetidos à ANOVA, não apresentando diferença estatística significativa ($p > 0,05$). A equação da reta obtida pela regressão linear foi $y = 100623x - 4458,7$. O coeficiente de correlação ($R = 0,9999$) foi considerado adequado, de acordo com as normas preconizadas pelo ICH.

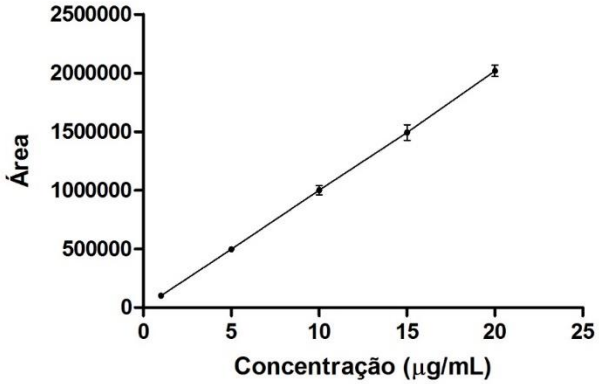

Figura 5 – Curva analítica da fenitoína em fase móvel por CLAE no comprimento de onda de 210 nm (n = 3).

A partir dos dados da linearidade, o método apresentou limite de detecção de 0,24 µg/mL e limite de quantificação de 0,80 µg/mL para a fenitoína. A precisão intra-dia (repetibilidade) e inter-dia (intermediária) foram determinadas a partir de 6 amostras, no mesmo dia, e 3 amostras em dias diferentes, respectivamente. As amostras utilizadas foram aquelas obtidas a partir da suspensão de nanocápsulas revestidas com quitosana e do pó contendo estas nanocápsulas, de modo a se obter a concentração do ponto médio da curva analítica (10 µg/mL). Foi realizada a extração do fármaco a partir da suspensão de nanocápsulas e do pó contendo estas nanocápsulas de acordo com metodologia descrita previamente no capítulo 1. Foram determinados os desvios-padrão relativos (DPR) entre as amostras analisadas (Tabela 1). Os resultados apresentaram DPR < 5%, indicando que o método se mostrou preciso para a quantificação do fármaco. Não houve diferença estatística significativa entre os resultados ($p > 0,05$) tanto na precisão intra-dia quanto na inter-dia.

Tabela 1 – Precisão intra-dia e inter-dia do método para quantificação da fenitoína.

Amostra	Precisão intra-dia DPR* (%)	Precisão inter-dia DPR* (%)
Suspensão de nanocápsulas	0,63	0,92
Pó contendo suspensão de nanocápsulas	1,31	0,32

*DPR: Desvio Padrão Relativo

A exatidão foi avaliada a partir da proximidade dos valores experimentais com o valor verdadeiro. Foi adicionada uma concentração conhecida de fármaco à amostras obtidas a partir de suspensão de nanocápsulas brancas e pó contendo estas nanocápsulas. Foram obtidas 9 amostras em 3 diferentes concentrações da curva analítica, uma concentração baixa (7,5 µg/mL), uma média (10 µg/mL) e uma alta (12,5 µg/mL). O método pode ser considerado exato, pois os resultados obtidos apresentaram recuperação mínima 95% e máxima 98% (Tabela 2). Estes foram submetidos à ANOVA e não apresentaram diferença estatística significativa ($p > 0,05$).

Tabela 2 – Exatidão (%) do método para quantificação da fenitoína.

Amostra	Exatidão (%)		
	Concentração baixa*	Concentração média*	Concentração alta*
Suspensão de nanocápsulas	98,16	96,11	96,98
Pó contendo suspensão de nanocápsulas	96,93	96,77	94,84

* n = 03 determinações (concentrações com DPR < 5%)

APÊNDICE C – Avaliação *in vivo* da atividade anticonvulsivante após administração de nanocápsulas de núcleo lipídico de fenitoína e de seus grânulos redispersos

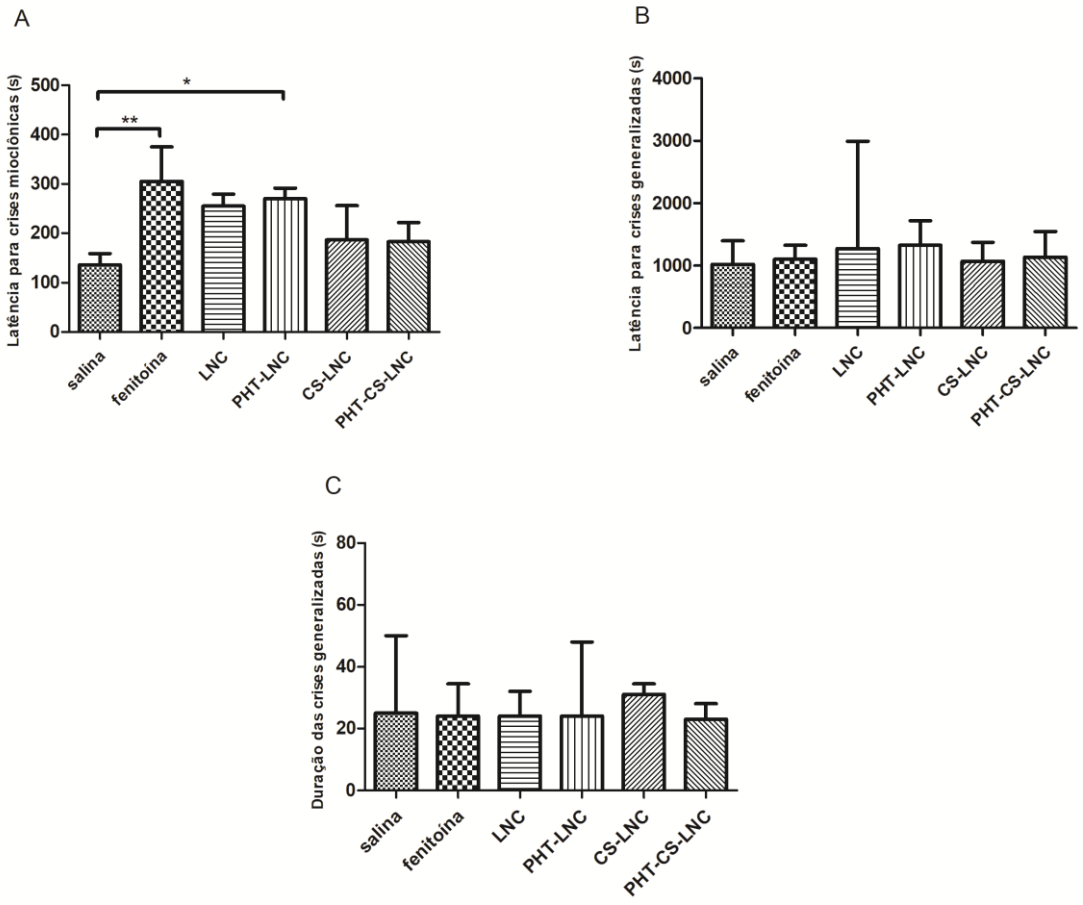

Figura 1 – Comparação entre o grupo controle, fenitoína não encapsulada, nanocápsulas sem fenitoína não-revestidas (LNC), nanocápsulas de fenitoína não-revestidas (PHT-LNC), nanocápsulas sem fenitoína revestidas com quitosana (CS-LNC) e nanocápsulas de fenitoína revestidas com quitosana (PHT-CS-LNC) na dose de 2,5 mg/kg (i.p.), em relação ao tempo de latência de crises mioclônicas (A), crises generalizadas (B) e duração das crises generalizadas (C) induzidas por pilocarpina (300 mg/kg, i.p.) (n = 5). * $p < 0,05$; ** $p < 0,01$, comparado ao grupo controle (teste de Kruskal-Wallis).

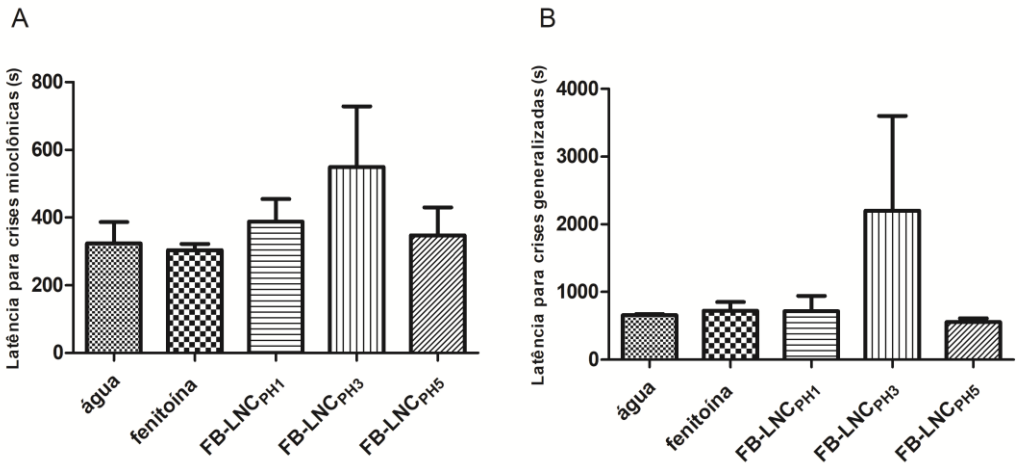

Figura 2 – Comparação entre o grupo tratado com água (controle), fenitoína não encapsulada (5 mg/mL), grânulos contendo nanocápsulas reconstituídos nas concentrações de 1, 3 e 5 mg/mL (FB-LNC_{PH1}, FB-LNC_{PH3} e FB-LNC_{PH5}), atingindo as doses de 10, 30 e 50 mg/kg (p.o.), respectivamente, em relação ao tempo de latência de crises mioclônicas (A) e crises generalizadas (B) induzidas por pilocarpina (300 mg/kg, i.p.) (n = 2).

CARTA DE APROVAÇÃO - CEUA/UFSM

Comissão de Ética no Uso de Animais
da
Universidade Federal de Santa Maria

CERTIFICADO

Certificamos que o Projeto intitulado "Avaliação do potencial anticonvulsivante de diferentes formas nanoestruturadas de fenitoína em modelos de epilepsia", protocolado sob o CEUA nº 3273040416, sob a responsabilidade de **Mauro Schneider Oliveira** e equipe; *Clarissa Vasconcelos de Oliveira; Ruy Carlos Ruver Beck* - que envolve a produção, manutenção e/ou utilização de animais pertencentes ao filo Chordata, subfilo Vertebrata (exceto o homem), para fins de pesquisa científica ou ensino - está de acordo com os preceitos da Lei 11.794 de 8 de outubro de 2008, com o Decreto 6.899 de 15 de julho de 2009, bem como com as normas editadas pelo Conselho Nacional de Controle da Experimentação Animal (CONCEA), e foi **aprovado** pela Comissão de Ética no Uso de Animais da Universidade Federal de Santa Maria (CEUA/UFSM) na reunião de 05/05/2016.

We certify that the proposal "Evaluation of anticonvulsivant potential of different forms of phenytoin nanoestructured in epilepsy models", utilizing 258 isogenics mice (males and females), protocol number CEUA 3273040416, under the responsibility of **Mauro Schneider Oliveira** *and team; Clarissa Vasconcelos de Oliveira; Ruy Carlos Ruver Beck* - which involves the production, maintenance and/or use of animals belonging to the phylum Chordata, subphylum Vertebrata (except human beings), for scientific research purposes or teaching - is in accordance with Law 11.794 of October 8, 2008, Decree 6899 of July 15, 2009, as well as with the rules issued by the National Council for Control of Animal Experimentation (CONCEA), and was **approved** by the Ethic Committee on Animal Use of the Federal University of Santa Maria (CEUA/UFSM) in the meeting of 05/05/2016.

Finalidade da Proposta: Pesquisa

Vigência da Proposta: de 07/2016 a 12/2018 Área: Farmacologia

Procedência:	Biotério Central UFSM						
Espécie:	Camundongos isogênicos	sexo:	Machos e Fêmeas	Idade:	30 a 90 dias	N:	258
Linhagem:	C57BL/6			Peso:	25 a 30 g		

Resumo: A epilepsia é considerada um problema de saúde pública porque atinge milhões de pessoas pelo mundo em todas as idades, sendo caracterizada pela recorrência de crises convulsivas, provocadas por eventos de atividade neuronal excessiva ou pela falta de sincronia no momento da transmissão do impulso nervoso.Além das crises epilépticas, a qualidade de vida dos pacientes com epilepsia é afetada por diversas comorbidades neurológicas, incluindo depressão, transtornos de ansiedade e déficit cognitivo. O objetivo do tratamento da doença é reduzir o número de crises convulsivas, com um mínimo de efeitos adversos, melhorando a qualidade de vida do paciente. No entanto, cerca de 30% dos pacientes são refratários, ou seja, continuam a ter crises, apesar de tratamento adequado com medicamentos anticonvulsivantes. A fenitoína é um fármaco modelo bastante utilizado no tratamento da epilepsia em crianças, adolescentes e adultos. Devido à estreita janela terapêutica, este fármaco necessita de frequente monitoramento dos níveis séricos. Seus efeitos adversos incluem tonturas,tremores, nistagmo, problemas de memória, sonolência e insônia. Diante disso, uma das vantagens dos sistemas nanoestruturados é o controle da liberação do fármaco, auxiliando na manutenção da concentração do fármaco na faixa terapêutica, diminuindo as flutuações plasmáticas e, consequentemente, os efeitos tóxicos. Além disso, a possibilidade de diminuição da quantidade de fármaco administrado e/ou do número de doses pode evitar o aparecimento de reações adversas. As nanocápsulas são agentes promissores para drug delivery no Sistema Nervoso Central (SNC) devido à passagem destes nanocarreadores pela barreira hematoencefálica, o que geralmente é limitada no caso de fármacos utilizados em doenças do SNC. Estas podem ser utilizadas na forma de suspensão, pós e grânulos. No entanto, as formas sólidas apresentam vantagens em relação às líquidas, principalmente no que diz respeito à estabilidade. Diante disso, é interessante avaliar as características físico-químicas, bem como a ação anticonvulsivante destas diferentes formas de fenitoína nanoestruturada, podendo auxiliar no desenvolvimento de uma formulação segura e eficaz para administração oral como alternativa ao tratamento anticonvulsivante convencional.

Local do experimento: Os experimentos propostos serão realizados em dois laboratórios no prédio 21 do Campus sede da Universidade Federal de Santa Maria: 1) Sala 5219 (prédio 21): Sala climatizada de 50 m2, dispõe de um espectrofotômetro UV-Visível, vibrátomo, sistema completo para realização de experimentos de western blot, capela de exaustão, estufa para secagem de material, agitadores diversos, balanças digitais com precisão de 0,01 g, 0,001 g e 0,0001 g, potenciômetro, microscópio óptico comum, refrigeradores, freezers e vidraria em geral. Neste laboratório há também dois computadores ligados à internet e rede de internet sem fio para uso dos alunos, assim como bibliografia específica da área (livros especializados). 2) Sala 5202 (prédio 21): Sala climatizada de 15 m2, subdividida em três salas menores onde são realizados os testes comportamentais. Possui computador com sistema de videomonitoramento para labirinto de Barnes, testes de Beam Walk, campo aberto, labirinto em cruz elevado, nado forçado, anedonia, medo condicionado e esquiva inibitória. Possui balança digital para pesagem de animais, assim como contadores manuais e cronômetros. Além disso, a equipe executora possui acesso à estrutura multiusuária que inclui sistema de

purificação de água para fornecimento de água destilada e ultrapura, leitor de placas, fotodocumentador, centrífugas, máquina de gelo e freezer a -80 oC,dentre outros equipamentos, bem como o biotério de experimentação animal do Departamento de Fisiologia e Farmacologia da UFSM. A preparação e caracterização das partículas será realizada na Faculdade de Farmácia da UFRGS, sob a coordenação local do Prof. Ruy Beck. Entre os equipamentos disponíveis estão:cromatógrafo a líquido, evaporadores rotatórios, equipamento para medidas de difração de laser (tamanho e distribuição de nano e micropartículas), equipamento para medidas de espalhamento de luz (tamanho e dispersão de nanopartículas), equipamentos para secagem por aspersão, equipamento de leito fluidizado, além de vidrarias e reagentes de uso rotineiro em laboratórios de pesquisa. O Centro de Microscopia Eletrônica da UFRGS dispõe de microscópio eletrônico de varredura, microscópio eletrônico de transmissão e metalizador para a realização das análises morfológicas propostas neste projeto.

Santa Maria, 26 de junho de 2016

Profa. Dra. Daniela Bitencourt Rosa Leal
Coordenadora da Comissão de Ética no Uso de Animais
Universidade Federal de Santa Maria

Prof. Dr. Denis Broock Rosemberg
Vice-Coordenador da Comissão de Ética no Uso de Animais
Universidade Federal de Santa Maria